MONTHLY NOTICES

OF THE

ROYAL ASTRONOMICAL SOCIETY

Vol. 116 No. 3 1956

Published and Sold by the
ROYAL ASTRONOMICAL SOCIETY
BURLINGTON HOUSE
LONDON, W.1

Price Thirteen Shillings and Sixpence

NOTICE TO AUTHORS

1. *Communications.*—Papers must be communicated to the Society by a Fellow. They should be accompanied by a summary at the *beginning* of the paper conveying briefly the content of the paper, and drawing attention to important new information and to the main conclusions. The summary should be intelligible in itself, without reference to the paper, to a reader with some knowledge of the subject; it should not normally exceed 200 words in length. **Authors are requested to submit MSS. in duplicate. These should be typed using double spacing and leaving a margin of not less than one inch on the left-hand side. Corrections to the MSS. should be made in the text and not in the margin.** Unless a paper reaches the Secretaries more than seven days before a Council meeting it will not normally be considered at that meeting. By Council decision, MSS. of accepted papers are retained by the Society for one year after publication; unless their return is then requested by the author, they are destroyed.

2. *Presentation.*—Authors are allowed considerable latitude, but they are requested to follow the general style and arrangement of *Monthly Notices*. References to literature should be given in the standard form, including a date, for printing either as footnotes or in a numbered list at the end of the paper. Each reference should give the **name and initials** of the author cited, irrespective of the occurrence of the name in the text (some latitude being permissible, however, in the case of an author referring to his own work). The following examples indicate the style of reference appropriate for a paper and a book, respectively :—

A. Corlin, *Zs. f. Astrophys.*, 15, 239, 1938.

H. Jeffreys, *Theory of Probability*, 2nd edn., section 5.45, p. 258, Oxford, 1948.

Alternatively, the Harvard reference system may be used.

3. *Notation.*—For technical astronomical terms, authors should conform closely to the recommendations of Commission 3 of the International Astronomical Union (*Trans. I.A.U.*, Vol. VI, p. 345, 1938). Council has decided to adopt the I.A.U. 3-letter abbreviations for constellations where contraction is desirable (Vol. IV, p. 221, 1932). In general matters, authors should follow the recommendations in *Symbols, Signs and Abbreviations* (London : Royal Society, 1951) except where these conflict with I.A.U. practice.

4. *Diagrams.*—**These should be designed to appear upright on the page, drawn about twice the size required in print and prepared for direct photographic reproduction except for the lettering, which should be inserted in pencil. Legends should be given in the manuscript indicating where in the text the figure should appear.** Blocks are retained by the Society for 10 years; unless the author requires them before the end of this period they are then destroyed.

5. *Tables.*—**These should be arranged so that they can be printed upright on the page.**

6. *Proofs.*—Costs of alteration exceeding 5 per cent of composition must be borne by the author. Fellows are warned that such costs have risen sharply in recent years, and it is in their own and the Society's interests to seek the maximum conciseness and simplification of symbols and equations consistent with clarity.

7. *Revised Manuscripts.*—When papers are submitted in revised form it is especially requested that they be accompanied by the original MSS.

Reading of Papers at Meetings

8. When submitting papers authors are requested to indicate whether they will be willing and able to read the paper at the next or some subsequent meeting, and approximately how long they would like to be allotted for speaking.

9. Postcards giving the programme of each meeting are issued some days before the meeting concerned. Fellows wishing to receive such cards whether for Ordinary Meetings or for the Geophysical Discussions or both should notify the Assistant Secretary.

MONTHLY NOTICES

OF THE

ROYAL ASTRONOMICAL SOCIETY

Vol. 116 No. 3

MEETING OF 1956 MARCH 9

Professor Sir Harold Jeffreys, President, in the Chair

The election by the Council of the following Fellows was duly confirmed :—

Vishnu Gianesh Bhide, Ph.D., Royal Holloway College, Englefield Green, Surrey (proposed by W. H. McCrea);

Rodney Deane Davies, 18 Granville Road, Wilmslow, Cheshire (proposed by A. C. B. Lovell);

Robert Allen Rach, Lick Observatory, Mount Hamilton, California, U.S.A. (proposed by W. P. Bidelman);

Ragihubir Saran Sharma, Ph.D., Royal Holloway College, Englefield Green, Surrey (proposed by W. H. McCrea); and

Stanislavs Vasilevskis, Lick Observatory, Mount Hamilton, California, U.S.A. (proposed by W. P. Bidelman).

The election by the Council of the following Junior Members was duly confirmed :—

Brian Geoffrey Marsden, Fixby, 7 Perne Road, Cambridge (proposed by D. W. Dewhirst);

Christopher John Millns, The Brow, The Brecks, Rotherham, Yorkshire (proposed by Z. Kopal); and

Brian Warner, 2 Diamond Cottages, Crawley Down, Sussex (proposed by P. Moore).

Ninety-four presents were announced as having been received since the last Meeting, including :—

Sir Harold and Lady Jeffreys, *Methods of Mathematical Physics, 3rd edition* (presented by the authors);

G. O. Jones, J. Rotblat and G. J. Whitrow, *Atoms and the Universe* (presented by G. J. Whitrow);

Sir John Herschel, *Outlines of Astronomy*, in Chinese (presented by Sir Eric Millar); and

Le Livre du Centenaire de la Naissance de Henri Poincaré (presented by Le Comité d'Organisation du Centenaire de la Naissance de Henri Poincaré).

MEETING OF 1956 APRIL 13

Professor Sir Harold Jeffreys, President, in the Chair

The election by the Council of the following Fellows was duly confirmed :—

Adly Salama Asaad, B.Sc., Helwan Observatory, Egypt (proposed by C. W. Allen);

Wilbur Norman Christiansen, D.Sc., C.S.I.R.O. Division of Radiophysics, University Grounds, Sydney, N.S.W., Australia (proposed by R. G. Giovanelli);

Bernard Yarnton Mills, B.Sc., Radiophysics Laboratory, University Grounds, City Road, Chippendale, N.S.W., Australia (proposed by R. G. Giovanelli);

Ali M. Naqvi, A.M., M.Sc., Ph.D., Professor of Physics and Astronomy, University of Sind, Hyderabad, W. Pakistan (proposed by M. K. Vainu Bappu);

Kevin H. Prendergast, Yerkes Observatory, Williams Bay, Wisconsin, U.S.A. (proposed by S. Chandrasekhar);

Elizabeth Roemer, Ph.D., Leuschner Observatory, University of California, Berkeley 4, California, U.S.A. (proposed by W. P. Bidelman);

Amos Hudson Ronan, M.C., Highover, Westerham, Kent (proposed by C. A. Ronan);

Alexander George Stanford, Thraves, Beech Close, Cobham, Surrey (proposed by A. Hunter); and

William Walton Wilson, 28 Norley Drive, Sale, Cheshire (proposed by Z. Kopal).

The President announced that the Council had elected the following Associates of the Society :—

Julius Bartels, Professor of Geophysics at the University of Göttingen, Germany;

Mrs. Cecilia Payne Gaposchkin, Phillips Astronomer at Harvard Observatory, Cambridge, Massachusetts, U.S.A.; and

Charles Donald Shane, Director of the Lick Observatory, Mount Hamilton, California, U.S.A.

Ninety presents were announced as having been received since the last Meeting, including :—

C. T. Moss, *The development of Spectroscopic Astronomy* (presented by the author);

R. H. Phillimore, *Historical records of the Survey of India* (presented by the Surveys-General of India);

Liège University, Institute of Astrophysics, *Atlas of representative cometary spectra* (presented by the International Astronomical Union);

E. F. Savarensky and D. P. Kirnes, *Elements of Seismology and Seismometry*; Seismological Council, Academy of Sciencies, U.S.S.R., *Guide to the performing and working of observations at seismic stations of the U.S.S.R.*; Geological Institute of the Academy of Sciences, U.S.S.R., *Questions of the Earth's internal structure and development* (these three, in Russian, presented by Colonel E. Tillotson); and

Three volumes of astronomical pamphlets, presented by Sir Eric Millar.

SIX VISUAL DOUBLE STAR ORBITS

W. D. Heintz

(Communicated by R. v. d. R. Woolley)

(Received 1956 February 29)*

Summary

Orbital elements and physical data of the pairs ADS 5949, 8949, 9392, 9425, 14412, 16057 are derived.

A 2855 (ADS 5949. $7^h\ 14^m{\cdot}2$, $+1°\ 4'$)

Elements:	P 71^y·3	e 0·16	i ± 135°	ω 282°
(precession neglected)	T 1953·5	a 0″·40	Ω 42°·5	μ 5·05

Observations	P_o	P_e	O–C	ρ_o	ρ_e	O–C
	°	°	°	″	″	″
1914·45 A	313·0	313·4	−0·4	0·32	0·33	−0·01
20·93 A	281·1	281·0	+0·1	36	35	+ 01
27·97 VBs	253·2	252·6	+0·6	44	40	+ 04
36·44 B	225·9	224·2	+1·7	37	41	− 04
38·54 VBs	214·9	216·7	−1·8	38	39	− 01
42·06 VBs/B	200·9	202·6	−1·7	28	36	− 08
46·00 VBs	182·4	181·5	+0·9	30	30	0
50·58 VBs	143·6	144·4	−0·8	24	24	0
54·23 Bz	...	...	...	round	24	...

Ephemeris:		°	″
	1956·0	93·7	0·27
	58·0	79·3	29
	60·0	67·5	32
	62·0	57·4	35
	64·0	48·6	37
	66·0	40·5	0·38

This very close couple is within reach only of the largest apertures, and the observations are not numerous. The predicted places diverge rapidly from those following from Baize's elements (*Circ. d'Inf.* **4**).

Σ 1757 (ADS 8949. $13^h\ 31^m{\cdot}7$, $-0°\ 4'$)

Elements :	P 334^y·0	e 0·24	i ± 58°·0	ω 140°·8
(1900)	T 1723·0	a 2″·35	Ω 97°·1	μ 1·078

Normal places :	P_o(1900)	P_e	O–C	ρ_o	ρ_e	O–C
	°	°	°	″	″	″
1825·0	12·3	13·8	−1·5	1·49	1·41	+0·08
35	26·9	28·3	−1·4	1·56	1·52	+ 04
45	41·3	40·4	+0·9	1·72	1·67	+ 05
55	51·4	50·4	+1·0	1·92	1·85	+ 07
65	58·9	58·6	+0·3	2·09	2·04	+ 05
75	65·4	65·3	+0·1	2·23	2·22	+ 01
85	70·9	71·0	−0·1	2·37	2·38	− 01
95	76·0	76·2	−0·2	2·48	2·53	− 05
1905·0	80·2	80·8	−0·6	2·58	2·64	− 06
15	84·6	85·0	−0·4	2·67	2·72	− 06
25	89·1	89·1	0	2·74	2·77	− 03
35	93·0	93·0	0	2·75	2·77	− 02
45	97·2	97·1	+0·1	2·67	2·72	− 05
55	101·4	101·4	0	2·64	2·63	+0·01

* Received in original form 1955 July 6. No changes in the resulting orbits have been made since that time.

Ephemeris	1956·0	101°·6	2″·62
(equinox of date):	60·0	103·5	2·56
	64·0	105·4	2·50
	68·0	107·4	2·43
	72·0	109·5	2·36
	76·0	111·8	2·27
	80·0	114·3	2·18

The point of maximum distance has been passed, and the companion closes in slowly. The observations show marked deviations from a constant areal velocity, but so far there is no periodicity indicated by the residuals. Also, the run in the distance differences could be partly due to error of the interpolation curve as the older measurements are unusually discordant. Accordingly, the recent elements published by Florsch (*Circ. d'Inf.* **3**) are based on a different areal constant. The couple has a proper motion and parallax not much different from the 19′ distant star ζ Virginis. The collection of observations in a previous paper on Σ 1757 by Luplau Janssen (**2**) was used and completed by more than 200 recent observations, especially the numerous measurements by Prof W. Rabe, which were kindly communicated to the writer, up to 1955·0.

Σ 1883 (ADS 9392. $14^h\,46^m\cdot4$, +6° 10′)

Elements :	P 1027^y	e 0·62	i ± 115°·8	ω 291°·5	
(1900)	T 1941·9	a 1″·45	Ω 88°·6	μ 0·3505	

Normal places :	P_o(1900)	P_c	O–C	ρ_o	ρ_c	O–C
	°	°	°	″	″	″
1830·74	269·9	269·47	+0·4	1·23	1·19	+0·04
43·01	266·8	267·12	−0·3	1·10	1·10	0
56·19	263·1	264·14	−1·0	1·03	1·00	+ 03
65·03	260·5	261·75	−1·2	0·85	0·93	− 08
74·89	260·5	258·54	+2·0	0·90	0·83	+ 07
83·32	256·1	255·13	+1·0	0·75	0·75	0
95·87	247·5	248·10	−0·6	0·62	0·60	+ 02
1903·62	242·3	241·68	+0·6	0·55	0·50	+ 05
10·69	236·0	233·22	+2·8	0·44	0·42	+ 02
18·55	218·4	218·51	−0·1	0·33	0·32	+ 01
25·98	197·6	196·09	+1·5	0·28	0·26	+ 02
31·92	169·0	172·30	−3·3	0·25	0·25	0
36·69	153·8	153·33	+0·5	0·27	0·26	+ 01
40·57	139·5	140·31	−0·8	0·28	0·29	− 01
45·91	125·6	126·60	−1·0	0·32	0·34	− 02
50·17	116·9	118·52	−1·6	0·34	0·39	− 05
52·95	114·7	114·24	+0·5	0·40	0·43	−0·03

Ephemeris	1956·0	110°·0	0″·46
(equinox of date):	58·0	107·8	48
	60·0	105·7	50
	62·0	103·7	52
	64·0	101·9	54
	66·0	100·3	56
	68·0	98·7	58
	70·0	97·3	0·60

Like Σ 2924 (below), this pair has been difficult during the last decades, but now the separation increases. Due to the fairly high inclinations, the orbital elements are less certain than would be expected from observed arcs of nearly 180°. The computation of these elements was dropped in 1953, after publication of orbits by Pensado (Σ 1883) and Arend (Σ 2924), cf. the ephemeris catalogue (**1**), but the work was resumed as recent observations seem to show residuals.

OΣ 288 (ADS 9425. $14^h\,51^m{\cdot}0$, $+15°\,54'$)

Elements : P 215$^y{\cdot}4$ e 0·60 i ± 112°·5 ω 0°
(1900) T 1819·3 a 1″·09 Ω 4°·7 μ 1·6715

Normal places :	P_o(1900)	P_c	O–C	ρ_o	ρ_c	O–C
	°	°	°	″	″	″
1844·85	224·5	224·31	+0·2	0·51	0·51	0·00
48·63	216·0	217·02	−1·0	0·50	0·62	− 12
64·46	203·0	202·41	+0·6	1·12	1·04	+ 08
73·74	197·4	198·07	−0·7	1·31	1·24	+ 07
82·18	195·4	195·12	+0·3	1·43	1·39	+ 04
88·49	193·5	193·27	+0·2	1·44	1·49	− 05
96·84	191·1	191·12	0	1·56	1·59	− 03
1903·42	189·8	189·59	+0·2	1·67	1·65	+ 02
12·51	187·4	187·61	−0·2	1·68	1·71	− 03
26·23	185·1	184·85	+0·2	1·78	1·74	+ 04
36·54	182·7	182·78	−0·1	1·74	1·73	+ 01
43·06	181·4	181·44	0	1·68	1·70	− 02
50·03	179·9	179·93	0	1·62	1·65	−0·03

		°	″
Ephemeris	1956·0	178·4	1·60
(equinox of date):	60·0	177·4	1·56
	64·0	176·3	1·51
	68·0	175·2	1·45
	72·0	174·0	1·39
	76·0	172·6	1·32
	80·0	171·1	1·25

A 751 (ADS 14412. $20^h\,52^m{\cdot}5$, $+59°\,7'$)

Elements : P 58$^y{\cdot}8$ e 0·51 i ± 134° ω 109°
(precession neglected) T 1918·0 a 0″·19 Ω13° μ 6·12

Observations	P_o	P_c	O–C	ρ_o	ρ_c	O–C
	°	°	°	″	″	″
1904·53 A	33·9	32·7	+ 1·2	0·16	0·21	−0·05
08·65 A	24·4	18·9	+ 5·5	17	17	0
11·51 A	16·1	5·3	+10·8	20	15	+ 05
14·71 A	336·4	336·7	− 0·3	13	10	+ 03
15–16				too close	<10	
20·68 A	212·5	205·6	+ 6·9	15	11	+ 04
21·54 A	195·9	196·3	− 0·4	13	12	+ 01
22·79 A	157·1	185·5	−28·4	14	13	+ 01
27·73 VBs	140·3	154·7	−14·4	17	16	+ 01
33·72 A	117·0	126·2	− 9·2	17	17	0
34·67 A	113·9	122·1	− 8·2	16	18	− 02
40·66 VBs	99·6	98·7	+ 0·9	19	19	0
43·78 VBs	89·0	88·0	+ 1·0	19	20	− 01
45·73 Jeff.	84·6	81·7	+ 2·9	17	21	− 04
48·65 VBs	71·0	73·0	− 2·0	19	21	− 02
53·70 Mu	60·9	59·0	+ 1·9	21	22	−0·01

Ephemeris:	1956·0	52°·9	0″·22
	58·0	47·6	22
	60·0	42·3	22
	62·0	36·7	22
	64·0	30·8	21
	66·0	24·3	0·19

Also for this pair, Baize (*Circ. d'Inf.* **4**) gives a recent set of elements, very similar to those derived here. Some measurements do not satisfy the law of areas, as seen from the leap in the residuals about 1920. The interferometer observations 1923·74 (3n) by Maggini are apparently spurious and have been rejected.

Σ 2924 (ADS 16057. $22^h\ 31^m.6$, +69° 39′)

Elements :	*P* 225ʸ·6	*e* 0·27	*i* ± 79°·0	ω 6°·7	
(1900)	*T* 1975·8	*a* 0″·78	Ω 82°·6	μ 1·596	

Normal places :	P_o(1900)	P_c	O–C	ρ_o	ρ_c	O–C
	°	°	°	″	″	″
1830·0	257·5	257·29	+0·2	0·80	0·85	−0·05
40	260·8	259·54	+1·3	0·86	0·93	− 07
50	263·1	261·70	+1·4	0·92	0·98	− 06
60	264·2	263·33	+0·9	0·95	0·99	− 04
70	265·1	265·20	−0·1	0·97	0·96	+ 01
80	266·3	267·24	−0·9	0·93	0·90	+ 03
90	268·6	269·69	−1·1	0·82	0·81	+ 01
1900·0	271·6	272·93	−1·3	0·66	0·68	− 02
10	275·9	277·94	−2·0	0·52	0·52	0
20	288·6	287·82	+0·8	0·36	0·34	+ 02
30	318·8	317·79	+1·0	0·19	0·18	+ 01
40	31·8	33·33	−1·5	0·20	0·18	+ 02
50	64·5	63·83	+0·7	0·36	0·34	+0·02

Ephemeris	1956·0	71°·4	0″·43
(equinox of date):	58·0	73·2	46
	60·0	74·8	49
	62·0	76·2	51
	64·0	77·5	53
	66·0	78·8	55
	68·0	80·0	56
	70·0	81·1	57

Last elements by Arend (1953, 2 orbits).

The following table gives the physical data of the six systems, total apparent magnitude *m*, magnitude difference Δ*m*, and spectrum, from which the dynamical parallaxes π_{dyn} and total masses $\mathfrak{M}$, according to Russell and Moore (**3**), have been calculated. The table also shows the radiation-energy parallax (strahlungsenergetische Parallaxe) π_{r-e}, and component masses, computed from tables given by Brill (**4**) and Hopmann (**5**). (This method uses as arguments the data also employed for the dynamical parallaxes, semi-axis major, period, apparent magnitudes and spectra, but also takes into account an empirically corrected mass-luminosity relation, thus obtaining individual instead of merely statistical parallaxes.) From the latter values the other data have been derived : absolute magnitudes *M*, radii *R* and mean densities *D* of the components (unit = Sun), and the semiaxis major in A.U.

ADS	5949	8949	9392	9425	14412	16057
m	8·20	7·36	6·72	6·43	6·82	6·02
Δm	0	1·1	0	0·7	0·3	0·5
Sp.	K0	K1	F8	F9	F2/A2	F2/A5
π_{dyn}	0·0178	0·0410	0·0085	0·0211	0·0074	0·0129
$\mathfrak{M}$	2·2	1·7	4·7	3·0	4·9	4·3
π_{r-e}	0·0192	0·0437	0·0098	0·0230	0·0079	0·0138
M_A	+5·37	+5·80	+2·42	+3·70	+1·91	+2·25
M_B	+5·37	+6·90	+2·42	+4·40	+2·21	+2·75
$\mathfrak{M}_A$	0·94	0·79	1·52	1·25	2·00	1·82
$\mathfrak{M}_B$	0·94	0·60	1·52	1·05	2·07	1·71
$\mathfrak{M}$	1·88	1·39	3·05	2·30	4·07	3·53
R_A	1·2	1·1	2·4	1·4	2·1	1·8
R_B	1·2	0·7	2·4	1·0	1·0	0·9
D_A	0·52	0·63	0·11	0·46	0·20	0·30
D_B	0·52	2·17	0·11	1·01	2·15	2·04
a (*AU*)	20·8	53·7	148·7	47·4	24·1	56·4

Commonwealth Observatory,
Canberra, A.C.T.:

1955 *June* 29.

References

(1) P. Muller, *J.O.*, **36**, 61, 1953.
(2) C. Luplau Janssen, *A.N.*, **241**, 67, 1931.
(3) H. N. Russell, C. E. Moore, *The masses of the stars*, 1940.
(4) A. Brill, *Veröff. Berlin-Babelsberg*, Vol. VII, 1, 1927.
(5) J. Hopmann, *Abh. Sächs. Akad.*, Vol. 43, No. 3, 1945.

MICROMETER OBSERVATIONS OF DOUBLE STARS

W. D. Heintz

(Communicated by R. v. d. R. Woolley)

(Received 1956 March 10)

Summary

Measurements made by a filar and by a Muller double image micrometer are given and the errors of both series discussed.

---

1. ***Filar Micrometer Observations.***—By courtesy of the Commonwealth Observatory, Mount Stromlo, the Oddie refractor (aperture 9″, focal length 139″), equipped with a filar micrometer, was made available for double star work in the winter of 1955. From June 18 to September 10, 925 observations were obtained, 873 of which are given below; the remainder consists mainly of negative or highly doubtful results of difficult pairs obtained under insufficient atmospheric conditions. Also, a few of the very first observations had to be rejected. 11 observations, also listed below, had been made in August 1954, in order to test the micrometer for other purposes. The separation limit of the telescope is 0″·52.

The programme consisted of stars, RA 12–24^h, with known orbits or appreciable orbital motion, "couples prioritaires" from the I.A.U. Double Star Circulars, and, for comparison, stars which are also regularly observed by Professor Rabe, Munich. A number of fairly close stars from the programme of Woolley, Gottlieb, and Simonow (**1**), 1945/47, at the same instrument (but by another micrometer) have been added. 190 double, 8 triple, 1 quadruple system, in total 209 objects, have been measured.

The angular revolution value resulting from 65 determinations is 29″·718 ± 0″·027. All measures are made with field illumination of properly adjusted brightness, a 1/4″ eyepiece, and with eyes parallel to the line joining the stars. The mean error of one observation in angle increases from ±0°·6 for the wide couples to 5° for the closest (not separated) ones; in distance it is ±0″·06 for the close pairs, and 0·11–0·13, practically constant, for all separations >1″. The increase in accuracy for bright stars and for couples with equal components is small.

The systematic differences of these observations minus the most recent values of 46 couples obtained by W. Rabe, Munich (11″ aperture), distributed according to brightness of primary and separation, are, after the small epoch differences have been made allowance for in all cases where an orbit exists, by interpolation from the orbit ephemeris (**2**):

m_A	ρ −0″·75		0″·75–2″·00		2″·00–	
	°	″	°	″	°	″
−5·0	+3·1	+0·04 (2)	+0·2	−0·02 (2)	+0·4	+0·12 (4)
5·0–7·5	+4·0	+0·12 (7)	+1·0	+0·04 (17)	+0·8	−0·01 (3)
7·5–	−0·2	+0·13 (3)	+0·6	−0·06 (4)	+0·7	+0·06 (4)

The position angles given here are apparently somewhat too large, and this difference increases for close couples. In separation, only the close pairs show

appreciable differences, due to the fact that Rabe corrects these measures by comparison with large-aperture observations. The agreement with his uncorrected values is satisfactory. Rabe's personal equations are well determined: he measures position angles, perhaps, slightly smaller than the mean of all observers does (**3**); his distance system shows no peculiarities. The writer's thanks are due to Professor Rabe for making his unpublished results available for this comparison, which is of interest with respect to the double-image results given later.

In the table of observations, only the means are given. A + sign with the number of nights indicates that the star has also been unsuccessfully observed on one or more nights. An asterisk refers to the remarks. For the comparison with orbits, the ephemeris catalogue (**2**) has been used, in some cases directly the elements in the orbit catalogue (**4**), where references to the orbits may be found.

For negative observations, the limiting distances (e.g. $<0''.4$) are based on the correctness of the ADS or SDS magnitude differences. It may be added that a number of these need revision, not only in the far south. For example, the companion of ρ Cap, given as $10^{m}.0$, is certainly brighter than 8^{m} (Wirtz, 1907, also estimated $7^{m}.7$); similarly the companions of β 227 and λ 244 seem brighter than 10·5 and 9·4, respectively. On the other hand, ξ Pav B, given as $8^{m}.6$, is certainly fainter than 10^{m}, about the same as δ PsA B (10·5).

ADS				α 1900+		P	ρ	n
				h		°	″	
—	λ	143		12·01	55·49	119·4	0·95	5*
8515	β	605		17	50	188± ?	0·7	6
8547	β	606		23	50	too difficult		5
—	—		α Cru	23	49	115·4	4·38	5
8555	B	228		25	51	too close		3*
8573	β	28		27	49	336±	0·95e	3+*
—	h	4539	γ Cen	39	49	6·2	1·46	4*
8630	Σ	1670	γ Vir	39	50	310·9	5·21	4*
—	Ru	207	β Mus	43	50	15·1	1·28	4
8708	OΣ	256		54	50	268·3	0·88	4
8728	I	1225		57	51	round	<0·35	3
8759	β	929	48 Vir	13·01	55·49	207·7	0·81	5
—	I	917		03	51	289·4	1·22	3
8864	Σ	1734		18	50	182·8	1·02	4
—	Hrg	86		29	51	239·3	1·62	4
8949	Σ	1757		32	51	100·3	2·71	6*
—	h	4596		33	51	282·6	1·30	4
—	I	365		34	52	127·1	0·47	4*
—	Howe	23		40	50	186·6	1·33	3
9019	Σ	1781		43	50	333·4	0·77	4*
—	β	343		49	53	68·1	0·87	3
—	Howe	28		50	53	round		3
9053	Σ	1788		52	49	89·2	3·26	5
—	Ru	227		53	52	5·6	1·73	4
—	β	1197		14·00	55·53	212·3	1·94	3
—	V	31	β Cen	00	57	253·5	1·18	4+
9106	β	938		03	50	—	<0·35	3
—	Slr	19		04	51	293·4	1·40	4

ADS				α 1900+		P	ρ	n
				h		°	″	
9170	β	939		14·11	55·52	85·7 :	0·51	3+
9182	Σ	1819		13	49	291·8	0·96	5*
—	h	4667		18	51	140·2	2·31	3
9258	β	225	AB	22	50	295·1	35·10	4
			BC	22	50	93·1	1·20	4
—	h	4687		32	54	104·2	1·22	3
—		—	α Cen	36	51	37·9	5·55	8*
—	β	414		39	54	347·1	0·94	3
9343	Σ	1865	ζ Boo	39	49	308·9	1·22	6*
9344	β	345		39	54	292·2	0·92	3
—	ϕ	309		43	48	round	<0·35	4*
9392	Σ	1883		46	52	110·7	0·46	6*
—	I	236		48	55	116·9	1·94	3
—	h	4707		50	52	33·7	0·79	4*
9425	OΣ	288		51	52	177·8	1·74	5*
9453	β	239	59 Hya	55	55	337·2	0·81	2
—	Cape	15		15·01	55·53	44·3	1·56	3
—	h	4728	π Lup	02	49	74·4	1·45	4
9532	β	618	ι Lib	09	54	—	″	3
—	I	329		10	54	336·6	0·78	3
—	I	228		10	52	26·3	1·32	4
9552	β	350		12	57	141·9	0·74	3
—	h	4753	μ Lup AB	15	49	322·6	1·21	5
			AB/2–C	15	49	128·7	22·98	4
9579	β	227		16	55	169·1	1·74	4
9586	β	228		16	55	292·8	0·73	4
—	Slr	20		19	53	87·2	0·61	4
—	Cop	2	ε Lup AB	19	52	251·3	0·71	4
			AC	19	53	170·9	26·11	2
—	h	4757	γ Cir	19	49	45·0	1·09	5
9659	β	1114		26	55	319·2	1·08	3
—	h	4786	γ Lup	32	56	282·6	0·45	7*
9701	Σ	1954	δ Ser	32	53	179·5	3·87	4
—	I	243		35	58	342·8	0·75	3
—	I	89		38	56	159·7	1·25	3
—	λ	244		38	56	40·0	0·97	3
9775	β	620		43	54	349·6	0·50	4
9823	β	36	2 Sco	50	53	273·2	2·35	4
9836	I	977		52	56	276·8	0·55	3
9880	OΣ	303		58	58	163·7	1·26	6
—	λ	258	ι^1 Nor AB	59	57	234·9	0·54	4*
			AB/2–C	59	56	245·2	10·78	2
9909	Σ	1998	ξ Sco AB	16·01	55·54	320·6	0·59	4*
			AB/2–C	01	55	53·7	7·78	2
—	λ	264	AB	02	56	183·1	0·72	4*
9913	β	947	β Sco AC	02	49	201·7	13·87	2*
9951	β	120	ν Sco AB	09	54	3·2	1·10	4
			AC	09	54	336·3	41·66	3
			CD	09	54	50·6	2·34	4
—	λ	268		11	56	176·7	1·78	4
9982	Σ	2026		13	55	30·4	2·20	5*
10049	Sh	228	ρ Oph	22	50	345·6	3·19	4
10050	λ	277		22	54	194·4	0·74	4
10074		—	α Sco	26	53	277·6	2·78	5
—	I	336		27	56	195·0	1·18	4

ADS				α	1900+	*P*	ρ	*n*
				h		°	″	
10087	Σ	2055	λ Oph	16·28	55·57	329·7	0·71	7*
10092	Σ	3105		29	58	—	<0·3	6
—	Slr	12		36	57	166·5	1·44	4
—	Ru	283		39	61	37·4	0·53	4
10229	Σ	2106		48	59	196·8	0·47	4+
10230	OΣ	315	21 Oph	49	51	136·4	0·63	4
10257	β	241		52	51	352·3	0·52	4
10265	β	1117	24 Oph	54	58	293·9	0·80	4
10312	Σ	2114		59	51	177·3	1·28	4
10341	β	823		17·04	55·51	82·5	0·80	4
—	I	407		04	57	175·8	0·51	4
10355	A	1145		05	50	round		4
10374	β	1118	η Oph	07	59	343·1	0·38	5*
10417	Sh	243	36 Oph	12	50	166·0	4·37	5
—	β	416		15	57	254·8	1·97	4
—	Brs	13		15	51	230·3	5·63	4*
10465	β	126	AB	17	51	263·8	2·06	4
10564	β	129		25	57	113·7	0·75	3
10598	Σ	2173		28	60	290·7	0·40	4*
10657	Hu	751		34	58	288±	<0·4	4
10696	β	631		37	57	unmeasurable		6
—	Hd	275		38	55	164·3	0·77	4
—	Cape	17		41	52	195·7	1·13	3
10828	OΣ	337		48	60	202·5	0·37	5
10858	Σ	3128		50	48	287?		2+*
—	I	1013		54	56	154·6	0·75	3
10912	Σ	2244		54	51	288·1	0·44	5
11005	Σ	2262	τ Oph	18·00	55·50	269·7	2·12	5*
11046	Σ	2272	70 Oph	03	49	97·9	5·18	4*
—	h	5014		03	53	29·3	1·55	4*
11111	Σ	2281	73 Oph	07	51	29·8	0·63	4*
11186	Σ	2294		12	49	94·8	0·89	5*
—	Gale	2	ξ Pav	18	63	154·5	3·26	4
11324	AC	11		22	51	358·0	0·74	7
11353	Σ	2316	59 Ser	24	50	318·1	3·78	4
11354	β	133		24	57	253·2	1·32	4
11378	HN	125		26	57	103·8	2·79	3
—	Stone	62		31	57	135·4	2·13	3
11483	OΣ	358		33	54·62	174·5	1·66	2*
					55·49	173·0	1·79	7*
11484	OΣ	357		33	48	—	<0·3	3*
11530	Ho	87		36	52	339·2	0·42	7
11622	λ	358		41	53	44·4	1·57	3
11643	B	405		43	50	round		4
—	Ru	314		43	56	270·0	1·83	3
—	h	5075		59	56	114·0	1·67	3
11950	Hd	150	ζ Sgr	59	63	242·5	0·56	5*
11971	Σ	2434	AB	19·00	55·49	106·1	24·32	3
			BC	00	57	15·0	1·01	5
11989	HN	126		01	49	221·9	1·05	5*
—	h	5084	γ CrA	03	52	37·0	2·37	7*
—	Gale	3		12	55	242	0·4	6
—	I	254		27	54	36·4	0·63	5

ADS				α	1900+	P	ρ	n
				h		°	"	
—	I	117		19·27	55·52	182·9	1·01	3
12715	Σ	2545		36	50	323·1	3·68	4
—	I	119		38	52	160·7	1·68	3
—	I	120		45	52	160·3	0·59	5*
13104	Σ	2597		52	53	78·1	0·76	5
13178	AC	12		56	51	308·0	1·28	4
—	Hd	294		58	59	359·4	0·73	4
13268	Hu	79		59	58	232·2	0·61	5
13493	β	1205		20·09	55·50	—		6*
13506	Σ	2644		10	54·62	26·4	2·62	2
					55·49	27·3	2·88	5
—	β	763	κ^2 Sgr	20	60	231·3	0·90	5
13860	β	60	π Cap	24	51	145·7	3·23	4
13887	Sh	223	ρ Cap	26	55	157·0	1·17	4
13961	λ	—		30	54	round		3
14086	I	1425		36	54	round		3
—	I	17		41	60	36·2	0·98	4
14233	Σ	2723		42	52	114·0	1·20	5
14280	β	153		44	61	265·3	1·62	5
14360	Σ	2729	4 Aqr	49	54·62	355·4	1·12	2*
					55·53	3·5	1·14	4*
—	I	669		56	61	63·1	0·96	4
14499	Σ	2737	ε Eql AB	56	60	287·9	0·85	6*
			AC	56	57	67·9	10·52	3
14573	Σ	2744		21·00	54·62	139·5	1·63	1
					55·57	139·1	1·44	6
14592	Σ	2745	12 Aqr	01	54·62	194·7	2·14	2
					55·55	193·5	2·38	4
14648	β	368		05	56	—	<0·35	3
14666	OΣ	527		05	64	236±?	<0·4	3+
—	Hu	1626		08	61	153·8	1·30	5
14759	β	270		11	64	18·5 :	0·56 :	2+
14773	OΣ	535	δ Eql	12	68	23·3	0·40	5*
—	h	5258	ϑ Ind	16	63	274·8	5·88	4
—	β	766	θ^2 Mic	21	61	270·4	0·66	5, 4
15007	Σ	2799		26	64	99·3	1·62	6
15176	β	1212	24 Aqr	37	66	282·5	0·60	6*
—	h	5278	λ Oct	43	63	68·1	3·04	4
15313	Σ	2825		44	62	125·5	0·85	5
—	I	19		45	64	317·0	1·24	3
15371	λ	460		48	64	144·4	0·59	4
15447	β	75		53	67	125±	0·41	2+
15536	β	276	η PsA	58	64	114·9	1·83	6
15596	Σ	2854		22·02	55·66	83·7	2·15	5
—	h	5319		09	64	127·8	2·09	4
15731	A	2292		10	66	201·4	0·64	4
15753	Sh	339	41 Aqr	11	66	115·1	5·09	4
—	I	134		19	64	287·1	0·55	4
15902	β	172	51 Aqr	21	65	328·7	0·62	5
15934	Sh	345	53 Aqr	24	64	322·3	4·16	5
15971	Σ	2909	ζ Aqr	26	54·60	275·3	1·95	1*
					55·65	272·5	1·87	7*
15978	λ	474	AB	26	65	320±?	<0·3	4
15988	Σ	2912	37 Peg	27	65	117·9	1·01	5*

ADS				α h	1900+	*P* °	ρ "	*n*
16131	Ho	479		22·36	55·66	330·4	0·66	5
16145	Σ	2928		37	65	120·4	3·70	4, 3
16208	Σ	2935		40	54·58	308·7	2·37	1
					55·63	309·2	2·44	4
16215	Hu	289		41	65	103·8	1·69	4
16270	Σ	2944	AB	45	66	274·7	2·52	5
			AC	45	68	106·0	49·68	3
—	I	340		49	67	352·3	0·88	4
—	h	5367	γ PsA	49	63	263·5	4·11	4
16365	β	178		52	64	—	<0·6	3
—	β	772	δ PsA	53	67	244·9	4·98	4
16428	OΣ	483	52 Peg	57	66	269·5	0·79	6
—	Jc	20	ϑ Gru	23·04	55·67	68·1	1·30	5
16613	β	714		11	67	121 ±		3+
16643	Hu	399		14	67	321·8	0·69	4
16649	β	79		15	67	35·3	1·29	5
16650	Hu	400		15	67	162·0	0·61	5
—	Stone	59		25	67	214·3	1·51	4
16791	Hu	599		27	67	single		5
16850	λ	492		33	67	64·0	0·68	5*
—	I	693		34	67	49·6	0·85	4
—	Rmk	27	ϑ Phe	36	66	275·1	4·03	4
16979	Sh	356	107 Aqr	43	65	137·3	6·47	4
—	Slr	14		48	67	300·7	0·75	5*
17107	Σ	3046		54	67	261·2	3·41	4
—	I	1477		57	67	292·1	0·49	4

Remarks: Comparisons with orbits.

— λ 143 +1°·5, −0″·04 (van den Bos 1936).

8555 B 228 Obs. irreconcilable, evidently spurious.

8573 β 28 The orbit Arend (1949) gives 328°·7, 1″·22, Baize (1954) 282·1, 0·92.

— γ Cen +0·6, +0·01 (van den Bos 1936).

8630 γ Vir +0·7, −0·05 (Strand 1937).

8949 Σ 1757 −1·1, +0·09 (Heintz 1955), −1·0, +0·14 (Florsch 1954).

— I 365 +0·5, +0·06 (van den Bos 1935).

9019 Σ 1781 +4·0, +0·07 (Rabe 1951, Elem. I), +0·2, +0·16 (Ziller 1954), 0·0, +0·13 (Arend).

9182 Σ 1819 −2·0, −0·03 (Hopmann 1945).

— α Cen +1·6, −0·40 (Finsen 1926).
The single observations are :

55·461	36·8	5·93	55·505	37·3	5·66
·480	37·5	5·61	·507	38·2	5·41
·483	37·6	5·49	·565	38·1	5·41
·494	38·2	5·63	·617	39·3	5·25

9343 ζ Boo −1·1, +0·05 (van den Bos 1937), −0·9, +0·06 (Wierzbinski 1954).

— φ 309 The separation according to van den Bos' orbit (1950) is 0″·56, but the recent elements of Finsen give 0·17.

9392 Σ 1883 +0·1, 0·00 (Heintz 1955).

— h 4707 +1·4, −0·03 (Woolley/Mason 1948).

9425 OΣ 288 −0·7, +0·13 (Heintz 1955).

— γ Lup The orbit Dawson 1919 is astray. A new determination is under work.

— ι^1 Nor −0·5, +0·08 (Woolley/Mason 1948).

9909 ξ Sco +3·9, +0·14 (Baize 1942).

— λ 264 +5·7, −0·02 (Woolley 1948).

9913 β Sco Close companion not seen.

9982 Σ 2026 −2·3, +0·06 (Woolley/Symms 1937).

10087	λ Oph	+3·6, −0·06 (Rabe 1948).
10374	η Oph	+4·8, +0·14 (Baize 1950).
—	Brs 13	+0·7, −0·13 (Wieth-Knudsen 1954).
10598	Σ 2173	−5·7, +0·15 (Duncombe/Ashbrook 1952).
10858	Σ 3128	Probably spurious, companion too faint.
11005	τ Oph	−1·0, +0·13 (Hertsprung 1942).
11046	70 Oph	−0·8, 0·00 (Strand 1952).
—	h 5014	−0·4, −0·14 (Dawson 1926).
11111	73 Oph	−9·7, +0·13 (van den Bos 1937).
11186	Σ 2294	−0·6, −0·03 (Wilson 1935).
11483	OΣ 358	1954 : +1·5, −0·16 1955 : +0·4, −0·03 (Heintz 1955).
11484	OΣ 357	Separation 0″·25 according to Florsch 1955.
11950	ζ Sgr	+1·6, +0·05 (Finsen 1937).
11989	HN 126	+1·8, +0·05 (Gottlieb 1948).
—	γ CrA	+2·0, −0·16 (Dawson 1924).
—	I 120	−8·4, −0·08 (Finsen 1935).
13493	β 1205	One obs. : 1955·50, 107°·9, 0″·6, but single at four subsequent good nights.
14360	4 Aqr	1954 : −5·0, +0·07 1955 : +2·7, +0·08 (Baize 1943).
14499	ε Eql	+0·9, 0·00 (van den Bos 1933).
14773	δ Eql	−0·7, +0·04 (Luyten/Ebbighausen 1934).
15176	24 Aqr	+2·5, +0·03 (Danjon 1942).
15971	ζ Aqr	1954 : +3·8, −0·15 1955 : +2·7, −0·20 (Rabe 1954).
15988	37 Peg	+0·9, −0·03 (van Biesbroeck 1927).
16850	λ 492	+2·7, −0·05 (Woolley/Mason 1948).
—	Slr 14	−5·0, −0·05 (Woolley 1948).

2. *Double Image Micrometer Observations.*—On invitation by Professor Woolley, some observations were made in September 1955 with a newly acquired Muller type double image micrometer at the same telescope. Muller's formula for the angular screw value, evaluated by Mr K. Gottlieb, yielded 0″·971 ± ″·002; from 5 determinations using circumpolar stars, 0″·963 ± ″·027, was obtained and adopted.

23 couples were selected from the previously observed programme in such a way as to give the widest possible range in brightness, magnitude difference, and separation. Usually, observations were made in two positions: having the four images in a straight line and in the vertices of a square, the latter was viewed from two sides (by turning the head 90°). The close couples δ Eql and Σ 2825, were measurable only in linear position, δ PsA (very wide, $\Delta m = 6$) only in the square. The linear arrangement generally seemed more easily to be judged, except for distance measures of close pairs. From 19 couples, the mean difference square minus line, is +0°·4, +0″·06, which is not significant.

The differences against the filar micrometer observations for various brightness and separation are as follows:

		Square minus Filar			Linear minus Filar		
		°	″		°	″	
m_A	<5·0	+1·5	−0·01	(2)	+2·0	0·00	(2)
	5·0–7·5, Δm<1	−0·8	+0·01	(10)	−1·5	−0·03	(11)
	5·0–7·5, >1	−1·1	−0·08	(6)	+0·2	−0·08	(4)
	>7·5	+0·5	−0·09	(3)	−0·1	−0·09	(4)
ρ	<0″·75	−1·4	−0·06	(5)	−1·4	−0·06	(5)
	0·75–2·00	+0·7	−0·01	(7)	−0·4	−0·02	(8)
	>2·00	−0·7	−0·04	(9)	−0·4	−0·07	(8)

Position angles and separations are both measured smaller (the opposite result for bright stars being caused by ζ Sgr only). Thus, according to the foregoing, the double image micrometer decreased the personal equations.

The accidental errors of both series of measurements cannot be fairly compared. The mean error of one double-image observation is throughout slightly larger than for the filar micrometer, but this is certainly due to the fact that the 115 observations made are insufficient to gain much experience with the instrument, and that they are made with a magnifying power of about 300 (against 560 before) and under almost continuously unfavourable seeing conditions. Thus it is preferable to list the double-image results separately:

ADS		α	1900+	P	ρ	n
		h		°	"	
11186	Σ 2294	18·12	55·72	98·3	0·90	4
11324	AC 11	22	71	353·0	0·72	6, 5
11353	Σ 2316	24	71	320·0	3·75	4
11483	OΣ 358	33	71	172·8	1·82	4, 3
11950	ζ Sgr	59	71	247·3	0·50	6
—	γ CrA	19·03	71	36·5	2·41	6
12715	Σ 2545	36	72	323·1	3·61	4
13860	π Cap	20·24	71	146·3	3·38	6
14499	ϵ Eql	56	72	285·4	0·79	6
14573	Σ 2744	21·00	71	139·2	1·52	4
14773	δ Eql	12	73	20·4	0·62	2, 1
15007	Σ 2799	26	71	98·0	1·52	6
15313	Σ 2825	44	73	122·9	0·87	2
15596	Σ 2854	22·02	72	82·3	2·10	6
15902	β 172	21	73	325·9	0·55	8
15971	ζ Aqr	26	72	271·2	1·92	10
16145	Σ 2928	37	73	120·0	3·51	4
—	δ PsA	53	73	239·2	4·51	2
16428	OΣ 483	57	73	269·2	0·62	3
16649	β 79	23·15	72	38·9	1·14	6
16850	λ 492	33	73	59·6	0·63	1
16969	107 Aqr	43	72	136·4	6·36	8, 7
17107	Σ 3046	54	72	259·9	3·42	4

It may be concluded that the Muller double image micrometer should not replace the filar micrometer but be employed together with it. The double image instrument yields less observations in a given time than the filar, but gives higher accuracy, especially at distances of, say, 1 to 2·5 times the separation limit of the telescope, over which range the filar measurements are frequently subject to errors. The loss of light by the division in two images is almost compensated by the fact that no field illumination is required.

Munich Observatory:
1955 *December* 14.

References

(1) R. v. d. R. Woolley, K. Gottlieb, G. V. Simonow, *Mem. Commonwealth Obs.* No. 9, 1948.
(2) P. Muller, *J.O.*, **36**, 61, and **37**, 153, 1953-54.
(3) Cf. W. Rabe, *Erg. Hefte A.N.* **12**, No. 3 (1953), and J. Hopmann, *Abh. Sachs. Akad.*, **43**, No. 3, p.24, 1945.
(4) P. Baize, *J.O.*, **33**, 1, 1950.

MEASURES OF DOUBLE STARS AND THEIR SYSTEMATIC ERRORS

F. Schmeidler

(Communicated by R. v. d. R. Woolley

(Received 1956 March 10)

Summary

Measures of double stars made at Mt Stromlo by a filar micrometer and by a double image micrometer of the Muller type are discussed and published. A systematic difference of 1° or 2° in position angle between both micrometers is found. A comparison of filar micrometer measures made by the author at Munich in 1938/39 with modern orbits shows that the position angles are systematically too great for pairs with a separation smaller than 2″. It is concluded that double image micrometer observations are less subject to systematic errors than filar micrometer observations.

---

1. *Purpose and programme of the observations.*—During the author's stay at the Commonwealth Observatory on Mt Stromlo, Canberra, measures of visual double stars were made with the 9-inch Oddie refractor in September 1955. The main purpose of these observations was to gain experiences with the newly constructed double image micrometer of the Muller type rather than to make a contribution to the number of existing series of double star observations.

The double image micrometer was constructed by the workshop of the Commonwealth Observatory, the prism having been sent to Canberra from France. Unfortunately, the only eyepiece available for the micrometer had a comparatively low power of about 300 times. The construction of an eyepiece with higher power was not completed before the author left Mt Stromlo and therefore the present double image micrometer measures are not as accurate as they could be.

A number of double stars within the greatest possible range as to distances, magnitudes and magnitude differences were selected as programme. Altogether 23 pairs were observed for which 45 measures were made by a filar micrometer and 63 measures by the double image micrometer. Observations by filar micrometer were included in the programme, as it was intended to test the results for systematic deviations.

The filar micrometer was the same as that used by W. D. Heintz (**1**); its screw value 29″·718 as determined by Heintz was adopted. For the double image micrometer the theoretical screw value 0″·971 was checked by two independent methods. The first method consisted in estimating the time interval between the passages of both images of any star of high southern declination through the same wire in the field. The second method compared distances of wide pairs as measured by the double image micrometer with measures of the same pairs by the filar micrometer. The following three results were found for the screw value of the double image micrometer

$R = 0''\cdot971 \pm 0''\cdot002$ as theoretical value
$1''\cdot010 \pm 0''\cdot017$ (m.e.) found from time intervals
$0''\cdot938 \pm 0''\cdot019$ (m.e.) found by comparison with filar micrometer measures of wide distances

No plausible explanation for the discrepancy between the two empirical values could be found, although the difference is greater than the mean errors would allow. As the mean of the two empirical values agrees very well with the theoretical value, the latter was definitely used.

The measures by the filar micrometer were made with the eyes parallel or perpendicular to the line joining both stars, whichever position was more convenient. Two different methods were used with the double image micrometer, the four images being arranged either in a square or in a straight line. In most cases, the same pairs were observed in both ways at the same night successively. The author believes that measures with the four images in a straight line are a little more convenient and more accurate, but the number of observations is too small for a definite judgment of this question.

2. *Systematic differences.*—For all stars for which double image micrometer measures were made in both ways, the difference between the results obtained with a square position of the four images (Dq) and those with a linear position (Dl) was formed. The mean difference in the sense Dq minus Dl is

$$\Delta p = -0^\circ\cdot55 \pm 0^\circ\cdot37 \text{ (m.e.)}$$
$$\Delta \rho = +0''\cdot02 \pm 0''\cdot04 \text{ (m.e.)} \qquad (13 \text{ stars})$$

As no difference significantly exceeding the mean error was found, all observations made by the double image micrometer by either method were combined in mean values (D) and compared with the mean values of the filar micrometer results (F) for the same stars. The mean difference F minus D is

$$\Delta p = +2^\circ\cdot37 \pm 0^\circ\cdot70 \text{ (m.e.)}$$
$$\Delta \rho = -0''\cdot06 \pm 0''\cdot03 \text{ (m.e.)} \qquad (15 \text{ stars})$$

The systematic difference in ρ is small enough to be neglected, but there is a remarkable amount Δp in the sense that all position angles measured by the filar micrometer are about 2° too great.

The question arises which of the two micrometers gives the wrong results. A comparison with the results of other observers strongly supported the assumption that the present author measures positon angles systematically too great with the filar micrometer. Some double stars of this programme were also observed by Rabe at Munich and by Heintz at Mt Stromlo (**1**) in 1955; the average differences between the present filar micrometer measures and the results of Rabe and Heintz are

Schmeidler–Rabe	$\Delta p = +2^\circ\cdot0 \pm 0^\circ\cdot62$ (m.e.)	$\Delta \rho = -0''\cdot02 \pm 0\cdot02$ (m.e.)
Schmeidler–Heintz	$+1^\circ\cdot6 \pm 0^\circ\cdot92$ (m.e.)	$-0''\cdot05 \pm 0\cdot02$ (m.e.)

which again indicate a systematic error in position angle.

In order to examine the question more carefully, the observations made by the author in 1938/39 at Munich (**2**) with a filar micrometer were compared with modern orbits. For 48 of the 224 couples contained in the above-mentioned publication orbits were found which agreed satisfactorily with all observations until at least 1940. Any residuals of individual observers against these orbits can therefore be considered as differences between the corresponding observers

and the "average" observer, at least for observations before 1940. The mean values for the 48 pairs were

$$\Delta p = +0^\circ.90 \pm 0^\circ.75 \text{ (m.e.)}$$
$$\Delta \rho = +0''.028 \pm 0''.013 \text{ (m.e.)}$$

in the sense Schmeidler minus average observer. The value of $\Delta\rho$ is neglegible, whereas Δp is again positive, although not much greater than its mean error. If the material is subdivided according to distances, the following results are found

$\rho < 1''$	$\Delta p = +1^\circ.0$	$\Delta\rho = +0''.10$	18 stars
$\rho = 1\text{–}2''$	$+1^\circ.2$	$0''.00$	19 stars
$\rho = 2\text{–}4''$	$-0^\circ.5$	$-0''.06$	5 stars
$\rho > 4''$	$+0^\circ.8$	$-0''.05$	6 stars

which are a clear indication that the position angles of pairs with a separation smaller than 2″ are measured 1° or 2° too great, whereas the observations of the wider pairs are systematically right. A similar result holds for the distances which are generally too great for pairs closer than 1″ and practically correct for wider pairs.

An additional confirmation that the measures made by the author in 1938/39 at Munich are systematically correct for pairs with a separation greater than 2″ can be found by comparison with photographic observations made by Hertzsprung (**3**) and Strand (**4**). After corrections for orbital motion had been applied wherever necessary, the following differences were found

Schmeidler–Hertzsprung	$\Delta p = +0^\circ.2$	$\Delta\rho = -0''.01$	22 pairs
Schmeidler–Strand	$+0.2$	-0.02	26 pairs

which are entirely neglegible. The distances of these pairs are, with very few exceptions, greater than 2″.

3. *Conclusions.*—It seems that the systematic difference of about $+2^\circ$ between the author's filar micrometer and double image micrometer measures of position angles is almost exclusively due to systematic errors of the filar micrometer observations. As the residuals of the Munich observations against modern orbits show a systematic error in position angle which is not much greater than 1°, it is possible that the double image micrometer measures also are subject to a small (negative) systematic error in position angle. The author is, however, inclined to believe that the mentioned discrepancy is due to the uncertainty of the used data and to consider the position angles as measured by the double image micrometer as systematically right.

It appears that double image micrometer observations are systematically more reliable than filar micrometer measures, specially for close pairs. The present discussion shows that it is still interesting to study the systematic errors of double star observations, a problem which has been rather neglected in the last decades.

4. *The observations.*—All individual measures are published. For each pair the usual designation is given and, if existing, also the ADS number. In the next line, the coordinates for 1950 and the magnitudes are given. For each observation, the date, the measured position angle and the measured distance are given; *F* means observations by the filar micrometer, *Dq* and *Dl* observations by the double image micrometer with the four images in a square or in a straight line respectively. For the *F* observations, .. means eyes parallel and : perpendicular to the stars.

Equal weight was given to all observations in combining the mean values. No systematic correction has been applied to the filar micrometer position angles, since the preceding discussion gives no clear result about the exact value of the error. As for most pairs the double image micrometer observations outnumber the filar micrometer measures, the mean of all observations should not be affected much.

The author wants to thank Professor Woolley for allowing him to work with the Oddie refractor. Acknowledgments are also made to Professor Rabe and to Dr Baize for communication of residuals against unpublished or unavailable orbits.

h 5084
$19^h\ 3^m{\cdot}1\ \ -37°\ 8'$; $5^m{\cdot}0\ 5^m{\cdot}0$

	°	″	
1955·694	37·2	2·32	*F* :
697	40·7	2·35	*F* · ·
702	36·6	2·16	*F* :
705	35·7	2·57	*Dq*
716	35·8	2·38	*Dq*
	38·2	2·35	*Dl*
719	36·4	2·28	*Dq*
1955·71	37·2	2·35	7*n*

β 142 = ADS 12469
$19^h\ 25^m{\cdot}4\ \ -12°\ 15'$; $7^m{\cdot}9\ 8^m{\cdot}2$

	°	″	
1955·716	15·1	1·17	*Dq*
	27		*Dl*
730	20	1·08	*F* :
1955·72	20·7	1·12	2, 3*n*

I 117
$19^h\ 27^m{\cdot}7\ \ -60°\ 23'$; $7^m{\cdot}6\ 8^m{\cdot}0$

	°	″	
1955·694	181·4	1·19	*F* :
697	181·5	1·05	*F* :
702	187·2	1·01	*F* · ·
705	177·8	1·22	*Dq*
1955·70	182·0	1·12	4*n*

Σ 2597 = ADS 13104
$19^h\ 52^m{\cdot}6\ \ -6°\ 52'$; $6^m{\cdot}9\ 8^m{\cdot}0$

	°	″	
1955·694	85·6	0·91	*F* · ·
697	82·7	0·71	*F* · ·
702	86·3	0·73	*F* · ·
1955·70	84·9	0·78	3*n*

h 5178
$20^h\ 10^m{\cdot}5\ \ -34°\ 17'$; $6^m{\cdot}9\ 8^m{\cdot}4$

	°	″	
1955·702	12·6	2·43	*F* · ·
705	10·2	2·76	*Dq*
	7·2		*Dl*
719	4·8	2·84	*Dq*
730	9·6	2·59	*F* :
1955·71	8·9	2·66	4, 5*n*

β 60 = ADS 13860
$20^h\ 24^m{\cdot}5\ \ -18°\ 22'$; $5^m{\cdot}1\ 8^m{\cdot}7$

	°	″	
1955·702	150·0	3·16	*F* · ·
705	149·3	3·22	*Dq*
	148·2		*Dl*
716	148·6	3·36	*Dq*
	148·1	3·07	*Dl*
733	148·3	2·96	*F* :
1955·71	148·8	3·15	6, 5*n*

β 151 = ADS 14073
$20^h\ 35^m{\cdot}2\ \ +14°\ 25'$; $4^m{\cdot}0\ 5^m{\cdot}0$

	°	″	
1955·694	23·6	0·65	*F* :
697	18·3	0·4 e	*F* :
733	21	0·45 e	*F* :
1955·71	21·0	0·50	3*n*

Σ 2725 = ADS 14270
$20^h\ 43^m{\cdot}9\ \ +15°\ 43'$; $7^m{\cdot}3\ 8^m{\cdot}0$

	°	″	
1955·697	8·6	5·46	*F* :
716	10·7	5·76	*Dq*
	9·2	5·73	*Dl*
722	4·8	5·61	*F* :
736	9·8	5·84	*Dq*
	7·5	5·53	*Dl*
1955·72	8·4	5·66	6*n*

Rmk 26
$20^h\ 47^m{\cdot}5\ \ -62°\ 37'$; $7^m{\cdot}2\ 7^m{\cdot}5$

	°	″	
1955·694	89·2	2·27	*F* · ·
697	88·8	2·29	*F* · ·
719	84·7	2·28	*Dq*
	84·2	2·30	*Dl*
1955·71	86·7	2·28	4*n*

Σ 2729 = ADS 14360
$20^h\ 48^m{\cdot}8\ \ -5°\ 49'$; $6^m{\cdot}3\ 7^m{\cdot}6$

	°	″	
1955·733	1·2	1·04	*F* :
738	0·1	1·08	*Dq*
	1·1	1·03	*Dl*
1955·74	0·8	1·05	3*n*

Σ 2737 = ADS 14449
$20^h\ 56^m.6$ $+4°\ 6'$; $5^m.7\ 6^m.2$

1955·694	289·9	0·85	*F* · ·
705	290·1	0·96	*Dq*
	285·2	0·79	*Dl*
716	290·5	0·89	*Dq*
	288·4	0·90	*Dl*
722	285·7	0·88	*F* · ·
733	285·5	0·90	*Dq*
	287·2	0·80	*Dl*
738	285·2	0·90	*Dq*
	287·3	0·86	*Dl*
1955·72	287·5	0·87	10*n*

h 5246
$21^h\ 6^m.7$ $-54°\ 49'$; $7^m.9\ 8^m.1$

1955·694	128·8	3·33	*F* · ·
700	129·5	3·06	*F* · ·
1955·70	129·2	3·20	2*n*

OΣ 535 = ADS 14773
$21^h\ 12^m.0$ $+9°\ 48'$; $5^m.3\ 5^m.4$

1955·694	5	0·35 e	*F* :
733	29	0·4 e	*Dl*
1955·71	17	0·38	2*n*

β 766
$21^h\ 21^m.2$ $-41°\ 13'$; $6^m.4\ 7^m.1$

1955·694	277·1	0·68	*F* · ·
722	281·0	0·57	*F* · ·
1955·71	279·0	0·62	2*n*

Σ 2799 = ADS 15007
$21^h\ 26^m.4$ $+10°\ 52'$; $7^m.0\ 7^m.0$

1955·694	280·5	1·27	*F* · ·
716	277·5	1·55	*Dq*
	278·5	1·64	*Dl*
733	279·8	1·62	*F* · ·
	278·6	1·45	*Dq*
738	275·7	1·70	*Dq*
1955·72	278·5	1·54	6*n*

h 5278
$21^h\ 43^m.5$ $-82°\ 57'$; $5^m.5\ 7^m.7$

1955·694	70·2	2·78	*F* · ·
705	64·4	2·50	*Dq*
	66·5	2·90	*Dl*
722	70·8	2·80	*F* · ·
1955·71	68·0	2·74	4*n*

β 172 = ADS 15902
$22^h\ 21^m.5$ $-5°\ 6'$; $6^m.7\ 6^m.7$

1955·716	314·2	0·68	*Dq*
	315·6	0·70	*Dl*
722	328·3	0·6 e	*F* :
733	343	0·6 e	*F* · ·
	314	0·74	*Dq*
	315	0·51	*Dl*
1955·73	321·7	0·64	6*n*

Σ 2909 = ADS 15971
$22^h\ 26^m.2$ $-0°\ 17'$; $4^m.4\ 4^m.6$

1955·702	271·3	2·09	*Dq*
705	269·9	1·86	*Dq*
	270·5	2·00	*Dl*
708	270·2	1·84	*Dq*
	271·0	1·93	*Dl*
716	271·5	1·74	*Dq*
	272·2	1·92	*Dl*
722	273·7	1·98	*F* · ·
733	270·7	1·92	*F* · ·
736	272·7	1·90	*Dq*
	269·6	1·96	*Dl*
1955·72	271·2	1·92	11*n*

Σ 2912 = ADS 15988
$22^h\ 27^m.4$ $+4°\ 11'$; $5^m.8\ 7^m.2$

1955·708	112·9	1·05	*Dl*
722	120·1	1·02	*F* :
733	123·0	0·99	*F* :
736	113·3	1·06	*Dq*
	115·8	0·82	*Dl*
1955·73	117·0	0·99	5*n*

Σ 2944 = ADS 16270
$22^h\ 45^m.3$ $-4°\ 29'$; $7^m.0\ 7^m.5$

1955·722	275·5	2·49	F · ·
733	274·8	2·44	*F* · ·
1955·73	275·2	2·46	2*n*

OΣ 536 = ADS 16417
$22^h\ 56^m.0$ $+9°\ 6'$; $7^m.0\ 7^m.5$

1955·708	191	0·45 e	*Dl*
722	157	0·5 e	*F* :
736	172	0·58	*Dq*
	184	0·51	*Dl*
1955·73	176	0·51	4*n*

β 384 = ADS 16465
$23^h\ 0^m{\cdot}0\ \ -18°\ 49'$; $7^m{\cdot}2\ 9^m{\cdot}2$

1955·708	68°·0	0″·87	*Dl*
716	63·3	1·13	*Dq*
	61·3	1·24	*Dl*
722	67·2	1·05	*F* · ·
1955·72	65·0	1·07	4*n*

Jc 20
$23^h\ 4^m{\cdot}1\ \ -43°\ 47'$; $4^m{\cdot}5\ 7^m{\cdot}0$

1955·705	67°·4	1″·03	*Dq*
	69·1	1·09	*Dl*
722	69·9	1·29	*F* · ·
733	67·0	1·27	*F* :
736	61·7	1·25	*Dq*
	65·6	1·15	*Dl*
1955·72	66·8	1·18	6*n*

Residuals against existing orbits were formed wherever possible. The theoretical values of position angle and distance were taken from Muller's catalogue of ephemerides (**5**). The following residuals in the sense O–C were found :

Star	Δp	$\Delta\rho$	Orbit computed by
	°	″	
h 5084	+2·6	−0·18	Dawson 1924
β 151	+3·1	+0·05	Finsen 1938
Σ 2729	−0·1	−0·01	Baize 1943
Σ 2737	+0·5	−0·01	van den Bos 1933
OΣ 535	−7	+0·02	Luyten 1934
Σ 2909	+1·4	−0·15	Rabe
Σ 2912	0·0	−0·05	van Biesbroeck 1927
OΣ 536	+10	+0·21	van den Bos 1934

Sternwarte München,
Munich, Germany:
1956 *February* 28.

References

(1) W. D. Heintz, *M.N.*, **116,** 248, 1956.
(2) F. Schmeidler, *A.N.*, **270,** 234; *Veröffentl. Sternw. Muenchen Band,* **2,** 7, 1940.
(3) E. Hertzsprung, *B.A.N.*, **9,** 113, 1940.
(3) K. Strand, *A.J.*, **52,** 1, 1946.
(5) M. P. Muller, *J. Obs.*, **36,** 61, 1953 and *J. Obs.*, **37,** 153, 1954.

THE ORBIT OF THE SPECTROSCOPIC BINARY HD 170523

William Buscombe

(Received 1956 February 11)

Summary

Radial velocities have been measured from twenty-four new spectrograms of the giant B-type star δ^2 Telescopii. The orbit has been derived by combining these with eleven observations made in Chile during 1908–17 and three in South Africa during 1952.

The mean velocity of the system is −7·6 km/sec and the velocity amplitude of the primary is 34·9 km/sec, with a minimum semi-major axis of $10{\cdot}2 \times 10^6$ km. The period is $21^d{\cdot}70564$, eccentricity 0·218 and mass-function 0·0891 solar masses.

Introduction and observations.—A three-prism spectrograph has been in use since early in 1954 at the Cassegrain focus of the 30-inch (Reynolds) reflector at the Commonwealth Observatory. The first principal programme is the determination of radial velocities of stars in the Scorpio-Centaurus cluster. At the outset, the observing time has been concentrated on stars brighter than visual magnitude 6·0 with uncertain velocities.

The star HD 170523 (δ^2 Tel), R.A. $18^h\,28^m{\cdot}3$, Dec. $-45^\circ\,48'$ (1950), vis. mag. 5·3, was announced as a spectroscopic binary from two plates obtained in 1908 by the D. O. Mills Expedition of the Lick Observatory at Santiago, Chile (**1**). Additional spectrograms were secured there between 1914 and 1917 (**2**), at Radcliffe Observatory in 1952 (**3**), and at Mount Stromlo in 1954, but the period of velocity variation remained unknown. During 1955 a determined effort yielded 22 additional spectra from which an orbit could be computed.

The observed radial velocities are listed in Table I. Column (1) shows the date and Universal Time. In column 2 is the phase in days, calculated on the basis of the finally adopted period and an arbitrary origin JD 2 435 200·0. The initials in column 3 indicate the observer and spectrograph used, for which a key is given in Table II. The numeral shows the number of prisms. Column 4 shows the mean plate velocity, reduced to the Sun, and column 5 the residual (observed − computed) from the final orbit in km/sec.

The design and operation of the spectrograph on Mount Stromlo will be described subsequently. The straight slit employed is 60 microns wide, corresponding to 15 μ projected on the plate. The star image is transmitted through a rocking plane-parallel glass plate to produce spectra of uniform density across a width of 0·6 mm at the slit. Eastman Kodak emulsion 103a-O was used throughout, developed for 5 minutes in D-19. Experiments on the distortion of emulsions (**4**) led to the adoption of Kodak Tropical Developer after 1955 August 15. Also at this time the exposure time could be reduced from 12 minutes to 6, due to the higher reflectance of freshly aluminized mirrors.

TABLE I

Radial velocity observations of HD 170523

Date (U.T.)			Phase	Observer	Velocity	Residual	Remarks
			d				
1908	July	21·22	5·353	—, L2	−31	+ 4	
	Sept.	7·10	9·822	—, L2	−11	+ 7	
1914	July	31·14	14·003	—, L2	+28	+ 7	
1915	July	27·21	6·078	—, L1	−34	0	
		28·20	7·068	—, L2	−22	+ 8	
		30·21	9·078	—, L1	−22	+ 1	
	Aug.	23·14	11·302	—, L1	− 4	+ 2	
		26·14	14·302	—, L1	+17:	− 7	
		30·10	18·262	—, L1	+18	− 3	
1917	June	5·30	12·293	—, L2	+ 5	− 2	
	Sept.	20·10	10·564	—, L2	− 8	+ 5	
1952	May	12·097	8·173	MF, R2b	−29	− 2	
		22·010	18·086	MF, R2b	+23	− 1	
	Sept.	10·767	21·315	MF, R2c	−11	+ 4	
1954	Aug.	16·437	9·699	AP, St3	−18	+ 1	
		19·508	12·770	WH, St3	− 2	−10	weak comparison
	Sept.	7·734*	10·290	MF, R2b	−18	− 3	
		16·777*	19·333	MF, R2c	+ 9	+ 2	
1955	May	7·729	13·523	HG, St3	+16	+ 1	
	June	1·653	16·742	WB, St3	+37	+ 3	
		7·608	0·991	WB, St3	−21	+ 5	
		10·617	4·000	WB, St3	−30	+ 5	
		11·618	5·001	HG, St3	−32	+ 3	
	July	4·567	6·244	WB, St3	−30	+ 4	
		7·553	9·230	WB, St3	−19	+ 3	
		9·505	11·182	WB, St3	−18	−10	underexposed
		25·484	5·456	AP, St3	−36:	− 1	fogged
	Aug.	1·477	12·449	WB, St3	−30:	−35	underexposed
		3·539	14·511	WH, St3	+15	−11	underexposed
		4·494	15·466	GH, St3	+10	−23	underexposed
		5·445	16·417	AP, St3	+35	0	
		28·451	17·717	WB, St3	+28	+ 1	
	Sept.	1·427	21·693	WB, St3	−32:	−14	overexposed
		4·449	3·010	GH, St3	−34	− 1	
		6·422	4·983	WB, St3	−38	− 3	
		7·442	6·003	HG, St3	−36	− 2	weak comparison
		8·425	6·986	GH, St3	−43	−11	
		10·408	8·969	WH, St3	−24	− 1	
		11·390	9·951	WB, St3	−21:	− 4	underexposed
		29·429	6·284	WB, St3	−35	− 1	

* These additional observations, communicated privately through the kindness of Dr A. D. Thackeray, are not included in Fig. 1.

TABLE II

Observers and Spectrographs

Obs.	Name
WB	W. Buscombe
MF	M. W. Feast
HG	H. Gollnow
GH	G. Hagemann
WH	W. D. Heintz
AP	A. Przybylski

Inst.	Location	Dispersion at Hγ
L1	Lick Obs., Santiago, Chile	37 A/mm.
L2	Lick Obs., Santiago, Chile	20
R2b	Radcliffe Obs., Pretoria, S. Africa	29
R2c	Radcliffe Obs., Pretoria, S. Africa	47
St3	Mount Stromlo, Canberra, Australia	36

The plates were measured on a Hilger long-screw engine with a microscope of 30-power. The reductions are based on the wave-length system developed by Petrie (**5**), with corrections for curvature of the iron-arc comparison lines. Standard-velocity stars are observed nightly; the velocities on 20 plates taken during the period, covered by the observations of the binary star, never departed by more than 2 km/sec from the corresponding values adopted by the International Astronomical Union. On each spectrogram of δ^2 Tel, from seven to twelve absorption lines were measured, depending on quality. The internal probable error of the plate mean velocity is in each case between 3 and 4 km/sec, which corresponds to the scatter from the final orbit. However for the weak plates, for which the velocity is followed by a colon (:) in Table I, the probable errors, due to the scatter of measures from diffuse lines, reach 6 to 9 km/sec.

The derivation of the elements.—From the observations obtained in the winter of 1955, the period was found to be approximately 21 days. Since a number of observations had already been secured 40 years previously, it was possible to determine a provisional period of $21^d{\cdot}707$ graphically by trial and error. However it is seen from Fig. 1 that those early observations fall almost entirely on the rising branch of the velocity curve, and do not delineate the extrema very precisely. The trial period was first adopted, and a graphical solution made by the method of Lehmann-Filhés. These elements were then adjusted by a

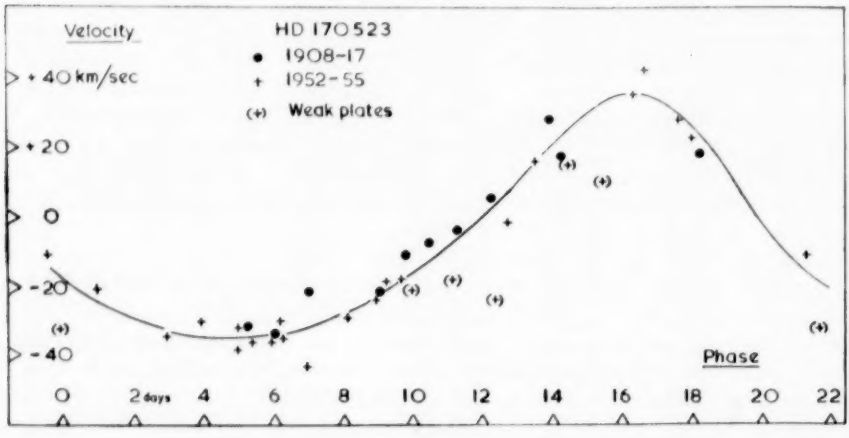

FIG. 1.—*The velocity curve of HD 170523, drawn according to the final elements. The origin of abscissae is taken arbitarily at J.D. 2,435,200·0.*

first least-squares solution based only on the individual observations made in 1955.

To facilitate the computation with a desk electric calculator, the equations of condition were expressed in terms of the Thiele-Innes rectangular coordinates

$$V = \gamma + L\,dX/dM + N\,dY/dM,$$

and

$$\Delta V = \Delta\gamma + \Delta L\, dX/dM + \Delta N\, dY/dM + P_v \Delta e + Q_v n \Delta T + R_v \Delta n,$$

where

$$P_v = L\frac{\partial}{\partial e}\left(\frac{dX}{dM}\right) + N\frac{\partial}{\partial e}\left(\frac{dY}{dM}\right),$$

$$Q_v = -L\frac{\partial}{\partial M}\left(\frac{dX}{dM}\right) - N\frac{\partial}{\partial M}\left(\frac{dX}{dM}\right),$$

$$R_v = -(t-T)Q_v;$$

$$L = 1{\cdot}92 \times 10^{-4} a \sin i \sin\omega,$$

$$N = 1{\cdot}92 \times 10^{-4} a \sin i \cos\omega.$$

The period was held unaltered.

The theory is given by van den Bos (**6**), who has also published tables of X and Y for each degree of the mean anomaly and each step of 0·01 in the eccentricity (**7**). Values of the derivatives (dX/dM and dY/dM) for any eccentricity can be interpolated easily, and the second partial derivatives with respect to eccentricity and anomaly obtained by differencing.

As the early Lick observations showed a mean residual of +6 km/sec from this orbit, it became clear that a slight decrease of the period was necessary. The amount was derived from the slope of the ascending branch of the velocity curve. For computing the final elements, eight normal points were adopted, representing all the observations in groups of from two to five within close intervals of phase. The unweighted normal equations were solved again by least-squares to yield the final elements shown in Table III. The individual residuals are shown in Table I. On many of the plates the density of the continuous background is not sufficient to permit a measurement of the velocity from the K line of Ca II, but from the measures shown it appears likely that the absorption feature is mainly stellar.

TABLE III
Orbital elements

	Preliminary	Adjusted	Final, with Probable Error	
P	21·707 days	21·707	21·70564 ±	0·00005
γ	− 10·0 km/sec	− 13·3	− 7·6	0·15
K_1	40·0 km/sec	34·0	34·9	0·3
L	+ 238·4 km/sec	+ 340·2	+ 429·9	8·7
N	+2171·0 km/sec	+1756·6	+1915·6	30·2
T-J.D.2435200	16·60 days	17·0958	16·6688	0·055
e	0·302	0·401	0·218	0·023
ω	6·26°	10·96	12·65	0·5
$a_1 \sin i$	$11{\cdot}4 \times 10^6$ km	9·3	10·2 (0·068 a.u.)	0·08
$f(m)$			0·0891 $\odot$	0·0021

Discussion.—By comparison with spectrograms exposed with the same equipment of standard stars in the MK system (**8**), the spectral class of HD 170523 is approximately B6 II-III. The hydrogen lines are always more diffuse at the phase six days, i.e. at maximum velocity of approach. Blaauw (**9**) lists it as a doubtful member of the Scorpio-Centaurus cluster, and in fact at

the probable distance of 1400 parsecs, this star would be far beyond the utmost extent of the cluster, whose known members are almost exclusively main-sequence stars.

The absolute (visual) magnitude of $-3{\cdot}5$: corresponds with that derived statistically from the assumption that the star's proper motion is purely a reflection of the solar motion. The corresponding mass of the primary from the mass-luminosity relation would be about 16 times the Sun's. Since no trace of the companion can be seen visually or spectroscopically, it must be at least a magnitude fainter, with a maximum mass of $8\odot$. If in the equation $f(m)=0{\cdot}0891\odot$ we insert the minimum value of $m_1/m_2=2$, we find that the least possible inclination is $i=29^\circ$, so that the maximum length of the semi-major axis is $a_1=21\times10^6$ km ($0{\cdot}14$ a.u.). A smaller value of the inclination could only occur if *both* components depart from the mass-luminosity relation.

On the other hand, any larger value of $i>29^\circ$ could be made consistent with the primary's mass and luminosity if we are willing to accept a larger value of the mass-ratio (i.e. a greater difference in magnitude of the two stars). The maximum value of the mass-ratio, in the case where $i=90^\circ$, is $m_1/m_2=5$. If the inclination is high, and the companion an A-type giant or main-sequence star, the chance of detecting it even from infra-red spectra would be very slight.

Detailed photometric studies have not been made, which would exclude the possibility of a shallow eclipse. However, from the absence of a deep eclipse, it is reasonable to infer that the inclination is not near 90°, as the radius of the primary component forms a large fraction of the radius of the relative orbit. Hence it appears probable that the mass of the secondary component is between four and eight times the Sun's.

Acknowledgments.—It is a pleasure to thank Professor Woolley and Dr Eggen for advice on the Thiele-Innes method, of which no previous application to exclusively spectrographic observations seems to have been published. I am also grateful for the helpful interest of Dr Gollnow throughout the work and for the share taken in the observing by Drs Hagemann, Heintz (of Munich) and Przybylski.

Commonwealth Observatory,
Canberra:
1956 *January* 12.

References

(1) H. D. Curtis, *Lick Obs. Bull.*, **5**, 140, 1909.
(2) W. W. Campbell *et al.*, *Lick Obs. Publ.*, **16**, 270, 1928.
(3) M. W. Feast *et al.*, *Mem. R.A.S.*, **67**, 67, 1955.
(4) H. Gollnow and G. Hagemann, *A.J.*, **61**, 1956 (in press).
(5) R. M. Petrie, *Publ. Dom. Astrophys. Obs.*, **9**, 297, 1953.
(6) W. H. van den Bos, *Union Obs. Circ.*, **68**, 354, 1926.
(7) *Ibid.*, **71**, 391, 1926.
(8) H. L. Johnson and W. W. Morgan, *Ap. J.*, **117**, 313, 1953.
(9) A. Blaauw, *Publ. Kapteyn Astr. Lab.*, Groningen, No. 52, 1946.

STELLAR PARALLAXES DETERMINED AT MILL HILL (THIRD LIST)

University of London Observatory

(Communicated by the Director)

(Received 1955 December 28)

The following is the third list of relative parallaxes determined with the Radcliffe 24-inch photographic refractor; the earlier lists were published in (**1**), (**2**). In the second list there was a mis-identification pointed out to us by the Naval Observatory at San Fernando, viz. the star No. 15 on that list was *A.C.* -6° 3939–98 and not *A.C.* -6° 3939–101.

There has been a noticeable deterioration in the quality of images on plates taken in recent years which is probably due to a small relative movement of the two components of the Radcliffe 24-inch lens. It is thought that this has had an adverse effect on the accuracy of the more recent parallax determinations and for this reason the measurements are being terminated with the list published in this paper. The mounting and performance of the lens is now under investigation.

All stars in the present list except No. 15 were taken from our first parallax programme. The results for two of the stars (Nos. 15 and 17),were obtained by measuring the plates with a recording microphotometer, as described by Kiang in (**3**). No. 17 was also measured with our usual measuring microscope, and the result, $\pi = 0''{\cdot}003 \pm 0''{\cdot}022$ was obtained. The very large probable errors obtained in both measurements were due, at least in part, to the fact that the comparison stars were very unsymmetrically placed; they were situated at three corners of a square surrounding the star.

All stars were photographed for at least six epochs. More specifically Nos. 11, 16, 17 were photographed for six epochs, Nos. 2, 3, 4, 5, 6, 8, 10, 12, 14 for seven, Nos. 1, 7, 13, 15 for eight, and No. 9 for nine epochs. Two exposures were made on each plate and an average of 4·5 plates per epoch was obtained. Most of the plates were taken between 1946 and 1951 inclusive. Nos. 1, 13, 16 each had an early epoch in 1939, and Nos. 15, 17 each had two late epochs in 1953 and 1954.

Details of exposures, types of plates, and reference plates were the same as before (**2**).

The photography was carried out by Mr C. C. L. Gregory, Dr E. M. Burbidge, Miss A. C. Robinson, Dr G. R. Burbidge, Mr R. W. Pring, Mr S. K. Wang, Mr T. Kiang and Professor C. W. Allen. Twelve stars were measured by Mr S. K. Wang and Mr T. Kiang, the remaining five by Mrs G. de Vaucouleurs, Miss A. C. Robinson, and Mr C. C. L. Gregory.

In the list, the second column gives the designation of each star. Radcliffe numbers give the number of the selected area followed by the Durchmusterung number, and are taken from the list of stars with proper motions exceeding $0''{\cdot}100$ in the Radcliffe Catalogue of Proper Motions, p. xl; Yale numbers refer to the 1935 General Catalogue of Stellar Parallaxes. The third column gives the approximate visual and photographic magnitudes. These, and also the spectral types, are taken from various sources and should be regarded as provisional only. Two values of the annual proper motion in R.A. are given, the first being a catalogue value and absolute (as are also the proper motions in declination;) the second value

is derived from the parallax plates and is relative; the average difference between this and the catalogue value is $\pm 0''.020$. The probable errors of unit exposure were divided by $\sqrt{2}$ to give the probable errors of unit plate, which are shown in the eighth column. In the last column the upper value refers to the parallax and the lower to the proper motion in R.A.

No.	Designation and B.D. or *A.C.* No.	Mag. Vis. Phot.	Spec. Type	R.A. Dec. 1900·0	Proper Motion (Unit = 0″·001) R.A.	Proper Motion (Unit = 0″·001) Dec.	P.E. Unit Wt.	Parallax	P.E.
				h m s					
1	Radcl. 68·384	..	G3d	0 10 54	− 2	−156	40	0*	13
	15° 27	10·8		+15° 43′	+ 3				3
2	Radcl. 22·752	..	G	2 39 57	+104	−113	25	+ 9*	5
	44° 574	10·6		+45° 11′	+118				4
3		..	M2	3 06 30	+380	+306	34	+87	7
	A.C. +79° 1584	12·6		+79° 34′	+381				4
4	Camb. IIIc, 67	8·3	G9	3 25 14	+307	−117	42	+29	10
	43° 744	9·3		+43° 20′	+283				6
5	Yale 1364	6·4	F8	4 19 55	+109	− 29	39	+34*	9
	15° 621	7·0		+15° 43′	+115				6
6	Yale 1567	var.	G5	4 54 30	− 30	0	42	+ 3	8
	39° 1138			+39° 49′	− 23				7
7	Radcl. 75.—	..	..	7 12 57	+ 91	−150	34	− 2*	8
	15° 1535	10·8		+15° 12′	+105				6
8	McC. 120·25	11·4	K0	8 42 54	+ 67	−148	34	+10*	7
	A.C. +29° 26176	12·5		+28° 53′	+ 78				6
9		11·0	A5	9 43 10	+ 2	−208	33	−11	7
	44° 1910	11·2		+44° 46′	− 1				3
10	Yale 3526	var.	A2	11 32 12	− 10	−130	33	0	9
	68° 652			+67° 53′	− 3				8
11	SW Dra	var.	F4	12 12 48	− 40	− 10	35	− 7	8
				+70° 4′	+ 15				7
12	Radcl. 57·192	9·0	G2	13 03 52	+196	− 78	36	+24*	9
	30° 2371	9·6		+29° 55′	+265				6
13	Yale 4495	10·1	K6	15 03 06	−826	+490	37	+58	9
	25° 2874			+25° 18′	−891				4
14	Yale 5071	4·8	F5	16 55 29	+247	+ 49	32	+28	9
	65° 1157	5·4		+65° 17′	+220				3
15	Yale 6323	10·0		20 28 00	+300	+300	52	+26†	12
	32° 3853			+32° 40′	+301				5
16	Camb. VIIa, 7		K2	21 58 56	+150	+140	32	−11*	11
		11·8		+59° 06′	+151				2
17	HD 5223	8·8	R3	00 48 54	+138	0	56	+19†	19
	23° 123			+23° 32′	+ 93				6

* No previous determination of parallax.
† Measured with a microphotometer

University of London Observatory,
Mill Hill Park:
1955 *December* 21.

References

(1) University of London Observatory, *M.N.*, **109**, 478, 1949.
(2) University of London Observatory, *M.N.*, **110**, 618, 1950.
(3) T. Kiang, *The Observatory*, **75**, 227, 1955.

IONIZED AND NEUTRAL CALCIUM IN THE ATMOSPHERES OF THE CEPHEIDS η AQUILAE AND ζ GEMINORUM

W. N. Abbott

(Communicated by F. J. M. Stratton)

(Received 1955 November 7)*

Summary

The equivalent widths of the ionized calcium H and K doublet and of the neutral calcium singlet at λ 4227 in the spectra of these two Cepheids have been measured in relation to the phase of the light variation. To render this possible, certain simplifying assumptions were necessary. Abundances of Ca I and Ca II as well as ionization temperatures in the atmospheres of these variables in relation to phase are derived. Gas-pressures permit, through the application of the perfect-gas formula, the computation of the values of the specific volume of the calcium atmosphere which is indicative of the general behaviour of the atmospheres of these stars in the course of their cycle. Results show a difference of phase existing between the general, photospheric, pulsation and the volume variations of the atmospheres of the Cepheids.

---

1. *Material.*—The spectrograms for this investigation of the variations of the equivalent widths, W_i, of the ionized calcium lines H and K, and of the neutral calcium line λ4227 (W_n), in the spectra of η Aql and ζ Gem were as follows. In the case of η Aql spectrograms were obtained at Ann Arbor with the 37-inch reflector, equipped with the Cassegrain two-prism spectrograph (24-inch camera), of the University of Michigan giving a dispersion of 12·8 A/mm at 4000 A. The plates used were IIa-O Kodak, and exposures depended on phase, the region of the spectrum, and seeing. The slit was open at 0·04 mm, and the plates were calibrated with the calibration spectrograph of the Observatory recently adjusted and equipped with a double-wedge slit. The spectrograms were very carefully developed, tracings were made with the MacMath–Hulbert deflection microphotometer, and results were, in general, satisfactory, although occasional poor seeing due to the position of the star, early evening hours and local conditions constituted a handicap. The spectrograms of ζ Gem, on the other hand, are Mt Wilson plates of a higher quality in all respects, taken with the coudé grating-spectrograph of the 100-inch at a dispersion of 2·9 A/mm. We took tracings of these with the Mt Wilson deflection microphotometer at Pasadena; after careful examination a number of plates of both groups were discarded as unsuitable, and those used, eight for η Aql and ten for ζ Gem, are given in Table I.

The equivalent widths W_i (the sum of the equivalent widths of the ionized calcium H and K lines) and W_n (of the neutral calcium line λ4227) were measured on these plates with the object of acquiring the maximum possible information on the respective abundances of these calcium ions and atoms, as well as on other physical data, such as ionization temperatures, gas pressures, and specific volumes in the calcium atmospheres in relation to phase.

* Received in original form 1955 May 19.

TABLE I

η Aql					ζ Gem				
Pl. No. R	Date*		Ph.	Sp.	Pl. No. Ce	Date*		Ph.	Sp.
19686 A	52 Oct.	10	0·06	cF3p	2301	42 Apr.	18	0·16	cF9p
19675 A	52 Sept.	28	·19		2263	40 Feb.	19	·30	
19677 A	52 Sept.	29	·33		2722	42 Jan.	30	·41	
19690 B	52 Oct.	8	·64	cG4p	2724	42 Jan.	31	·51	
19659 A	52 Sept.	25	·76		2764	42 Apr.	2	·51	cGop
19696 A	52 Oct.	9	·78		2742	42 Mar.	4	·66	
19664 B	52 Sept.	26	·91		2977	43 Mar.	25	·67	
19683 B	52 Oct.	3	0·92	cF4p	2980	43 Mar.	26	·77	
					2707	42 Jan.	4	·85	
					2988	42 Mar.	28	0·91	cF9p

* The decimal fraction of the date is about +0·8 for mid-exposure.

2. *The* λ 4227 *line.*—This resonance singlet is the first member of the principal series of the singlet system of the Ca I atom and its study presents no difficulty. Although small, the variations of W_n were easily measurable.

3. *The Ca* II *doublet.*—This resonance doublet, being the first member of the principal series, arises in absorption through the transition of this potassium-like ion from ground level, 4^2S to 4^2P. The wave-number interval between the two components is 223 cm^{-1}. The duplicity of the P level gives these two lines, $4^2S_{1/2} \rightarrow 4^2P_{3/2}$ and $4^2S_{1/2} \rightarrow 4^2P_{1/2}$, the shortward one $4^2S_{1/2} \rightarrow 4^2P_{3/2}$ being more intense, and in the doublet energy levels of atomic systems containing but one valence electron the fine-structure level, $j = 1 - \frac{1}{2}$ generally lies deeper than the corresponding level $j = 1 + \frac{1}{2}$. Between levels 4^2S and 4^2P there lies in the calcium ion a metastable level, 3^2D, from which allowed transitions to 4^2D give, in absorption, the infra-red triplet λ 8662, very pronounced in the Sun and probably so in the classical Cepheids if we could explore that region; unfortunately we are restricted to the H, K doublet, and information on the Ca II ion and its abundance may be gained only through measurements of the W values of these lines. A formidable obstacle to such measurements, however, especially to precise absolute measurements, constitutes the very heavy blending of this region in these spectral classes. Hundreds of metallic lines of atoms and ions crowd this area and in assigning the contours of H and K we have made due allowance for the W of the blends. The systematic errors, important in the case of research on the absolute values of W, are in our case unimportant, as we are interested in the variations of W as a function of phase and not in the absolute W values themselves.

4. *Assumptions.*—Short of abandoning the problem altogether we have made the following working assumptions:

(*a*) The contours of H and K are assumed to be exact provided they do not cut the line of zero intensity. If they do so they are discarded as useless; no correction is made on the reduced contours even if they merely touch the zero line. The effect of instrumental scattering is therefore neglected. In the case of the Ann Arbor plates, instrumental scattering cannot but be negligible; the Mt Wilson plates are more affected by it and the contours of the ζ Gem lines are markedly less deep than the contours of the η Aql lines.

(*b*) As the blends are fine and belong both to atoms and ions, the resulting variation of their total W, or ΣW within the region of H and K as a function of phase may be assumed $\int dW = 0$ for all practical purposes. The dW are of the order of $\pm$0·01 A while the variation of H and K is of the order of 10 A.

(*c*) The non-systematic errors made under the above assumptions (*a*) and (*b*) are no greater than, but are of the order of, errors resulting from measurements on curves, the use of a slide rule, plotting, tracing, reducing, and, in general, errors of approximation.

5. *The Hε line.*—This blend comes under assumption (*b*) as the variations of its equivalent width cannot exceed ±0·03 A; and these are probably balanced by the contrary variations of other blends.

6. *Continuum.*—Placing the continuum may, especially in cases like this, be a highly controversial undertaking. Wherever we place it, however, it is important to keep it there all along. The highest-peak method gives a continuum which is too low, as the actual continuum certainly lies a good deal above the peaks of the microphotometer tracing, its actual location being to all practical purposes unknown. The highest-peak method offers nevertheless the advantage of supplying a conventional continuum which is solidly anchored. As the spectral classes of these stars are G and F we assume that we may advantageously, if not decisively, check the continuum thus obtained by comparing it with the continuum of the Utrecht *Atlas*. Line 100 of this *Atlas* was taken as the continuous background; if A_c is our continuum intensity, A the intensity of a point on our spectrum, and U_c and U are, respectively, the Utrecht continuum intensity and our intensity at the same point, we have:

$$\frac{1}{A_c}\int_{\lambda_1}^{\lambda_2} A\,d\lambda = \frac{1}{U_c}\int_{\lambda_1}^{\lambda_2} U\,d\lambda; \qquad A_c = U_c \frac{\int_{\lambda_1}^{\lambda_2} A\,d\lambda}{\int_{\lambda_1}^{\lambda_2} U\,d\lambda}.$$

The agreement for the two sets of spectrograms is satisfactory.

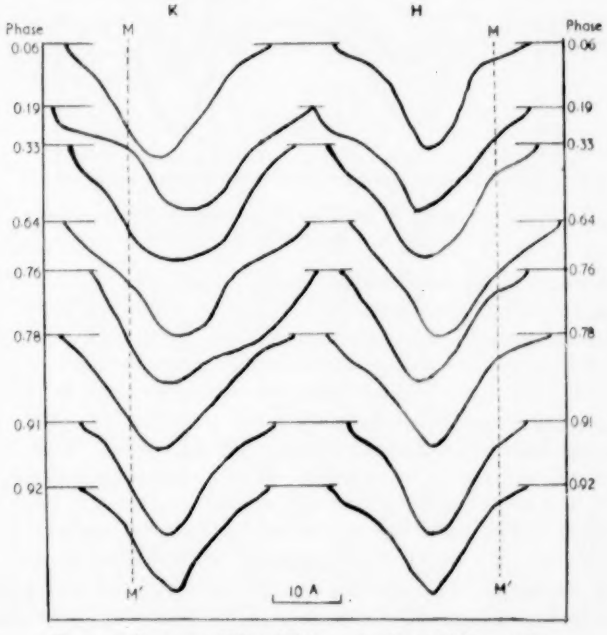

FIG. 1.—*Contours of* H *and* K *in η Aquilae at different phases. (The vertical lines are metallic lines of reference.)*

7. *Profiles.*—The profiles of H and K for the two stars resulting from the reduction of the tracings by means of the characteristic curves are shown in Figs. 1 and 2. The variation of their contours as a function of phase is very similar for both stars and will be discussed more at length in a subsequent paragraph.

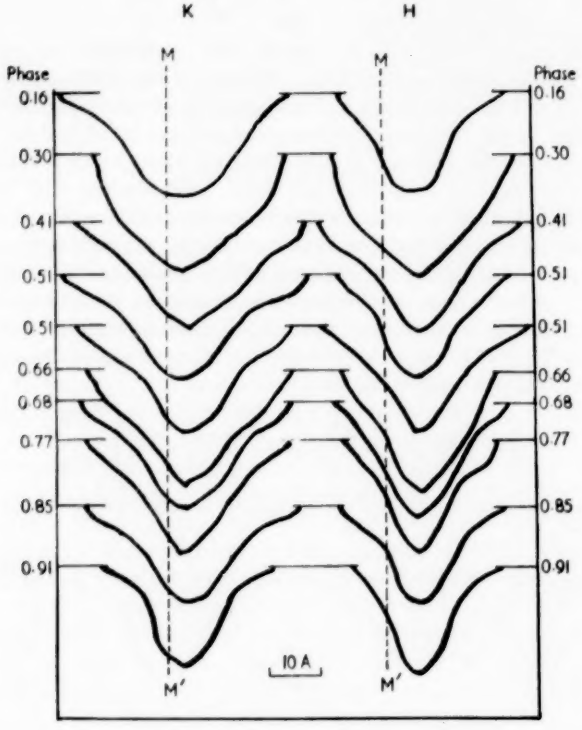

FIG. 2.—*Contours of* H *and* K *in* ζ *Geminorum at different phases. (The vertical lines are metallic lines of reference.)*

8. *W-values.*—These were derived in the usual way: areas of the contours were measured with a planimeter and $W = S/A_c$ values for H and K and for λ4227 are tabulated in Table II and plotted in Fig. 3; the scattering of the points is comparatively small and mean curves illustrating the mode of variation of W_i and W_n may be easily traced. The two different values of W_i of ζ Gem at phase 0·51 may give an idea of the mean error, provided the differences are not real and due to different conditions in two different cycles. The mean error is for η Aql ± 1·3 A and for ζ Gem ± 0·8 A. In Fig. 3 the light curve of η Aql is by Wylie (**1**) and of ζ Gem by Harris (**2**), whom we thank for his collaboration on this occasion. The radial velocity curves are both by Jacobsen (**3**).

9. *Abundances.*—To derive the abundances of Ca II from W_i values we used the curve of growth for the Schuster–Schwarzschild model and pure radiation damping for the line K (3933 A) which Aller (**4**) has computed, with pure radiation damping absorption coefficient $a = 0{\cdot}0287$ and oscillator strength value

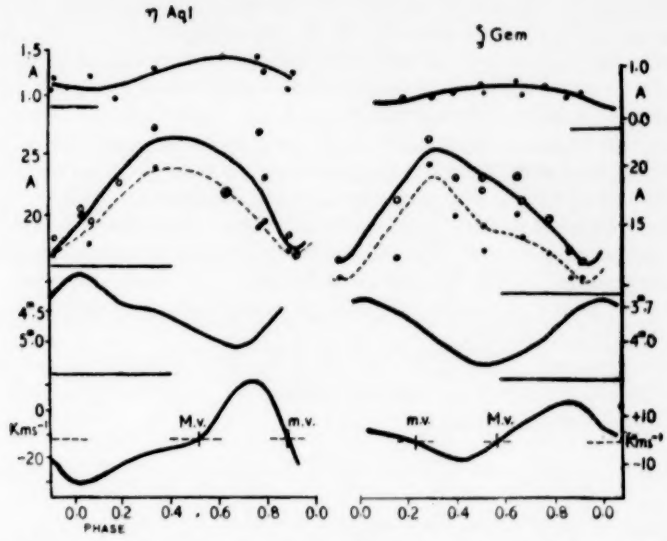

FIG. 3.—*Variation of the W values of λ 4227 and of* H (*dotted*), *and* K (*full*) *with phase for η Aquilae and λ Geminorum* (*higher curves*).
Middle curves are light curves.
Lower curves are radial velocity curves.

$f = 2/3 \times 1{\cdot}19$. To simplify things we used the same curve of growth for the λ4227 line and the values of $\log N_i$ and $\log N_n$ thus derived are tabulated in Table II (columns 4 and 5). The lower W_i values and the resulting lower N_i values for ζ Gem are probably real.

TABLE II

Ph.	log W_i	log W_n	log N_i	log N_n	log P_e	log P_g	T deg. K	5040/T	V 10^7 cm³
η Aql									
0·06	1·568	0·087	19·95	17·05	0·30	3·68	5,200	0·97	8·9
·19	1·624	− ·042	20·07	16·80	·18	3·45	5,400	0·93	15·9
·33	1·708	·134	20·24	17·14	·03	3·43	5,100	0·99	15·8
·64	1·644	·170	20·10	17·22	− ·52	3·00	4,600	1·1	38·2
·76	1·653	·179	20·13	17·25	− ·12	3·26	4,800	1·05	22·0
·78	1·634	·170	20·08	17·22	− ·10	3·38	4,900	1·03	17·0
·91	1·545	·046	19·88	16·97	·33	3·80	5,030	1·0	6·7
0·92	1·519	0·152	19·85	17·20	0·33	3·78	5,100	0·99	7·0
ζ Gem									
·16	1·463	−0·409	19·75	16·06	0·28	3·43	5,700	0·89	17·5
0·30	1·634	− ·252	20·08	16·38	·23	3·44	5,600	0·90	16·5
·41	1·544	− ·143	19·88	16·61	− ·02	3·37	5,200	0·97	18·4
·51	1·506	− ·194	19·83	16·52	− ·23	3·18	5,040	1·00	28·0
·51	1·519	− ·104	19·85	16·67	− ·23	3·18	4,940	1·02	27·0
·66	1·532	− ·060	19·90	16·75	− ·52	3·00	4,670	1·08	39·0
·68	1·478	− ·222	19·77	16·45	− ·52	2·95	4,800	1·05	43·3
·77	1·449	− ·137	19·73	16·54	− ·12	3·31	5,000	1·01	20·4
·85	1·381	− ·284	19·60	16·33	·13	3·52	5,140	0·98	13·0
0·91	1·362	−0·244	19·56	16·42	−0·33	3·68	5,340	0·95	9·3

10. *Electron pressures.*—M. and B. Schwarzschild and W. S. Adams have given values of the electron pressures in the reversing layer of η Aql (**5**) derived by an ingenious if a rather indirect method, by comparing metal abundances in the Sun to metal abundances in η Aql and using rather freely the method of least squares. Relative values are given by them of $\log P_e/P_e\odot$. We used their relation and by taking $P_e\odot = 1{\cdot}48$ dyne cm^{-2} we derived P_e values for the calcium atmosphere which to all practical purposes are the same for the reversing layer. The same values of P_e were assumed for the calcium atmosphere of ζ Gem. The calcium lines are probably formed higher in the atmosphere than the neutral Fe lines but we may assume that the increase in degree of ionization is approximately compensated by the diminution of the density, at least within the practical limits of error of this research. Under this assumption the values of $\log P_e$ are given in Table II, column 6.

11. *Temperatures.*—The Saha formula was used to derive the temperatures from the abundances and the electron pressures; thus for each phase of the cycle of light variation we have:

$$\log N_i - \log N_n + \log P_e = -\frac{5040}{T} J + 2{\cdot}5 \log T - 0{\cdot}48 + \log 2B_i/B_n \qquad (J = 6{\cdot}09 \text{ ev})$$

The ratio of the partition functions was assumed $B_i/B_n = 1{\cdot}0$, and we have for the temperatures:

$$\frac{\log N_i - \log N_n + \log P_e + 0{\cdot}28}{2{\cdot}5} + \frac{12250}{T} = \log T.$$

The temperatures were derived by a graphical method and their values as a function of phase are tabulated in Table II, column 8. Thus we see that ζ Gem has higher ionization temperatures all along the cycle than η Aql. Maximum temperature for both stars, in the calcium atmosphere which is formed of the mean and higher layers, is at phase 0·15 to 0·20 instead of 0·00, and minimum ionization temperature is at phase 0·65; this is indicative of a certain independence of ionization temperature from surface temperature, as minimum light or minimum surface temperature of η Aql is at phase 0·7 while for ζ Gem it is at phase 0·5, the light curve of this star being almost perfectly symmetrical. The temperature curves have a steeper descending branch than the ascending one and the respective gradients are:

η Aql $\Delta T/\Delta t = -200$ K for $\Delta t = 0{\cdot}10$ phase
ζ Gem $\Delta T/\Delta t = +226$ K

on the descending branch, and:

η Aql $\Delta T/\Delta t = -145$ K
ζ Gem $\Delta T/\Delta t = +233$

on the ascending.

As the use of the Saha formula is based on the assumption of thermodynamical equilibrium, the ionization temperatures derived therefrom may legitimately be considered as being the actual thermodynamical temperatures of the atmosphere at these levels, such temperatures being defined by the Maxwellian distribution relation:

$$\xi_0 = \sqrt{2\frac{k}{m}T}.$$

12. *Gas pressures.*—By using Aller's relation (6) between electron pressure, temperature, and gas pressure we derive for each phase the gas pressure, P_g, at the calcium level. Values of $\log P_g$ in dyne cm^{-2} are tabulated in Table II, column 7.

13. *Specific volume.*—As we have assumed the existence of thermodynamical equilibrium we may consistently associate T and P_g through the perfect-gas formula; and we have for the specific volume of the calcium atmosphere which we assume to be representative of the medium-to-high atmosphere of these supergiants:

$$V = \frac{T}{P_g}\mathscr{R} \quad (\mathscr{R} = 8{\cdot}31 \times 10^7 \text{ erg mole deg}).$$

These values of the specific volume are contained in column 10 of Table II and are plotted in Fig. 4. The full curve shows the variation of the specific volume of the calcium atmosphere with phase for η Aql, and the broken curve for ζ Gem.

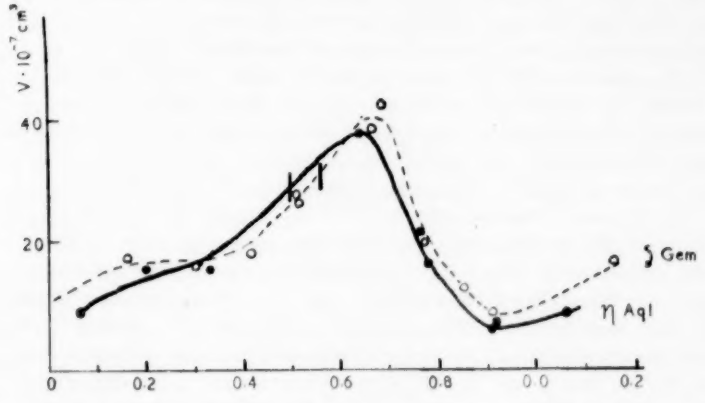

FIG. 4.—*Variation of the specific volume of the calcium atmosphere with the phase for* η *Aquilae and* ζ *Geminorum.*

The vertical dashes locate the phase of maximum volume of the pulsating photosphere resulting from the radial velocities as deduced from the metallic lines. Apart from cycle peculiarities there is a very marked difference of phase between maximum star-volume and maximum volume of the calcium atmosphere, the dynamics of which may definitely be assumed to be the dynamics of the higher atmosphere. This assumption together with the mode of variation V is, if not conclusive, at least indicative that this difference in phase of maximum volumes, photospheric and atmospheric (which is about $\pi/3{\cdot}65$ for η Aql, and $\pi/4$ for ζ Gem), is real, the maximum atmospheric volume following by these quantities the maximum photospheric volume.

Working with the metallic lines on the lower atmosphere the Schwarzschilds (5) find that, while the pulsation of the photosphere has the characteristics of a wave which is neither standing nor progressive but intermediate between the two, the pulsation of the higher atmosphere has the characteristics of a progressive wave. These results are interesting in the light of our measurements, notwithstanding the doubts which may exist as to the validity of some of the Schwarzschilds' assumptions.

14. *Asymmetries of the lines.*—Figs. 1 and 2 show that the profiles of H and K present asymmetries slightly after maximum equivalent width, at least in the case of η Aql. The theory of the influence of a moving atmosphere on the line profiles developed by Miss Underhill (**7**) is not applicable to H and K as this would imply velocities of the order of 1,000 km sec^{-1} which is impossible. The condition of existence of the star fixes an upper limit to velocities in radial motion of the material. The velocities cannot exceed for any length of time the critical velocity, otherwise gravitational disintegration of the star would be unavoidable. There is therefore a relation

$$v_r < \sqrt{2GM/R}$$

which links radial motion to the potential; a pulsating star is less stable at maximum volume than at minimum volume, since, the potential being lower, the condition of disintegration is less remote.

15. *Fluctuations in the position of the* H, K *lines.*—Such fluctuations in the position of H and K as compared to the metallic lines as are suggested by Fig. 1 and 2 where the lines marked M-M′ are metallic lines of reference, are not very convincing and may be due to the variation of the depths and intensities of the lines.

16. *Conclusion.*—The variation of the equivalent widths of the Ca II and Ca I lines reveals the variation of the abundances of ionized and neutral calcium in the atmospheres of η Aql and ζ Gem, two Cepheids of different optical characteristics but physically very much alike. By using the Saha formula and assuming thermodynamical equilibrium we derive the temperatures in relation to the phase, and their variation reveals a certain independence of surface temperature. By associating these temperatures with the gas pressures, derived from available electron pressures by means of the perfect gas relation, we obtain the specific volumes of the calcium atmosphere and its variations related to phase. A difference in phase amounting to about $\pi/3{\cdot}65$ for η Aql and to $\pi/4$ for ζ Gem between the volume variation of the atmosphere and the pulsation of the photosphere and reversing layer is rendered very obvious. The asymmetries of the contours of H and K at maximum W, and certain apparent oscillations of the centre of the lines compared to the metallic lines, would be, if real, subjects open to further investigation.

Acknowledgments.—I wish to express my thanks to Dr L. Goldberg for making available to me the facilities of the Observatory of the University of Michigan, to Dr D. McLaughlin for his assistance, and to Dr I. Bowen and Dr W. S. Adams for making available to me the facilities of the Mt Wilson and Palomar Observatories in Pasadena. I likewise thank the Committee of the Fulbright–Smith–Mundt Fund for their grant.

Athens:
1955 *April* 20.

References

(1) C. C. Wylie, *Ap. J.*, **56**, 217, 1923.
(2) D. Harris III, *Ap. J.*, **118**, 346, 1953.
(3) T. S. Jacobsen, *L.O.B.*, **12**, 138, 1926.
(4) L. Aller, *Astrophysics*, 1953, Ronald Press, p. 289.
(5) M. and B. Schwarzschild *et al.*, *Ap. J.*, **108**, 207, 1948.
(6) L. Aller, *Astrophysics*, 1953, Ronald Press, pp. 91, 223.
(7) A. B. Underhill, *Ap. J.*, **106**, 128, 1947.

EQUIVALENT WIDTHS OF THE *K* LINE

Antoinette de Vaucouleurs

(Communicated by the Commonwealth Astronomer)

(Received 1955 December 30)

Summary

Determinations of the equivalent widths of the *K* line were made for 46 stars of spectral types ranging from A0 to M3. The observations are compared with the theoretical gradient—equivalent width relation for radiative models computed by Przybylski. Comparisons are also made with the results of other observers and it appears that the equivalent width of the *K* line is fairly constant for stars later than type K0.

Determinations of the equivalent widths of the *K* line were made for 46 stars of spectral types ranging from A0 to M3. The plates were those taken with an objective-prism telescope of four inches aperture for the monochromatic magnitudes programme of Woolley, Gascoigne and de Vaucouleurs (**1**). The dispersion was 212 A/mm at *K*.

Additional material, obtained with the same equipment, was provided recently by Dr Heintz; from this were selected late-type stars (F6 to M3) taken with a longer exposure on 103a-E plates and for which the density in the *K* line region is more adequate.

The spectra were recorded partly with the Leeds and Northrup microphotometer of the National Standards Laboratory (Sydney) and partly with the new Hilger microphotometer now in use at the Observatory. The enlargements of the tracings were $\times 42$ and $\times 61{\cdot}5$ respectively. For each plate at least four spectra of a star taken with sectors varying by steps of 0·5 magnitude were recorded for calibration.

Most of the densities used for the contours were on the straight part of the characteristic curves but for some late-type stars the density at the centre of the *K* line was too small for accurate measurements. To this source of error is added the usual difficulty of drawing the continuous background and the wings of the lines.

The contours were drawn for values of I/I_0 at intervals of 0·03 or 0·04, where I is the intensity of any point along the line and I_0 the intensity of the continuum. The two wings were integrated separately at $I/I_0 = 0{\cdot}95$, 0·85, 0·75, etc., along a smooth curve through the points.

Table I gives the name of the star, its MKK spectral type and luminosity (or that given by Miss Woods in her catalogue of southern stars (**2**)), the Stromlo or Greenwich gradients (when in parentheses the interpolated value corresponding to the spectral type was used), the equivalent width in angströms with its mean error, and $\log EW$. The weights are the number of spectra measured (on two plates or more).

On Fig. 1 the logarithms of the equivalent widths were plotted against the relative gradients. Open circles represent supergiant stars and though their scatter, especially for F and G type stars, is rather high, they were included in the mean curve. On this figure is also shown the theoretical gradient–equivalent

TABLE I

Star	Spectral Type	Gradient	E.W. in A	Mean error	log *EW*	(Weight)
γ Cent	Ao III	−0·03	1·26	±0·06	0·100	3
β Cari	Ao III	0·02	1·63	0·11	0·212	7
α Cor B	Ao V	−0·04	0·70	0·09	−0·155	7
γ Tr Au	Ao V Eu	0·08	1·74	0·08	0·240	3
ζ Sgtr	A2 IV	0·13	2·76	0·31	0·441	3
α Psc A	A3 V	0·12	4·3	0·15	0·633	7
α Libr	A3 met	0·25	2·74	0·15	0·438	4
β Erid	A3 V	0·25	2·53	0·11	0·403	3
β Leon	A3 V	0·14	1·96	0·13	0·292	8
α Ophi	A5 III	0·28	3·49	0·13	0·543	5
δ Capr	A5 met	0·57	4·7	(0·02)	0·672	2
α Aqil	A7 V	0·41	4·3	0·18	0·633	9
α Cari	Fo Ia	0·35	7·2	0·42	0·858	6
α Leps	Fo Ib	0·49	10·0	0·4	1·000	6
θ Scor	Fo I–II	0·81	11·9	0·5	1·075	4
α Hydi	Fo V	0·60	7·9	0·24	0·898	6
α Circ	Fo V Sr	0·41	9·6	0·3	0·982	4
β Tr Au	F2 V	0·65	8·5	0·6	0·929	3
α C Min	F5 IV	0·88	9·2	0·32	0·964	5
ρ Pupp	F6 II	0·87	10·3	0·3	1·01	3
δ C Maj	F8 Ia	1·18	20·5	1·35	1·31	3
β Aqar	Go Ib	1·24	13·2	0·4	1·12	4
ξ Pupp	Go I	(1·25)	17·3	(0·7)	1·24	2
η Boot	Go IV	1·05	11·0	0·5	1·04	6
β Hydi	G1 IV	1·08	13·1	0·46	1·12	5
α Cent	G2 V	1·22	13·0	0·7	$1{\cdot}11_5$	8
β Leps	G2 II	1·34	11·4	0·3	1·06	6
β Corv	G5 II	1·46	10·8	0·2	1·03	5
μ Velr	G5 III	1·53	10·6	0·4	$1{\cdot}02_5$	5
χ Erid	G5 IV	(1·55)	22·4	0·9	1·35	4
β Ceti	G8 III	1·73	23·2	$1{\cdot}2_5$	$1{\cdot}36_5$	8
ϵ Ophi	G8 III	(1·75)	23·1	2·7	1·36	6
τ Sgtr	Ko	(1·90)	21·8	(0·8)	1·34	2
α Phoe	Ko III	(1·90)	24·6	1·8	1·39	7
ζ Lupi	Ko III	(1·90)	24·1	2·6	1·38	4
θ Cent	Ko III–IV	1·66	23·8	1·0	$1{\cdot}37_5$	8
α Indi	Ko III	(1·90)	23·6	1·1	1·37	5
τ Pupp	Ko III	(1·90)	21·8	0·7	1·34	4
β Colm	Ko	(1·90)	20·4	(1·8)	1·31	2
α Tr Au	K2 III	2·60	23·8	2·6	$1{\cdot}37_5$	3
λ Sgtr	K2 III	(2·10)	24·7	1·1	1·39	5
δ Sgtr	K2 III	(2·10)	27·3	0·5	$1{\cdot}43_5$	5
ν Hyda	K2 III	(2·10)	20·8	(0·2)	1·32	2
α Hyda	K3 III	2·38	21·9	0·9	1·34	6
β Grus	M3 II	(3·50)	21·5	1·1	1·33	10
γ Cruc	M3 II	3·38	19·1	(2·1)	1·28	2

width relation for radiative models computed by Przybylski (**3**), with a correction of $-0{\cdot}15$ applied to the logarithm of the computed equivalent width and a zero adjustment of $+1{\cdot}10$ to the observed relative gradients. The agreement between the observed and the theoretical curves is very good and the zero point for the relative gradients agrees exactly with the value determined by Greaves (**4**). Our observed curve indicates a maximum value of log EW for gradients approximately equal to 2·0 (corresponding to the spectral type K0) and the values of the K line for later-type stars seem to stay fairly constant, within the limit of the precision of the measurements.

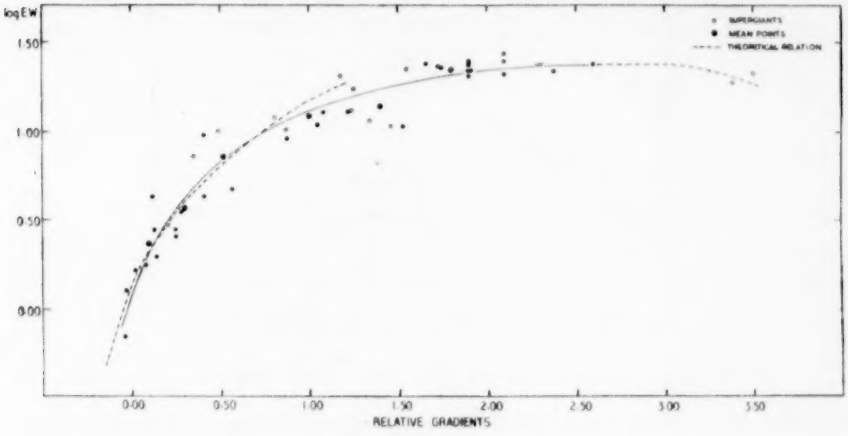

FIG. 1.—*Observed gradient—equivalent width relation (Mt Stromlo determinations).*

A list of contours of the K line for late-type stars was published by Hogg (**5**). These contours were integrated to obtain equivalent widths. The 15 stars ranging from K2 to M7 (2·1 to more than 4·0 for relative (interpolated) gradients) give a mean value for log EW of 1·18 with an average deviation of only 0·06, thus showing a fairly constant value of the K line over this range.

Our observed curve can be compared too with the curve given by Unsöld (**6**) and based on Williams' values (**7**). The constant intensity of the K line, reached for type G1 approximately, is $\log EW = 1{\cdot}45$, to compare with the value $\log EW = 1{\cdot}37$ on our curve.

A comprehensive list of K line intensities has been published by Barbier, Chalonge and Morguleff (**8**). Their values for K, determined by the wide-slit method, are expressed in logarithms of the total intensity of the line, i.e. $\log I/I_0$ for the minimum of the line. A direct comparison of our equivalent widths with their logarithms of the intensities has shown that the relation between these two quantities is not linear for late-type stars. But if we plot $\sqrt{EW}$ against $\log I/I_0$ the points fit closely to a straight line. Fig. 2 shows this relation for the stars in common with Barbier, Chalonge and Morguleff. The most discordant point is for δ CMaj, a supergiant, which has a low weight in both lists. Even in this case the error is only 25 per cent of the value in A. It has been shown that such a difference between observers is quite possible; thus we felt justified in transforming the K values of B.C.M. into equivalent widths, to allow a direct comparison with our observed curve.

Fig. 3 gives for their data the relation between $\log EW$ and the relative gradients (Stromlo or Greenwich gradients, or the interpolated value corresponding to the spectral type). The scatter is more pronounced than for our

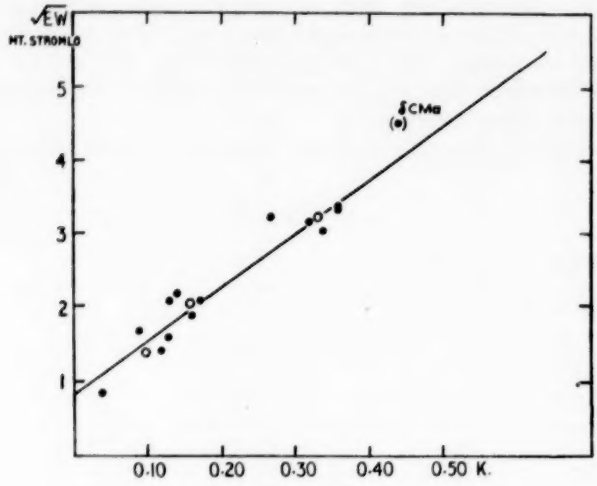

Fig. 2.—*Comparison EW Mt Stromlo with K values B.C.M.*

values and the mean curve includes the supergiants as well. When a correction of $-0{\cdot}26$ is applied to the logarithm of the computed equivalent width and, of course, the same zero point to the observed gradients, the theoretical relation computed by Przybylski fits exactly the observed mean curve.

The mean of the two corrections to the logarithm of the computed equivalent width, i.e. $-0{\cdot}15$ (Stromlo) and $-0{\cdot}26$ (B.C.M.), equals $-0{\cdot}20_5$, in agreement

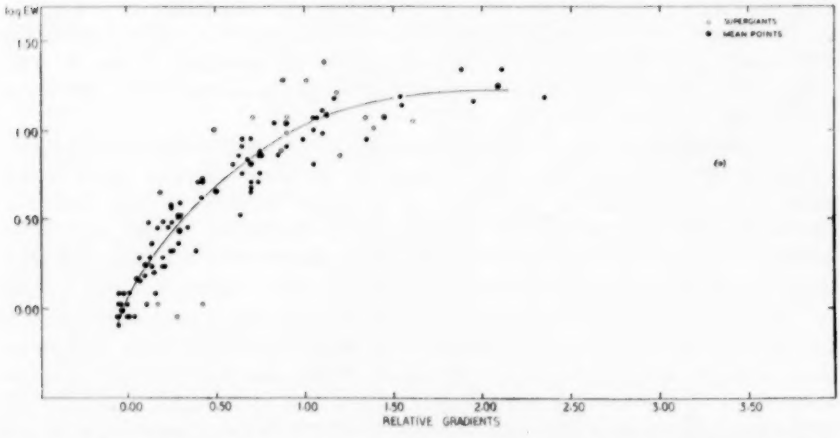

Fig. 3.—*Observed gradient—equivalent width relation (Barbier, Chalonge, Morguleff values).*

with the correction derived by Przybylski from the mean observed curve obtained with other data.

Przybylski's results do not extend to relative gradients greater than 1·2. On the other hand, curves published by Unsöld (**6**), Russell (**9**) and Pannekoek (**10**) indicate that the logarithm of the number of Ca II atoms, or the intensity of the *K* line should decrease for stars of types later than Ko. Of this there is no sign in our observations and it seems likely that any correction for difficulties in drawing the continuum would tend to increase rather than decrease the observed equivalent widths.

Acknowledgments.—The present work was carried out at the suggestion of Professor R. v. d. R. Woolley to whom the author is grateful for help and advice.

Commonwealth Observatory,
Canberra:
1955 *December* 20.

References

(**1**) R. v. d. R. Woolley, S.C.B. Gascoigne and A. de Vaucouleurs, *M.N.*, **114,** 490, 1954.
(**2**) M. L. Woods, *Mem. Comm. Obs.*, **3,** No. 12, 1956 (in press).
(**3**) A. Przybylski, *M.N.*, **114,** 407, 1954.
(**4**) W. M. H. Greaves, *M.N.*, **108,** 131, 1948.
(**5**) F. S. Hogg, *H.B.*, 859, 1928.
(**6**) A. Unsöld, *Physik der Sternatmosphären*, pp. 339–340, Berlin, 1938.
(**7**) E. G. Williams, *Publ. A.S.P.*, **48,** 113, 1936.
(**8**) D. Barbier, D. Chalong, and N. Morguleff, *Ann. Astrophys.*, **4,** 137, 1941.
(**9**) H. N. Russell, *Ap. J.*, **78,** 239, 1933.
(**10**) A. Pannekoek, *Publ. Astro Inst. Amsterdam*, No. 4, 1935.

THE RADIO SOURCE IN THE DIRECTION OF THE GALACTIC CENTRE

F. G. Smith, P. A. O'Brien and J. E. Baldwin

(Received 1956 March 9) *

Summary

Measurements have been made over a range of frequencies from 38 to 500 Mc/s of the flux density of radio waves from the intense source in Sagittarius. Aerials with high resolving power in the East-West direction were used, giving a strip distribution of brightness across the source. It was found that the flux density increases with decreasing frequency in this range of frequencies, and that the brightness temperatures exceed those expected from H II regions. The suggestion is now put forward that there is in this direction a non-thermal source of radio waves lying behind ionized hydrogen, and it is shown that this might account for the unusual spectrum indicated by the available measurements of flux density, including those at high frequencies. The source itself may be similar to other non-thermal galactic radio sources, and its position suggests that it might lie in the galactic nucleus.

Introduction.—Although the radio source IAU 17S2A in Sagittarius, close to the direction of the galactic centre, is one of the most intense in the sky, it has proved difficult to observe owing to its peculiar location in the intense band of radiation from the galactic plane. This band, and the source itself, are not easy to resolve with the aerial beam-widths used, and observations are therefore particularly difficult at the longer wave-lengths. In this paper we describe measurements using aerials with high resolving power in the East–West direction, at frequencies from 38 to 500 Mc/s. The measurements at 38 Mc/s and at 210 Mc/s were made with interferometers with various spacings up to 60λ, sufficient to resolve the source completely. At the latitude of Cambridge the source reaches an elevation of only 10° above the horizon, so that resolving power in declination is necessarily very restricted. In right ascension the resolving powers of the various aerials were of the order of 1°.

1. *Observations.*—Two different kinds of observation were made. On 38 Mc/s, 210 Mc/s and 500 Mc/s two small aerials were used as phase-switched interferometers of variable spacing in the way described by O'Brien (1953) in his measurements of the distribution of radio brightness across the Sun. On 81·5 Mc/s and 160 Mc/s individual aerials of the large Cambridge interferometer were used; these were used both in a conventional manner with a receiver which measured total power, and also in an arrangement in which two parts of one aerial were used with a phase-switching receiver. This latter arrangement provides better discrimination between radiation from the discrete source and that from the intense belt of radiation along the galactic plane.

The axes of all the interferometers were aligned nearly East–West. The receivers for all frequencies were calibrated against thermal sources with an accuracy which we believe to be about 10 per cent.

* Received in original form 1955 August 25.

(*a*) 38 *Mc/s.*—The interferometer aerials consisted of pairs chosen from seven fixed-corner reflectors, each containing one capacity-loaded dipole one wave-length long. The aerials were directed at $\delta = +7°$, and although the directivity in the declination plane was very small the sensitivity at $\delta = -29°$ is uncertain owing to the effects of ground reflection. The flux density may therefore be in error by a factor as great as 2.

Fig. 1 shows the recorded amplitude as a function of interferometer spacing (a curve referred to as the visibility curve), and the strip brightness distribution resulting from a Fourier transformation of this curve. (The latter curve will represent the actual East–West strip distribution provided it is symmetrical in R.A.) The width to half brightness is 1°·6, and the total flux density is $1{\cdot}0 \times 10^{-22}\,\mathrm{wm^{-2}(c/s)^{-1}}$.

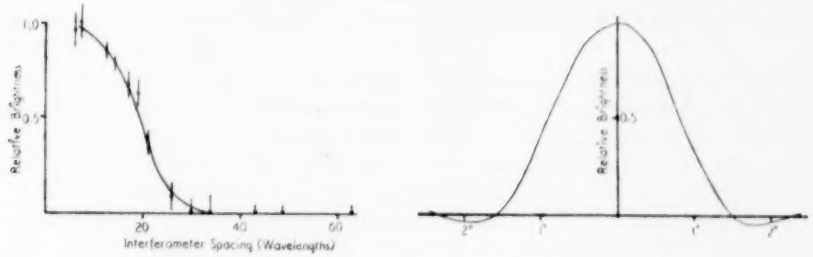

FIG. 1.—*Amplitude-spacing curve at 38 Mc/s and the corresponding strip brightness distribution.*

(*b*) 81·5 *Mc/s.*—Observations were made at spacings of 12, 15 and 18λ, using various sections of one aerial of the large interferometer (Ryle and Hewish, 1955). Each section had a beam of either $4° \times 15°$ or $8° \times 15°$, and in conjunction with the resolving power of the interferometer it was then possible to distinguish between the discrete source and the general background of radiation near the galactic centre. The source itself was only partially resolved in the East–West direction. Fig. 2 shows the record obtained with a 12λ spacing, together with the shape of the beam with which the source was scanned in right ascension.

At the 1955 General Assembly of the I.A.U. some preliminary results were presented of a survey of the galactic centre region made at nearly the same frequency with a large cross aerial. This survey, by B. Y. Mills, shows the source to be somewhat extended along the plane, so that it appears to have an extent of about 3° North–South and 1½° East–West. The East–West distribution found in our observations is in good agreement with Mills' observations.*

Our measurement of the total flux density at 81·5 Mc/s is

$$1{\cdot}2 \times 10^{-22}\,\mathrm{wm^{-2}(c/s)^{-1}}.$$

(*c*) 160 *Mc/s.*—At this frequency the beam of one aerial of the large interferometer is $1° \times 7\frac{1}{2}°$. Observations were made of the total power received by one aerial, and also by using two halves of one aerial as an interferometer. In this arrangement the main lobe of the interference pattern was 1°·2 wide between zeros. A record obtained with this system, and the shape of the aerial beam, are shown in Fig. 2. On this record the rise at 1½° in the following

* We are indebted to Mills for allowing us to make measurements on a copy of his map prior to publication.

direction cannot be due to the main source, and must be due to a separate object. This separate source is also seen on the record of total power. The asymmetry in the 81·5 Mc/s record is possibly to be attributed to this object.

The East–West distribution observed with these arrangements was very similar to that found at 81·5 Mc/s, and to the distribution of brightness found by Mills at 85 Mc/s. The source was nearly symmetrical, and extended with fairly uniform brightness over about $1\frac{1}{2}°$. The total flux density was

$$0{\cdot}9 \times 10^{-22}\,\mathrm{wm^{-2}(c/s)^{-1}}.$$

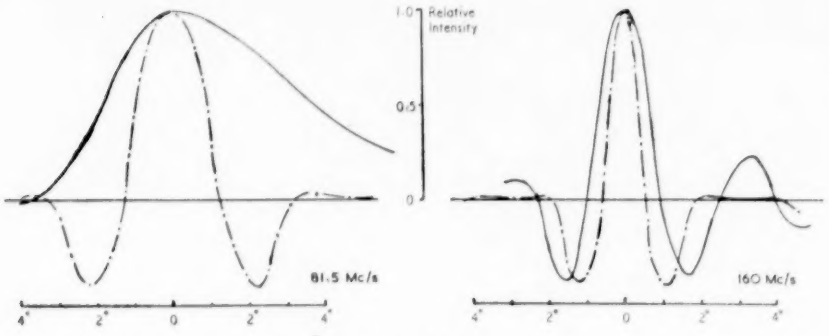

FIG. 2.—*Records obtained at 81·5 Mc/s and at 160 Mc/s. Full line: recorder deflection; broken line: aerial beam.*

(*d*) 210 *Mc/s.*—Two movable aerials were used: each one was a broadside array of 20 half-wave dipoles in front of a reflecting sheet. The receptivity pattern was sufficiently narrow in the vertical plane to avoid effects from ground reflection. Spacings up to 60λ were used, giving the visibility curve in Fig. 3. The Fourier transforms here show the source superimposed upon part of the background radiation. This background derives in the Fourier transformation from the low order components of the visibility curve, which were not included in the observations at 38 Mc/s. The width to half brightness in this strip distribution is 1°·0, and the apparent flux density is $1{\cdot}0 \times 10^{-22}\,\mathrm{wm^{-2}(c/s)^{-1}}$. The subsidiary source observed on 160 Mc/s with about one-quarter the flux density will have been confused with the main source, giving a flux about 25 per cent too high, and an uncertainty in the diameter of about 0°·2.

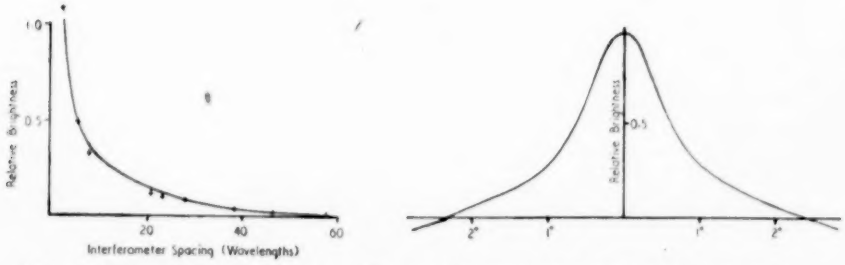

FIG. 3.—*Amplitude-spacing curve at 210 Mc/s and the corresponding strip brightness distribution.*

(*e*) 500 *Mc/s.*—Two movable broadside arrays were used, each comprising 22 full-wave dipoles in front of a reflecting sheet. No detailed visibility curve could be obtained since the signal-to-noise ratio was insufficient at the larger spacings, but it was found to be similar to that obtained at 210 Mc/s. The flux density was found to be $0{\cdot}45 \times 10^{-22}\,\mathrm{wm}^{-2}(\mathrm{c/s})^{-1}$.

2. *Positional observations.*—Accurate measurements were made of the R.A. of the centre of the source at 81·5 Mc/s and 160 Mc/s, and these both gave R.A. $17^{\mathrm{h}}44^{\mathrm{m}}$. At 81·5 Mc/s the declination was found to be $-28^{\circ} \pm 3^{\circ}$.

These values agree well with optical determinations by Oort (1952) of the position of the centre of the Galaxy. Kraus and Ko (1955) have summarized the results of other radio determinations, particularly at higher frequencies, and these all give similar positions. The close coincidence of positions over the whole range of frequencies may, however, be accidental, since the source may not be one single object.

3. *Discussion of results.*—The present observations show the existence of a source of radiation virtually unchanged in size over the frequency range 38–500 Mc/s. The measurements with high resolving power at 38 Mc/s and at 210 Mc/s show that there is no appreciable fine structure in the source.

The experimental values of flux density are given in Table I, together with the corresponding values of brightness temperature. These latter values are based on our experimental determinations of the East–West distribution combined with the North–South distribution given by Mills, and represent an average brightness over the source.

Frequency Mc/s	38	81·5	160	210	500
Flux Density $\times 10^{-22}\,\mathrm{wm}^{-2}$ (c/s)	1·0	1·2	0·9	1·0	0·45
Brightness Temperature	150 000	40 000	7 000	4 500	300 deg. K

The experimental values of flux density are known to an accuracy of about 20 per cent, except at 38 Mc/s where the value is less certain.

We note first that our values of flux density are considerably higher than those for higher frequencies, which have been discussed by Davies and Williams (1955) and by Priester (1955). These authors suggest that the flux density is independent of frequency, a relationship which is expected in thermal radiation from ionized hydrogen. There is, however, only incomplete evidence on the size of the source at higher frequencies; it has been suggested that at 9500 Mc/s the source appears to be considerably smaller (Haddock and McCullough, 1955).

It, therefore, appears that the simple behaviour which we have noted at the lower frequencies does not extend over the whole range. We note, however, that some experimental values are in doubt: for example McGee, Slee and Stanley (1955) find a flux density $0{\cdot}16 \times 10^{-22}\,\mathrm{wm}^{-2}(\mathrm{c/s})^{-1}$ at 400 Mc/s, lower than our value at 500 Mc/s, whereas the preliminary results of Denisse, Leroux and Steinberg (1955) at 900 Mc/s indicate a flux as high as $0{\cdot}3 \times 10^{-22}\,\mathrm{wm}^{-2}(\mathrm{c/s})^{-1}$. Nevertheless there seems little evidence against our conclusion that, except at the highest frequencies, the source can be treated as one simple object, and we shall propose a model which will explain the apparent departures from this simple picture at high frequencies.

If we bear in mind that the flux densities at 38 Mc/s and at 81·5 Mc/s must be affected by absorption in ionized hydrogen in the galactic plane to an extent depending on the distance of the source, it is clear that at the lower frequencies the flux density corrected for absorption cannot be independent of frequency, but could be represented by a spectrum in which flux density decreased with frequency. The brightness temperatures may similarly have been reduced by absorption, but even without allowance being made for this the experimental values greatly exceed 10 000 deg. K, the temperature usually assigned to H II regions. These two conclusions immediately remove the possibility that we are here observing thermal radiation from an H II region.

4. *The identification of the source.*—The close coincidence of the position of the source with the direction of the centre of the Galaxy has naturally suggested that the source is, in fact, a nucleus at the galactic centre. On the other hand a remarkable coincidence with the position of a compact group of H II regions has also been pointed out (Davies and Williams, 1955; Priester, 1955), and it has been shown that the flux density observed at the higher frequencies is not incompatible with such an origin. At 1420 Mc/s, from studies of the absorption in the hydrogen line by Davies and Williams and by McClain (1955), there is evidence that the source lies at a distance of about 3 kpc, the distance of the H II region.

The possibility now arises that radiation is received from two sources, one of which is the group of H II regions and the other a non-thermal source which may reasonably be considered to lie in the galactic nucleus. The flux density of the non-thermal source may be assumed to decrease with increasing frequency. Some evidence that the non-thermal source lies behind the ionized hydrogen is provided by the apparent broadening of the source at 38 Mc/s, which is consistent with the effects of absorption by ionized hydrogen lying between us and the galactic centre and concentrated within ± 100 pc from the galactic plane.

Under these circumstances the spectrum of the source would show the following characteristics:

(i) At frequencies where the optical depth of the hydrogen is small and where the brightness temperature of the non-thermal source exceeds that of the hydrogen, the non-thermal source will be seen relatively unaffected by the ionized hydrogen.

(ii) At lower frequencies, say below 100 Mc/s, appreciable absorption will occur and the spectrum will become flatter.

(iii) At higher frequencies, say above 1000 Mc/s, the brightness of the source may become less than that of the ionized hydrogen, so that the source may not be clearly distinguishable from irregularities in the distribution of the hydrogen.

5. *Conclusions.*—We have shown that the radiation observed from this source at frequencies from 38 Mc/s to 500 Mc/s cannot be thermal radiation from ionized hydrogen, although the group of H II regions which may be mainly responsible for the radiation observed at higher frequencies may, however, produce appreciable absorption at 38 Mc/s and at 81·5 Mc/s. Allowing for this absorption, the brightness temperature at 38 Mc/s would probably reach 400 000 deg. K, and the flux density vary as $(\text{frequency})^{-0.4}$, a spectrum comparable with those from other non-thermal sources. The absorption varies across the source, so

that a unique value of emission measure of the ionized hydrogen regions cannot be found without more detailed observations. Values between 10^3 and 10^4 are consistent with our hypothesis.

It seems reasonable to suggest that this source is situated in the nucleus of the Galaxy. At this distance its size would be about 150 parsecs by 400 parsecs, the longer dimension lying in the plane of the Galaxy. Nuclei of dimensions as small as 20 pc have been observed in Sc galaxies (Seyfert, 1954) and in these a high degree of turbulence is apparent. No nuclei of such small dimensions as 150 pc have been reported from optical observations of Sb galaxies, but Kwee, Muller and Westerhout (1954) have shown that in our own Galaxy large turbulent velocities exist in neutral hydrogen over a region several kiloparsecs across. It seems possible that the discrete source represents a central concentration in this region.

Cavendish Laboratory,
Cambridge:
1956 *March* 8.

References

Davies, R. D. and Williams, D. R. W., 1955, *Nature*, **175,** 1079.
Denisse, J-F., Leroux, E. and Steinberg, J-L., 1955, *C. R.*, **240,** 278.
Haddock, F. T., and McCullough, T. P., 1955, *Astr. J.*, **60,** 161.
Kraus, J. D. and Ko, H. C., 1955, *Ap. J.*, **122,** 139.
Kwee, K. K., Muller, C. A. and Westerhout, G., 1954, *B.A.N.*, **12,** 211.
McClain, E. F., 1955, *Ap. J.*, **122,** 376.
McGee, R. X., Slee, O. B., and Stanley, G. J., 1955, *Aust. J. Phys.*, **8,** 347.
O'Brien, P. A., 1953, *M.N.*, **113,** 597.
Oort, J. H., 1952, *Ap. J.*, **116,** 233.
Priester, W., 1955, *Zeit. f. Astrophys.*, **38,** 73.
Ryle, M. and Hewish, A., 1955, *Mem. R.A.S.*, **67,** 97.
Seyfert, S. K., 1954, Conference notes, Leuschner Observatory, Berkeley, California.

STUDIES IN THE EQUILIBRIUM OF GLOBULAR CLUSTERS (II)

R. v. d. R. Woolley and Denise A. Robertson

(Received 1956 January 3)

Summary

Times of relaxation are calculated for radial and circular motion in an "isothermal gas sphere." The times of relaxation increase outwards with the radius. A model is developed in which relaxation is complete only up to a limited distance from the centre. Calculations with this model give projected densities which agree much better with observation than do those from the simple isothermal case.

In a previous paper, *M.N.* **114**, 191, 1954 (Paper I), attention was given to the distribution of density in globular clusters, with special reference to (1) the fact that the "isothermal gas sphere" is not a finite object and (2) that it is only a correct solution of the differential equation concerned (Poisson's equation) if the stars all have the same mass.

The first point has been dealt with by many authors by introducing an arbitrary cut-off in the solution. In Paper I this appeared as an arbitrary upper limit to the stellar velocities. The second point was examined by introducing a spread of stellar masses—a mass function. In the present paper we attempt to enquire more closely into the nature of the cut-off, in other words to suggest a physical justification for one. Throughout the present paper we deal only with the case where the stars all have the same mass: firstly, to avoid complication, and secondly to avoid producing results which only have meaning in relation to an arbitrary mass function. (All stellar masses equal is also an arbitrary mass function, but it is the simplest.) Secondly, observations of globular clusters continue very obstinately to give no support to the theoretical expectation that massive stars are concentrated towards the centres of clusters.* Perhaps this only means that the mass luminosity law for nearby stars is quite inapplicable to stars in clusters, but it does suggest some caution in assigning a mass function and a mass luminosity law to cluster stars, both derived from observations of "main sequence" stars.

1. By "globular cluster" we mean an assembly of stars possessing spherical symmetry. The relation between the gravitational potential ϕ and the radius r is then Poisson's equation

$$\frac{1}{r^2}\frac{d}{dr}\left(r^2\frac{d\phi}{dr}\right) = -4\pi\Gamma\rho. \qquad (1.1)$$

If the cluster is in complete equilibrium, Liouville's theorem can be applied to it, and hence so can Jeans' theorem. The only satisfactory† solution for the

* But the galactic cluster M37 as analysed by von Zeipel shows a concentration of luminous stars towards the centre, and so do the Hyades, according to van Bueren.

† i.e. stable against collisions.

velocity distribution is Maxwell's distribution, and if $\nu_m(v, r)\,dm\,dv$ is the number of stars per unit volume at r with velocities between v and $v+dv$ and masses between m and $m+dm$,

$$\nu_m(v, r) = N_0 f(m)\,\frac{4}{\sqrt{\pi}}\,(\beta m)^{3/2}\,.\,\exp\{2\beta m(\phi-\phi_0)\}\,.\,v^2\,.\,\exp\{-\beta m v^2\} \qquad (1.2)$$

where N_0 is the number of stars per unit volume at the centre of the cluster, $f(m)$ the mass function at the centre of the cluster, and β is a constant.*

Then if $\nu_m(r)\,dm$ is the number of stars at r with masses between m and $m+dm$, integrated over all velocities,

$$\nu_m(r) = N_0 f(m) \exp\{2\beta m(\phi-\phi_0)\}$$

leading to an expression for the density, $\rho(r) = \int m\nu_m(r)\,dm$, which depends on the central mass function $f(m)$. However, throughout this paper we confine ourselves to the case where all the masses are the same, and then

$$\nu_m(r) = N_0 \exp\{2\beta m(\phi-\phi_0)\}.$$

We write $\beta m = j^2$ and $2j^2(\phi-\phi_0) = -\psi$. Then

$$\rho = \rho_0\,e^{-\psi}. \qquad (1.3)$$

Further we introduce a dimensionless radius z defined by

$$z = r \times (8\pi\Gamma\rho_0 j^2)^{1/2} \qquad (1.4)$$

and then equation (1.1) becomes

$$\frac{d}{dz}\left(z^2\frac{d\psi}{dz}\right) = z^2\,e^{-\psi}. \qquad (1.5)$$

Equation (1.5) is the well known equation of the isothermal gas sphere and its solution has been tabulated.

In passing we may note that if in (1.4) $z = r/l$, where l is a length, then if ρ_0 is in solar masses per cubic parsec and j in $(\mathrm{km/sec})^{-1}$,

$$l = 3{\cdot}05(\rho_0 j^2)^{-1/2}\ \text{parsecs}.$$

2. We now turn to the calculation of the time of relaxation in the cluster. It was remarked in Paper I that "once a high velocity star has got a velocity anywhere near the velocity of escape it spends almost all its time well away from the centre of the cluster and experiences very few collisions relative to the number experienced by a low velocity star which spends its time near the centre." In this section we follow up this remark.

A formula, number 2.355, given by Chandrasekhar in his *Principles of Stellar Dynamics* asserts that $\Sigma\Delta E^2$ the sum of the squares of the exchanges of energy experienced in time dt by a star of mass m_2 and velocity v_2 moving through a field of N stars per unit volume, all of mass m_1, and having a Maxwellian distribution of velocities with a parameter j, is given by

$$\Sigma\Delta E^2 = 8\pi N\Gamma^2 m_1^2 m_2^2 v_2 G(x_0)\ln(qv_2^2)\,dt$$

where

$$G(x_0) = (2x^2)^{-1}\left\{\operatorname{erf} x - \frac{2}{\sqrt{\pi}}\,x\exp(-x^2)\right\}$$

$$x_0 = jv_2$$

$$q = \left(\frac{6}{\pi N}\right)^{1/3}\,.\,\{\Gamma(m_1+m_2)\}^{-1}.$$

* cf. Paper I, section 4.

Here $m_1 = m_2 = m$. If we take* as our definition of the time of relaxation $dt = T$ when $\Sigma\Delta E^2 = \bar{E}^2/e$, where $\bar{E} = 3m/4j^2$, then

$$T^{-1} = \tfrac{128}{9}\pi e N j^4 \Gamma^2 m^2 v_2 G(jv_2) \ln (qv_2^2). \tag{2.2}$$

To calculate this for a star moving in a circular orbit is simple, as v_2 is constant throughout the history of the star, but for any other motion it is necessary to follow the history of the velocity of the star as it describes its orbit.

Consider first a star which has the circular velocity at some point in the cluster. Since $g\,dr = -d\phi$ we have $2j^2 gl\,dz = d\psi$, where $l = (8\pi\Gamma\rho_0 j^2)^{-1/2}$. But $v_c^2 = gr$ so that

$$2j^2 v_c^2 = 2j^2 glz = z\frac{d\psi}{dz}.$$

In any motion $v^2 - 2\phi = \text{constant} = 2E/m$ where E is the energy in the motion: hence $j^2v^2 + \psi = \text{constant} = 2j^2E/m$. Hence if an object moves radially with the speed of the circular velocity at a point where $\psi = \psi_1$ the apocentre of the movement occurs where $\psi = \psi_2$ such that

$$\psi_2 = \psi_1 + \tfrac{1}{2}\left(z\frac{d\psi}{dz}\right)_1 \tag{2.3}$$

and from tabulated solutions of equation (1.5) giving ψ as a function of z, the value of ψ_2 can always be found for any ψ_1.

The circular velocity at ψ_1 is given by

$$jv_c = (\psi_2 - \psi_1)^{1/2} = \left\{\tfrac{1}{2}\left(z\frac{d\psi}{dz}\right)_1\right\}^{1/2}. \tag{2.4}$$

Substitution in equation (2.2) now gives T_c, the time of relaxation for a star moving with the circular velocity. We have in fact

$$T_c^{-1} = \tfrac{128}{9}\pi e\rho j^3 \Gamma^2 m(\psi_2 - \psi_1)^{1/2} G\{(\psi_2 - \psi_1)^{1/2}\} \ln\{qj^{-2}(\psi_2 - \psi_1)\} \tag{2.5}$$

where

$$q = \left(\frac{6m}{\pi}\right)^{1/3} (2\Gamma m)^{-1}\{\rho_0 \exp(-\psi_1)\}^{-1/3}.$$

Then

$$T_c^{-1} = \tfrac{16}{9}\, e\,\frac{\Gamma m j}{l^2} \exp(-\psi)(\psi_2 - \psi)^{1/2} G\{(\psi_2 - \psi)^{1/2}\} \ln\{qj^{-2}\{\psi_2 - \psi)\}$$

using $l^{-2} = 8\pi\rho_0\Gamma j^2$.

On the other hand if a star is moving radially so that its apocentre occurs where $\psi = \psi_2$, at any other point $j^2v^2 = \psi_2 - \psi$ so that the time dt required to pass through an element of dimensionless radius dz is

$$dt = \frac{l\,dz}{v} = \frac{jl\,dz}{(\psi_2 - \psi_1)^{1/2}}. \tag{2.6}$$

Hence the time to complete an oscillation is

$$4\mathrm{T} = 4jl\int_{\psi=0}^{\psi=\psi_2} (\psi_2 - \psi)^{1/2}\left(\frac{d\psi}{dz}\right)^{-1} d\psi \tag{2.7}$$

and T can be found from the tabular solution. Now by (2.1) and (2.6) the sum of the squares of the energy exchanges experienced in moving through dz is

$$\Sigma\Delta E^2 = 8\pi N_0 \exp(-\psi)\,\Gamma^2 m^4 l\, G\{(\psi_2 - \psi)^{1/2}\} \ln\{qj^{-2}(\psi_2 - \psi)\}\, dz$$

*i.e. e^{-1} of the quantity defined by Chandrasekhar as $\bar{\tau}_E$.

Hence in performing a quarter oscillation (moving from $\psi = 0$ to $\psi = \psi_2$) in time T,

$$\frac{\Sigma \Delta E^2}{\bar{E}^2} = \frac{128\pi}{9} N_0 \Gamma^2 m^2 j^4 l \int_{\psi=0}^{\psi=\psi_2} \exp(-\psi)\, G\{(\psi_2-\psi)^{1/2}\} \ln\{qj^{-2}(\psi_2-\psi)\} \frac{dz}{d\psi}\, d\psi.$$

Accordingly $\Sigma \Delta E^2/\bar{E}^2 = 1/e$ in time. $T_r = n\mathrm{T}$ if

$$1 = ne \frac{128\pi}{9} \rho_0 j^3 \Gamma^2 m j l \int_0^{\psi_2} \exp(-\psi) G\{(\psi_2-\psi)^{1/2}\} \ln\{qj^{-2}(\psi_2-\psi)\} \frac{dz}{d\psi}\, d\psi.$$

Hence T_r, the time of relaxation for radial oscillation is given by

$$T_r^{-1} = \frac{16e}{9} \frac{\Gamma m j}{l^2} \frac{\int_0^{\psi_2} \exp(-\psi)\, G\{(\psi_2-\psi)^{1/2}\} \ln\{qj^{-2}(\psi_2-\psi_1)\}(dz/d\psi)\, d\psi}{\int_0^{\psi_2} (\psi_2-\psi_1)^{-1} (dz/d\psi)\, d\psi}. \quad (2.8)$$

From formulae (2.2) and (2.8) we can calculate the times of relaxation for the extreme cases of circular and radial motion for any total energy $E = \frac{1}{2} m j^{-2} \psi_2$. Both times of relaxation are inversely proportional to j/l^2, characteristic of the particular cluster, and also inversely proportional to m, the common mass of the individual stars.

Numerical results are given in Table 1. For the purposes of this table we have taken m = the solar mass, $j^{-1} = 1$ km/sec, and $l = 1$ parsec.

TABLE I

Times of relaxation for circular and radial motions, etc., in the isothermal gas sphere

$\xi = \ln z$ (where z is dimensionless radius)	2	3	4	5
log τ years	7·11	7·60	8·05	8·48
log T_c years	8·86	9·88	10·78	11·55
log T_r years	8·37	8·96	9·50	10·01
log T_c/T_r	0·49	0·92	1·28	1·54
log ρ/ρ_0	2·71	3·64	4·76	5·95
ψ_1	2·97	5·42	7·47	9·32
ψ_2	4·22	6·55	8·42	10·26

In the example shown in Table 1 complete equipartition cannot be established beyond $\xi = 3$ or 4 in a life of 10^{10} years : and if the life of the cluster is substantially less than that the full quota of circular velocities can hardly extend much beyond $\xi = 3$ (or $z = e^3 = 20$). The effect of this defect on the distribution of density in the cluster is discussed in the next section.

3. We are led to the idea that at some considerable time after the formation of a cluster, relaxation is substantially complete at and near the centre, but that in any finite time after formation there are some great distances from the centre at which there has not yet been time to relax the stellar velocities. If the cluster started out in a restricted volume, it would push out some stars beyond this initial volume, at first on orbits initially present in the distribution, and later on orbits arising as a result of relaxation of velocities at and near the centre.

We now investigate a model of a cluster in which relaxation is complete inside a certain radius R, but stars only occur outside this radius if they travel in orbits part of which lie within R (or touch R). The stars outside R are thrown out, as it were, by the equilibrium at and inside R.

Consider an orbit such that the velocity is v_1 and the direction makes an angle α_1 with the radius vector at R. Then if the corresponding quantities are v_2 and α_2 at a distance xR, from the centre of the cluster (where $x>1$), we have, since the force is always central,

$$v_1 \sin\alpha_1 = xv_2 \sin\alpha_2.$$

Again,

$$j^2(v_1^2 - v_2^2) = \psi_2 - \psi_1.$$

Accordingly if V_1, V_2 are the velocities in the orbit which touches both $r=R$ and $r=xR$ (i.e. such that $\sin\alpha_1 = \sin\alpha_2 = 1$),

$$V_1 = xV_2$$

$$j^2V_1^2 = (\psi_2 - \psi_1)\,x^2/(x^2-1), \quad j^2V_2^2 = (\psi_2 - \psi_1)/(x^2-1).$$

Three cases arise, as follows,

Case I. If $j^2v_1^2 < \psi_2 - \psi_1$, the orbit cannot get to xR for any value of α_1.

Case II. If $\psi_2 - \psi_1 < j^2v_1^2 < j^2V_1^2$, the orbit intersects $r=xR$ for some values of α_1 (see Fig. 1).

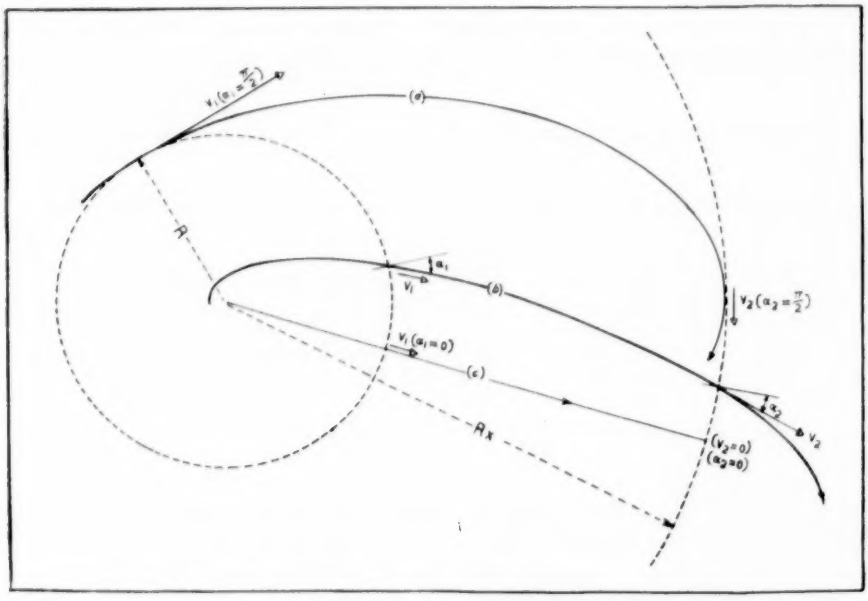

FIG. 1.—*Examples of orbits intersecting* $r=xR$.
(*a*) $\alpha_1=\alpha_2=\pi/2$.
(*b*) $0<\alpha_1<\pi/2$.
(*c*) $\alpha_1=\alpha_2=0$.

Case III. If $j^2v_1^2 > j^2V_1^2$, the orbit intersects $r=xR$ for all values of α_1.

These cases arise from

$$\sin\alpha_2 = \sin\alpha_1 \cdot \frac{v_1}{xv_2} = \sin\alpha_1 \cdot v_1 \{x^2v_1^2 - (x^2-1)\,V_1^2\}^{-1/2}.$$

Hence, $\sin\alpha_2 > 1$, which is impossible, unless $\alpha_1 < A$, where

$$\sin^2 A = x^2 - (x^2-1)\,V_1^2/v_1^2.$$

When $j^2v_1^2=\psi_2-\psi_1=\{(x^2-1)/x^2\}.j^2V_1^2$, $\sin^2 A=0$.

When $v_1^2=V_1^2$, $\sin^2 A=1$.

Accordingly in Case II, $0<\sin^2 A<1$, and A can always be found. All (v_1, α_1) stars for which $0<\alpha<A$ get to xR. In Case III, all values of α_1 give a possible value of α_2, (but not all values of α_2 are possible.)

These rules enable us to calculate the number of stars at xR from the number at R. If ν_1 is the number of stars per unit volume at R, the number with velocities between v_1 and v_1+dv_1, moving in directions between α_1 and $\alpha_1+d\alpha_1$ is

$$\nu_1\frac{4}{\sqrt{\pi}}j^3v_1^2\exp(-j^2v_1^2)\,dv_1\,|\sin\alpha_1|\,d\alpha_1.$$

The number moving inwards and outwards over the sphere of radius R in unit time is

$$\nu_1\frac{4}{\sqrt{\pi}}j^3v_1^3\exp(-j^2v_1^2)\,dv_1\,|\sin\alpha_1|\cos\alpha_1\,d\alpha_1\,.\,4\pi R^2$$

integrated over all values of α_1 from 0 to $\pi/2$ and v_1 from 0 to ∞. The number crossing the sphere at xR is the same integrated over all permissible values of α_1 and v_1. Each class (v_1, α_1) contributes to ν_2, the number per unit volume at xR, inversely as $v_2\cos\alpha_2$, so that

$$\nu_2=\nu_1\,.\,\frac{4}{\sqrt{\pi}}\int_{\alpha_1=0}^{\alpha=A}\int_{j^2v_1^2=\psi_2-\psi_1}^{v_1=\infty}\frac{v_1^3\exp(-j^2v_1^2)\,dv_1\,.\,\sin\alpha_1\cos\alpha_1\,d\alpha_1}{v_2\cos\alpha_2}\,.\,\frac{R^2}{xR^2}.$$

Since $v_1\sin\alpha_1=xv_2\sin\alpha_2$, we have $xv_2\cos\alpha_2=(x^2v_2^2-v_1^2\sin_2\alpha_1)^{1/2}$ and, carrying out the α integral, we get

$$\frac{\nu_2}{\nu_1}=\frac{4}{\sqrt{\pi}}j^3\int_{j^2v_1^2=\psi_2-\psi_1}^{j^2v_1^2=\infty}v_1\exp(-j^2v_1^2)\,dv_1\left\{v_2-\left(v_2^2-\frac{v_1^2\sin^2 A}{x^2}\right)^{1/2}\right\}.$$

When $\psi_2-\psi_1<j^2v_1^2<j^2V_1^2$ we have $\sin^2 A=x^2V_2^2/V_1^2$ and when $j^2v_1^2>j^2V_1^2$ we have $\sin^2 A=1$. Accordingly

$$\begin{aligned}\frac{\nu_2}{\nu_1}&=\frac{4}{\sqrt{\pi}}j^3\int_{j^2v_1^2=j^2v_1^2}^{j^2v_1^2=\psi_2-\psi_1}v_1v_2\exp(-j^2v_1^2)\,dv_1\\&\quad+\frac{4}{\sqrt{\pi}}j^3\int_{j^2v_1^2=j^2V_1^2}^{\infty}v_1\exp(-j^2v_1^2)\,dv_1\left\{v_2-\left(v_1^2-\frac{v_1^2}{x^2}\right)^{1/2}\right\}\\&=\frac{4}{\sqrt{\pi}}j^3\int_{j^2v_1^2=\psi_2-\psi_1}^{\infty}v_1v_2\exp(-j^2v_1^2)\,dv_1\\&\quad-\frac{4}{\sqrt{\pi}}j^3\int_{j^2V_1^2}^{\infty}v_1\left(v_2^2-\frac{v_1^2}{x^2}\right)^{1/2}\exp(-j^2v_1^2)\,dv_1\end{aligned}$$

and remembering that $j^2v_2^2=j^2v_1^2-(\psi_2-\psi_1)$, $v_1dv_2=v_1\,dv_1$,

$$\frac{\nu_2}{\nu_1}=\exp\{-(\psi_2-\psi_1)\}\left\{1-\frac{4}{\sqrt{\pi}}\int_{y_1}^{\infty}\tfrac{1}{2}\left(y-\frac{j^2v_1^2}{x^2}\right)^{1/2}\exp(-y)\,dy\right\}$$

in which $y=j^2v_2^2$ and $y_1=j^2V_1^2-(\psi_2-\psi_1)=(\psi_2-\psi_1)/(x^2-1)$.

Again

$$y-\frac{j^2v^2}{x^2}=\frac{x^2-1}{x^2}(y-y_1),$$

so that

$$\frac{\nu_2}{\nu_1}=\exp\{-(\psi_2-\psi_1)\}\left[1-\left(\frac{x^2-1}{x^2}\right)^{1/2}\exp\left(-\frac{\psi_2-\psi_1}{x^2-1}\right)\right]. \qquad (3.1)$$

The differential equation to be solved is

$$\frac{d}{dz}\left(z^2\frac{d\psi}{dz}\right) = z^2\exp(-\psi)$$

from $z=0$ to $z=R/l$ (say $z=z_1$) subject to $\psi=0$ and $\dot{\psi}=0$ at $z=0$. (3.2)

$$\frac{d}{dz}\left(z^2\frac{d\psi}{dz}\right) = z^2\exp(-\psi)\left[1-\left(\frac{z^2-z_1^2}{z_1^2}\right)^{1/2}\exp-\left\{\frac{z_1^2(\psi-\psi_1)}{z^2-z_1^2}\right\}\right]$$

for all $z>z_1$, subject to ψ and $\dot{\psi}$ being continuous at $z=z_1$. ψ_1 is the value of ψ at $z=z_1$.

A solution of equations (3.2) was made, with $z_1=30$, and carried from $z=30$ to $z=100$. It is shown in Table 2, with some comparisons, including projections. It was found that if we denote ρ/ρ_0 by η, then ηz^3 was approximately constant (there is a small term linear with z) from $z=60$ to $z=200$, and in making the projection it was supposed that this relation held good outwards for such a distance as could sensibly affect the projection. Notice that this gives a projected density roughly proportional to r^{-2}, as compared with r^{-1} for the isothermal case.

TABLE 2

Solutions and projections of isothermal and modified isothermal

z	ψ		$\log\eta$		log projected intensity	
	Iso.	mod.	Iso.	mod.	isothermal	modification
0	0·00		0·00		1·52	1·75
2	0·56		$\bar{1}$·76		1·36	1·59
5	2·04		$\bar{1}$·11		0·96	1·18
10	3·74		$\bar{2}$·38		0·54	0·75
20	5·41		$\bar{3}$·65		0·18	0·34
30	6·29	6·29	$\bar{3}$·27	$\bar{3}$·27	0·00	0·00
40	6·87	6·86	$\bar{3}$·02	$\bar{4}$·85	$\bar{1}$·88	$\bar{1}$·75
50	7·31	7·27	$\bar{4}$·83	$\bar{4}$·57	$\bar{1}$·79	$\bar{1}$·58
60	7·66	7·57	$\bar{4}$·67	$\bar{4}$·35	$\bar{1}$·70	$\bar{1}$·45
70	7·96	7·80	$\bar{4}$·55	$\bar{4}$·16	$\bar{1}$·65	$\bar{1}$·34
80	8·20	7·99	$\bar{4}$·46	$\bar{4}$·00	$\bar{1}$·60	$\bar{1}$·24
90	8·41	8·14	$\bar{4}$·35	$\bar{5}$·87	$\bar{1}$·55	$\bar{1}$·16
100	8·61	8·28	$\bar{4}$·26	$\bar{5}$·74	$\bar{1}$·52	$\bar{1}$·08

To obtain a good comparison of these results with Gascoigne's observed curves,* the zero of the log of projected light was chosen at

$z=30$ for isothermal and modified isothermal solutions

$r=3.5$ minutes for 47 Tuc.

and $r=7{\cdot}23$ minutes for ω Cen.

These four points were plotted as one in Figure 2, thus determining the scale of the abcissae.

* *M.N.*, **116** (in press).

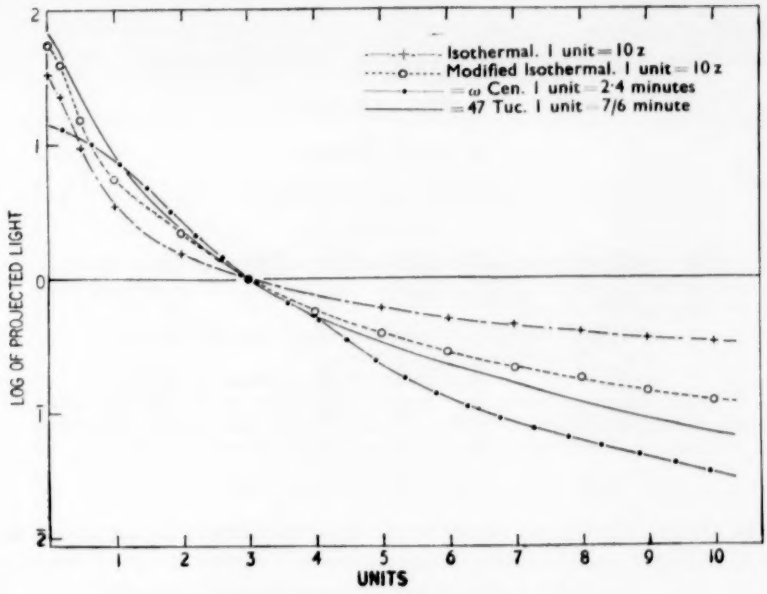

FIG. 2.—*Comparison of theoretical models with observations.*

The modification certainly agrees better with observation than does the unmodified isothermal solution, but much more work is needed, both theoretical and observational, to decide these outstanding questions :

What is the mass function in clusters ?

What is the mass-luminosity law ?

How far out in radius do clusters extend and what is the nature of the cut-off ?

Is equipartition of energy confined to the centres, or even absent ?

Commonwealth Observatory,
Mount Stromlo,
Canberra, Australia:

1955 *December.*

ON THE EQUILIBRIUM OF CLUSTERS

III. THE PLEIADES

R. v. d. R. Woolley

(Received 1956 January 4)

Summary

Data concerning the Pleiades, principally from Hertzsprung's catalogue, are compared with a model (a truncated negative polytrope of index 3) with the following constants:

central density ρ_0 = 15·6 solar masses per cubic parsec,
velocity parameter j^{-1} = 0·60 km/sec,
truncation = 0·72 × velocity of escape at centre.

The projected density, the relative distribution of the brighter stars and the observed internal motion are reasonably well represented. The time of relaxation of the inner parts is between 10^7 and 10^8 years.

The Pleiades form a star cluster which has few members in comparison with the large numbers seen in great clusters such as ω Centauri and 47 Tucanae and has perhaps been regarded as unsuitable for comparison with equilibrium theory on this account. On the other hand the relative closeness of the Pleiades makes it comparatively easy to sort out members of the cluster from background stars by using proper motions, and also enables us to identify members with low absolute luminosities. These advantages appear to make an attempt to represent the Pleiades by a theoretical model worth while.

Hertzsprung* in Table 4 of his *Catalogue de 3259 étoiles dans les Pléiades* lists 291 stars which are "plus ou moins suspectes de participer au mouvement propre d'Alcyone." Only one star in eleven in the region is a member: a fact which illustrates the great difficulty in eliminating non-members from clusters (when stars of low luminosity are taken into account.) The area measured by Hertzsprung was 160′ × 160′, and according to Trumpler† a number of stars well outside the area considered by Hertzsprung have the same proper motion as Alcyone. Again, Hertzsprung's limiting magnitude is $16^{m}{\cdot}8$, while van Maanen‡, using the 100-inch telescope at Mt Wilson, found some stars fainter than the 17th magnitude which he considered to show the proper motion of the cluster. Hertzsprung's list of 291 stars is therefore almost certainly incomplete in extension (distance from Alcyone) and faintness, but it is nevertheless the most complete catalogue of membership that we possess for any cluster.

The stars listed by Hertzsprung are catalogued with photographic magnitudes determined by Binnendijk. If the stars are grouped according to apparent photographic magnitude, and according to distance from Alcyone, as in Table I, it can be seen at once that there is a tendency for the brighter stars to be concentrated towards the centre.

* *Ann. Sterrewacht te Leiden*, **19**/1, A, 1947.
† *L.O.B.*, **10**, 110, 1921.
‡ *Ap. J.*, **94**, 399, 1941.

TABLE I

Distribution of 290 stars less than 85′ from Alycone in Hertzsprung's catalogue, arranged in annuli of equal area, centred on Alcyone and according to apparent photographic magnitude. (One star is 88′ from Alcyone.)

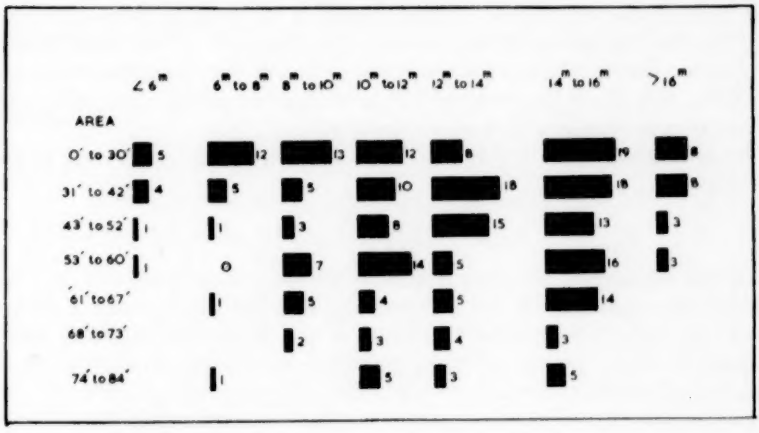

We now attempt to estimate the masses of these groups of stars, in terms of the solar mass. According to Eggen* the modulus of the Pleiades is $5^{m}\cdot68$. On account of absorption the corresponding parallax is $0''\cdot0077$ (and not $0''\cdot0073$ as would be deduced from this modulus if there were no absorption). From the modulus we can convert apparent photographic magnitudes to absolute photographic magnitudes, and then make an estimate of the mass, following Eggen† for stars of mass $<\odot$ and Kuiper‡ for stars of mass $>\odot$. Masses are adopted as follows:

Apparent photographic magnitude	Number of stars (Hertzsprung)	Adopted mean mass ($\odot=1$)
<6	11	6·3
6–7	11	3·3
7–8	9	2·4
8–9	18	1·7
9–10	17	1·3
10–11	20	1·1
11–12	36	1·0
12–13	28	0·85
13–14	31	0·68
14–15	41	0·57
15–16	47	0·47
>16	22	0·4

We can now form a table showing the distribution of mass in various annuli. These annuli are of course as seen projected on the plane of the sky, and the annular densities could be transformed into space densities in the manner used

* *A.J.* (in press).
† *A.J.* (in press).
‡ *Ap. J.*, **88**, 429, 1938.

by von Zeipel, namely, if $\rho(r)$ is the space density and $\sigma(a)$ the projected density at annular radius a, then

$$\pi\rho(r) = \int_r^\infty \frac{\sigma'(a)da}{(r^2-a^2)^{1/2}}.$$

This method was used by von Zeipel himself in his analysis of the open cluster M 37, and by van Bueren in his analysis of the Hyades. It has disadvantages if the annular function $\sigma(a)$ as observed is so rough that its differential $\sigma'(a)$ is unreliable, and also if the observed $\sigma(a)$ is incomplete through lack of knowledge of faint stars or of stars with large values of a.

An alternative method is to start with a model of the cluster and project it by using

$$\sigma(a) = 2\int_a^\infty \frac{\rho(r).rdr}{(r^2-a^2)^{1/2}}$$

which has advantages for numerical work as the values of $\rho(r)$ are theoretical and therefore smooth. It is a disadvantage that one has to select a particular model of a cluster and make a solution of the differential equation before a comparison can be made, and that one is in some danger of finding out more about the model than about the cluster. However, in the inner parts of a cluster the potential as a function of the radius is not at all sensitive to the choice of model, nor is the projected density critically sensitive*. In this paper we have chosen a particular model and projected the density (and also the distribution of the bright stars) for comparison with the annular results for the Pleiades.

The model chosen is similar to some described in the writer's first paper† but it is more sharply restricted (cut off) than any yet given. It is, in fact, similar to models C, D and E in the first paper but the cut off is at $c = 2{\cdot}5$ (or $k = 4{\cdot}5$).

The notation used is $m = \mu\overline{m}$ where m is the mass of any star and $\overline{m}$ a suitably defined mean mass. The velocity distribution is such that $\nu_\mu(v, r)d\mu dvdr$ is the number of stars per unit volume with masses between μ and $\mu + d\mu$, velocities between v and $v + dv$ and distances between r and $r + dr$ from the centre of the cluster. It is supposed that

$$\begin{aligned} \nu_\mu(v,r) &= C_\mu v^2 e^{-\mu j^2 v^2} e^{-\mu\psi} \quad \text{for} \quad j^2v^2 < k-\psi \\ &= 0 \qquad\qquad\qquad\qquad\quad \text{for} \quad j^2v^2 > k-\psi \end{aligned}$$

where k is a constant and ψ is related to the gravitational potential ϕ by

$$\psi = 2j^2(\phi_0 - \phi)$$

and ϕ_0 is the value at the centre of the cluster. Here ϕ is reckoned decreasing outwards, so that ψ increases outwards from zero at the centre of the cluster. This arrangement of velocities satisfies Jeans' relation.

Integrating over all velocities we have

$$\nu_\mu(r) = \frac{4}{\sqrt{\pi}} e^{-\mu\psi}(\mu j^2)^{-3/2} C_\mu \operatorname{erf}_2\{\mu(k-\psi)\}^{1/2}$$

where

$$\operatorname{erf}_2 x = \frac{4}{\sqrt{\pi}}\int_0^x y^2 e^{-y^2} dy.$$

* A. W. Rodgers and D. M. Myers, *M.N.*, **114**, 620, 1954.
† *M.N.*, **114**, 191, 1954.

At the centre, in particular,

$$\nu_\mu(0) = \frac{4}{\sqrt{\pi}}(\mu j^2)^{-3/2} C_\mu \operatorname{erf}_2(\mu k)^{1/2}$$

so that

$$\nu_\mu(r)/\nu_\mu(0) = e^{-\mu\psi} \operatorname{erf}_2 \sqrt{\{\mu(k-\psi)\}} / \operatorname{erf}_2 \sqrt{(\mu k)}.$$

It is necessary to adopt a particular case of C_μ as a function of μ, and the models have

$$C_\mu = \text{const.} \times \mu^{5/2} e^{-3\mu}$$

which gives

$$\nu_\mu(0) = \text{const.} \times \mu e^{-3\mu} \operatorname{erf}_2 \sqrt{(\mu k)}$$

and

$$\nu_\mu(r) = \text{const.} \times \mu e^{-(3+\psi)\mu} \operatorname{erf}_2 \sqrt{\{\mu(k-\psi)\}}$$

Poisson's equation, assuming spherical symmetry, is

$$\frac{1}{r^2}\frac{d}{dr}\left(r^2 \frac{d\phi}{dr}\right) = -4\pi\Gamma\rho$$

and if we put $r = lz$ where $l = (8\pi\Gamma\rho_0 j^2)^{-1/2}$ and $\rho = \eta\rho_0$ the equation is

$$\frac{d}{dz}\left(z^2 \frac{d\psi}{dz}\right) = \eta z^2$$

subject to $\psi = 0$ and $\dot{\psi} = 0$ at $z = 0$. From the expression for $+\nu_\mu(r)$ we get

$$\eta = \rho/\rho_0 = (1 + \psi/3)^{-3}\left(\frac{k-\psi}{k}\right)^{3/2}\left\{1 + \frac{(126 + 12k)\psi + 15\psi^2}{315 + 84k + 8k^2}\right\}.$$

The solution for $k = 4{\cdot}5$, called model F, is given in Table 2.

TABLE II

Model F

z	ψ	η	z	ψ	η
0	0	1·000	8	3·14	0·035
1	0·159	0·839	9	3·42	0·023
2	0·552	0·555	10	3·68	0·014
3	1·04	0·341	11	3·90	0·009
4	1·54	0·210	12	4·09	0·005
5	2·05	0·132	13	4·25	0·002
6	2·43	0·084	14	4·40	0·001
7	2·81	0·055	14·84	4·50	0·000
$z_\infty = 14{\cdot}84$			$(z^2\dot{\psi})_\infty = 26{\cdot}4$		

Truncation of velocity at centre

$$\frac{v_0^2}{u_0^2} = \frac{kz_\infty}{kz_\infty + (z^2\dot{\psi})_\infty} = 0{\cdot}717$$

where u_0 is the velocity of escape at the centre of the cluster and $j^2 v_0^2 = k$.

The projected densities $\sigma(a)/\sigma(0)$ in model F are as follows

a	0	1	2	3	4	5	6	8	10
$\sigma(a)/\sigma(0)$	1·00	0·89	0·67	0·47	0·33	0·25	0·16	0·07	0·03

Here the projected radius a is in the same dimensionless units as are used for z, so that the annular radius in real units is al. Before comparing these projections with densities from Hertzsprung's catalogue we consider briefly the results given by Trumpler. For stars brighter than $10^m{\cdot}0$ photographic, his "very probable members" and "probable members", distant more than 1° from Alcyone, and not given by Hertzsprung, are as follows:—

Distance from Alcyone	$6^m{\cdot}0$ to $6^m{\cdot}9$	$7^m{\cdot}0$ to $7^m{\cdot}9$	$8^m{\cdot}0$ to $8^m{\cdot}9$	$9^m{\cdot}0$ to $0^m{\cdot}9$
1°·1 to 1°·5	0	0	2	3
1°·6 to 2°·0	2	2	0	3
2°·1 to 2°·5	1	2	2	0
2°·6 to 3°·0	0	2	0	4

Trumpler's additions indicate an extension to at least 3° from Alcyone and also (for stars brighter than $10^m{\cdot}0$) a twenty-five per cent increase over the mass derived from Hertzsprung's catalogue, which gives a total mass of 337⊙. We therefore suppose that the total mass of the Pleiades is about 500⊙ (probably an underestimate) and that $a = 14{\cdot}84$, the limit of model F, corresponds to 180′. These two identifications fix the scale of a and the mass, and we now proceed to compare the projection of model F with the observed values. The quantity chosen for comparison is the mass inside annular radius a, and the result is shown it Fig. 1. The break in the observed curve at about 60′ from Alcyone is taken to indicate that the data are incomplete beyond this radius.

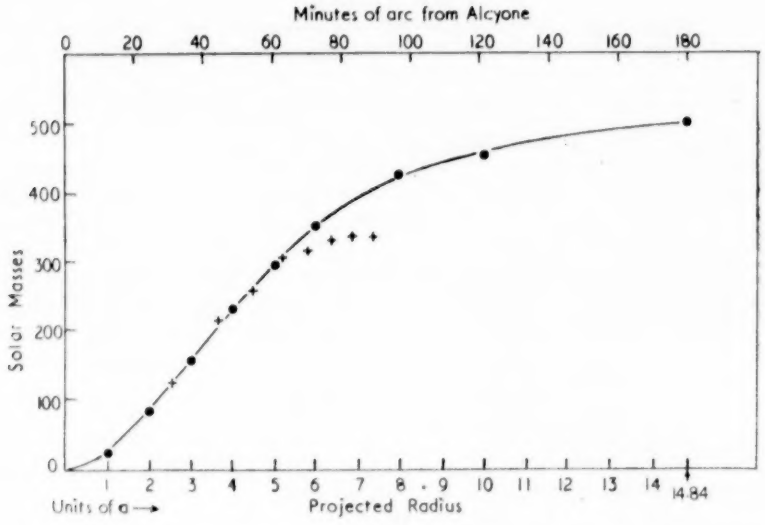

FIG. 1.—*Projected mass inside annular radius a from model F (full line) compared with values derived from Hertesprung's catalogue and adopted masses (crosses).*

Since in model F

$$\int \frac{\sigma(a)}{\sigma(0)} \cdot 2\pi a\, da = 4\pi(z^2\dot{\psi})_\infty = 331,$$

the mass of model F is $331\rho_0 l^3$, in solar masses if ρ_0 is in solar masses per cubic parsec and l is in parsecs. Now since 180′ at a distance of 130 parsecs is 6·79 parsecs, we have $14{\cdot}84l = 6{\cdot}79$ parsecs or $l = 0{\cdot}46$ parsecs, and then from $331\rho_0 l^3 = 500$ we have

$$\rho_0 = 15{\cdot}6 \text{ solar masses per cubic parsec.}$$

Again $l=(8\pi\Gamma\rho_0 j^2)^{-1/2}$ so that $j^{-1}=l\,.\,(8\pi\Gamma\rho_0)^{1/2}$, from which $j^{-1}=0{\cdot}60$ km/sec.

In a full Maxwellian distribution, the average projected velocity of stars relative mass μ is $\frac{1}{2}\pi^{1/2}(\mu j^2)^{-1/2}$, but if the distribution is truncated to $j^2v^2<L^2$ the average projected velocity is

$$\sqrt{\frac{\pi}{2}}(\mu j^2)^{-1/2}\,\mathrm{erf}_2\,L/\{1-\exp(-L^2)\}.$$

Using $k=4{\cdot}5$ and the empirical mass function derived in the next section for the Pleiades the average of the reduction factor

$$\mu^{-1/2}\,\mathrm{erf}_2\sqrt{\{\mu(k-\psi)\}}/\{1-\exp(-\mu(k-\psi))\}$$

is about 0·9. Accordingly, the average projected velocity with $j^{-1}=0{\cdot}60$ km/sec is $\bar{v}=0{\cdot}54$ km/sec. This corresponds to a proper motion of 0″·9 per 1000 years at Eggen's distance of the Pleiades. Discussing the observed proper motions Hertzsprung says "le mouvement interne des Pléiades semble d'être environ $\pm 0''{\cdot}7/1000a$". Titus* gives 0″·8/1000 years for the average internal motion, and Smith and Struve† concluded from spectroscopic observations that "there may exist internal motions of the order of 1 km/sec." Most weight should be given to Hertzsprung's value of 0″·7/1000 years. The theoretical value of 0″·9/1000 years is, however, in quite satisfactory agreement with the observations.

We now compare the adopted mass function of model F with the observed distribution of stellar masses in Hertzsprung's catalogue. Before we can do this it is necessary to convert the *central* mass function of model F

$$\nu_\mu(0)=\text{const.}\,\mu e^{-3\mu}\,\mathrm{erf}_2\sqrt{(k\mu)}$$

to a mass function *for the cluster as a whole*, which can only be done by calculating the quantities

$$\lambda_\mu=\{\nu_\mu(0)\}^{-1}\,.\,4\pi\int\nu_\mu(z)z^2dz$$

the mass function of the cluster being $f_\mu=\text{const.}\,\lambda_\mu\nu_\mu(0)$. The following values were found (constants having been subtracted from the natural logarithms).

μ	2	1·5	1	0·75	0·50	0·25
$\ln\lambda_\mu$	−1·46	−0·79	0·00	0·42	0·81	1·16
$\ln(\nu_\mu(0)/\mu)$	−2·97	−1·47	0·00	0·70	1·29	1·54
$\ln(f_\mu/\mu)$	−4·38	−2·21	0·00	1·17	2·15	2·75
$\log(f_\mu/\mu)$	−1·90	−0·96	0·00	0·50	0·93	1·19

From $\mu=0{\cdot}5$ to $\mu=1{\cdot}5$ we have $d/d\mu\log(f_\mu/\mu)=2{\cdot}0$, nearly.

On the other hand the mass function of the cluster from $m=0{\cdot}60\odot$ to $m=1{\cdot}7\odot$ is quite well represented by

$$\frac{d}{dm}\log(f_m/m)=1{\cdot}6\odot^{-1}$$

and by comparison $\bar{m}=1{\cdot}25\odot$.

The projected annular distributions of stars with $\mu=2$ and $\mu=1$ in model F, $\sigma_2(a)$ and $\sigma_1(a)$, are now given:

a	0	1	2	3	4	5
$\sigma_2(a)$	1·00	0·76	0·39	0·17	0·073	0·033
$\sigma_1(a)$	1·00	0·88	0·65	0·44	0·28	0·18
a	6	7	8	10	12	
$\sigma_2(a)$	0·015	0·008	0·004	0·001	—	
$\sigma_1(a)$	0·12	0·076	0·048	0·027	0·004	

* *A.J.*, **47**, 25, 1938.
† *Ap. J.*, **100**, 360, 1944

With $\bar{m}=1\cdot25\odot$, $\mu=2$ gives $m=2\cdot5\odot$ or about $7^{m}\cdot5$ apparent photographic magnitude. We can compare the 9 stars between 7^{m} and 8^{m} with $\sigma_2(a)$ using $a=12'\cdot1$, and we find

Annulus	Expected from $\sigma_2(a)$	Hertzsprung's catalogue
′ ′		
0 to 12	1·3	1
13 to 24	2·6	2
25 to 36	2·2	4
37 to 48	1·4	1
49 to 60	0·8	0
61 to 73	0·4	0
>74′	0·2	1

an agreement fully as good as could be expected.

Stars with $\mu=1$ have $m=1\cdot25\odot$ or about $9^{m}\cdot8$ apparent photographic magnitude. We compare the theoretical distribution $\sigma_1(a)$ with 37 stars from 9^{m} to 11^{m} and with 91 stars from 8^{m} to 12^{m}.

Annulus	37 stars from $9^{m}\cdot0$ to $11^{m}\cdot0$		91 stars from $8^{m}\cdot0$ to $12^{m}\cdot0$	
	Expected $\sigma_1(a)$	Hertzsprung's catalogue	Expected $\sigma_1(a)$	Hertzsprung's catalogue
′				
0 to 12	2·5	6	6·2	8
13 to 24	6·2	3	15·4	9
25 to 26	7·5	3	18·5	14
37 to 48	7·0	6	17·2	16
49 to 60	5·8	11	14·2	25
61 to 73	4·6	8	11·4	13
74 to 85	3·4	0	8·3	6

The agreement is as good as could reasonably be expected. Trumpler's bright stars, well away from Alcyone, do not fit into the scheme: to this question we will briefly return later.

The time of relaxation of the system can now be mentioned. According to calculations by Woolley and Robertson*, based it is true on another model (the "isothermal gas sphere"), we should expect the following results with $\bar{m}=1\cdot25\odot$, $l=0\cdot46$ parsecs, $j^{-1}=0\cdot60$ km/sec and $z=e^2=7\cdot39$ (i.e. 3·4 parsecs from Alcyone, or 90′ apparent distance):

$$\log T_c=7\cdot96 \qquad \log T_r=7\cdot47$$

Here T_c is the time of relaxation, in years, of stars having the circular velocity at $a=7\cdot39$ and T_r is the time of relaxation, in years, of stars describing radial orbits and having the speed of the circular velocity at $a=7\cdot39$. These figures suggest that if the age of the Pleiades as a cluster is 10^7 or 10^8 years (or more) the stars within 3 parsecs of Alcyone should be substantially in a state of equipartition of energy. The present analysis appears to support this view.

On the other hand the bright stars ($<8^{m}\cdot0$) at distances greater than $1^{\circ}\cdot5$ from Alcyone seem to be too far out to be in equilibrium with the centre of the cluster†. There is nothing inherently unreasonable about this, and it may indicate that the cluster is not more than 10^8 years old. More light would

* *M.N.*, **116**, 288, 1956.

† There is a suggestion in Fig. 1 that equilibrium may fail at 60′ from Alcyone and outwards but one would have to be very certain that the data were complete before pursuing this.

thrown on this question, as well as on the appropriateness of model F as a representation of the Pleiades, by the collection of more data about membership of the Pleiades concerning stars too distant from Alcyone or too faint to be covered by the work of Hertzsprung or of Trumpler.

Acknowledgments.—The writer is indebted to Olin J. Eggen for many valuable discussions about the Pleiades, and to Denise Robertson for her conscientious checking of this paper.

Commonwealth Observatory,
Mount Stromlo,
Canberra, Australia:
1955 *December.*

Note added, 1956 May

The question has been raised whether the Pleiades can be considered as a self-gravitating object, in the presence of the galactic gravitational field. The paper examines this question whether the Pleiades behaves like a model cluster, by appealing to the observations, and suggests that it does: but the theoretical point may be pursued. Clearly a uniform gravitational field would affect the Pleiades as a whole: and the question is whether differences in the galactic field over the diameter of the cluster are comparable with (particularly greater than) the internal field. Stability of a cluster in the presence of the galactic field has been investigated by Bok (H.C.O. Circular No. 384). Bok finds that the cluster is least stable along that axis which is radial to the centre of this galaxy, and that the cluster is stable at a distance r from its centre if the density $\Delta(r)$ satisfies the inequality

$$\Delta(r) > \frac{3\Theta A}{\pi\Gamma a}$$

where Θ is the circular velocity in the galactic field, A is Oort's constant and a the distance to the galactic centre. With $\Theta = 216$ km/sec, $A = 19{\cdot}5$ (km/sec)/kpc and $a = 8{\cdot}2$ kpc we have $\Delta(r) > 0{\cdot}114 \bigcirc$ pc^{-3}.

If the mass of the Pleiades is $500 \bigcirc$ and we take the distance r as 6·79 pc. the limiting radius in the paper $\Delta(r) = 0{\cdot}353 \bigcirc$pc^{-3}, which satisfies the Bok criterion with something to spare.

The cluster is therefore stable in Bok's sense. The effect of this galactic field is to destroy gravitational spherical symmetry, but not presumably to an extent which would easily be observed. It is tempting to suppose that since Bok's limit for a mass of $500 \bigcirc$ is reached at 10·2 pc, not very far outside the adopted limit of the Pleiades, it is the galactic gravitational field actually which limits the cluster (causes the cut off)—a point of view which has been put to me privately on many occasions by S. C. B. Gascoigne, while discussing clusters generally.

FINITE ATMOSPHERES WITH ISOTROPIC SCATTERING
II. INCREASE OF LINE STRENGTH TO THE LIMB

I. W. Busbridge

(Received 1955 December 29)

Summary

The following problem in the theory of the formation of absorption lines is solved by the method developed in Paper I: An atmosphere of finite thickness lies above a photosphere of infinite extent, both being stratified in plane parallel layers. The absorption lines are formed by coherent isotropic scattering in the atmosphere, and there is continuous emission according to a linear Planck function throughout both photosphere and atmosphere. It is required to find the emergent intensity at any point of the line profile. Subject to certain assumptions, the exact solution is found in terms of the X- and Y-functions and their moments. Some numerical results are obtained and a theory is put forward to account for the variations in the intensities of faint and strong lines across the solar disk.

---

1. ***Introduction.***—In recent years, most of the theoretical papers on the formation of absorption lines have dealt with the Milne–Eddington model, in which lines are formed throughout an atmosphere of infinite extent. One phenomenon which cannot be accounted for in this way is the strengthening of faint lines to the limb of the sun. This was first observed by Dr Adam (**1**). She found that strong lines, on the other hand, decrease in strength towards the limb.*

In some circumstances, a model which comes closer to physical reality is that in which the absorption lines are formed in a layer near to the surface and such a model will be considered in this paper. For the sake of clarity, the layer in which the absorption lines are formed will be called the atmosphere, and the semi-infinite layer below this will be called the photosphere, though there will, in fact, be no difference between the two outside the line frequencies.

With this nomenclature, the following problem will be considered: A plane parallel atmosphere of thickness x_1 lies above a plane parallel photosphere of infinite extent. Throughout both atmosphere and photosphere there is continuous emission according to a linear Planck function. Absorption lines are formed by coherent isotropic scattering in the atmosphere. It is required to find the emergent intensity at any point of the line profile considered.†

In (**3**), to which I shall refer as Paper I, I have developed a method for finite atmospheres, which was originally given by Ambartsumian (**2**) for semi-infinite atmospheres. With the aid of this, it is a comparatively simple matter to find the

* Houtgast (**6**) found that the wings of some strong lines are strengthened. An account of all such investigations is given by Unsöld in (**7**).

† This model is almost the same as that considered by Houtgast in (**6**). In obtaining the emergent intensity, he used the Eddington approximations.

exact solution of the stated problem in terms of the X- and Y-functions and their moments. This is done in Sections 2–4.

Extensive tables of X- and Y-functions (**5**) have been compiled, with the aid of an electronic computer, by Chandrasekhar, Breen and Franklin. For reasons which will appear in Section 5, only a few numerical results can be calculated with the aid of these tables. These results are, however, of considerable interest, and with these as a basis it is possible to suggest an explanation of the phenomenon referred to above.

2. *The Milne integral equation.*—We shall solve the problem outlined above subject to certain conditions. Throughout both the photosphere and the atmosphere we assume that

(i) the variations of the continuous absorption coefficient κ over the range of frequencies considered may be neglected;

(ii) κ is independent of the depth x below the surface of the atmosphere;

(iii) the Planck function $B(\nu, T)$ can be represented in the form

$$B(\nu, T) = b_0 + b_1\tau, \tag{2.1}$$

where

$$\tau = \int_0^x \kappa\rho\, dx, \tag{2.2}$$

and where the variations of the coefficients b_0 and b_1 over the range of frequencies considered may be neglected.

Throughout the atmosphere we assume, in addition, that

(iv) the ratio η_ν of the line scattering coefficient to κ is independent of τ;

(v) the scattering in the line frequencies is coherent, i.e. the frequency re-emitted within the line depends only on the radiation absorbed at the same frequency;

(vi) the coefficient ϵ, introduced to allow for thermal emission within the line, is independent of both ν and τ.

Let $\tau = \tau_1$ when $x = x_1$. In the photosphere ($\tau \geqslant \tau_1$) and outside the line frequencies in the atmosphere ($0 \leqslant \tau \leqslant \tau_1$) the intensity $I(\tau, \mu)$ at the optical depth τ and at an angle $\cos^{-1}\mu$ with the outwards drawn normal satisfies the transfer equation

$$\mu \frac{dI(\tau,\mu)}{d\tau} = I(\tau, \mu) - (b_0 + b_1\tau). \tag{2.3}$$

The solution of this, subject to the boundary condition

$$I(0, -\mu) \equiv 0 \qquad (0 < \mu \leqslant 1) \tag{2.4}$$

together with the condition that $I(\tau, \mu)$ is at most $O(\tau)$ for large τ, is given by

$$I(\tau, +\mu) = b_0 + b_1(\mu + \tau), \tag{2.5}$$

$$I(\tau, -\mu) = b_0 + b_1(\tau - \mu) - (b_0 - b_1\mu)e^{-\tau/\mu} \tag{2.6}$$

where $0 \leqslant \mu \leqslant 1$. Hence the intensity emerging from the surface of the photosphere is

$$I(\tau_1, +\mu) = b_0 + b_1\tau_1 + b_1\mu, \tag{2.7}$$

and that emerging in the continuous spectrum is

$$I(0, +\mu) = b_0 + b_1\mu. \tag{2.8}$$

Now consider the radiation in the atmosphere in the line frequencies. Here the intensity $I_\nu(\tau,\mu)$ satisfies the transfer equation

$$\mu\frac{dI_\nu(\tau,\mu)}{d\tau}=(1+\eta_\nu)I_\nu(\tau,\mu)-\tfrac{1}{2}(1-\epsilon)\eta_\nu\int_{-1}^{1}I_\nu(\tau,\mu')\,d\mu' -(1+\epsilon\eta_\nu)(b_0+b_1\tau), \tag{2.9}$$

and the boundary conditions

$$\left.\begin{aligned} &I_\nu(0,-\mu)=0 \qquad (0<\mu\leqslant 1),\\ &I_\nu(\tau_1,+\mu)=b_0+b_1\tau_1+b_1\mu \qquad (0<\mu\leqslant 1). \end{aligned}\right\} \tag{2.10}$$

The latter comes from equation (2.7).

If we write

$$t_\nu=(1+\eta_\nu)\tau, \qquad t_1=(1+\eta_\nu)\tau_1, \tag{2.11}$$

$$\lambda_\nu=\frac{1+\epsilon\eta_\nu}{1+\eta_\nu}, \qquad n_\nu=\frac{1}{1+\eta_\nu}, \tag{2.12}$$

and if we replace $I_\nu(\tau,\mu)$ by $I_\nu(t_\nu,\mu)$ (as can be done without ambiguity), then (2.9) and (2.10) become

$$\mu\frac{dI_\nu(t_\nu,\mu)}{dt_\nu}=I_\nu(t_\nu,\mu)-\tfrac{1}{2}(1-\lambda_\nu)\int_{-1}^{1}I_\nu(t_\nu,\mu')\,d\mu' -\lambda_\nu(b_0+b_1n_\nu t_\nu), \tag{2.13}$$

and

$$\left.\begin{aligned} &I_\nu(0,-\mu)=0,\\ &I_\nu(t_1,+\mu)=b_0+b_1n_\nu t_1+b_1\mu, \end{aligned}\right\} \tag{2.14}$$

where $0<\mu\leqslant 1$.

Let

$$\mathfrak{I}_\nu(t_\nu)=\tfrac{1}{2}(1-\lambda_\nu)\int_{-1}^{1}I_\nu(t_\nu,\mu')\,d\mu'+\lambda_\nu(b_0+b_1n_\nu t_\nu). \tag{2.15}$$

Then (see Paper I, Section 2) $\mathfrak{I}_\nu(t_\nu)$ satisfies the Milne equation

$$\mathfrak{I}_\nu(t_\nu)=(1-\lambda_\nu)\bar{\Lambda}_{t_\nu}\{\mathfrak{I}_\nu(t')\}+B_\nu(t_\nu), \tag{2.16}$$

where

$$\begin{aligned} B_\nu(t)&=\lambda_\nu(b_0+b_1n_\nu t)+\tfrac{1}{2}(1-\lambda_\nu)\int_0^1(b_0+b_1n_\nu t_1+b_1\mu')e^{-(t_1-t)/\mu'}d\mu'\\ &=\lambda_\nu(b_0+b_1n_\nu t)+\tfrac{1}{2}(1-\lambda_\nu)[(b_0+b_1n_\nu t_1)E_2(t_1-t)+b_1E_3(t_1-t)]. \end{aligned} \tag{2.17}$$

The operator $\bar{\Lambda}$ in (2.16) is defined by [cf. Paper I, equation (2.10)]

$$\bar{\Lambda}_t\{f(t')\}=\tfrac{1}{2}\int_0^{t_1}f(t')E_1(|t'-t|)\,dt', \tag{2.18}$$

and

$$E_n(t)=\int_1^\infty e^{-tx}\frac{dx}{x^n}. \tag{2.19}$$

The exact solution of (2.16), when $B_\nu(t)$ is given by (2.17), is a sum of multiples of the solutions of (2.16) when $B_\nu(t)$ has the values 1, t, $E_2(t_1-t)$,

$E_3(t_1-t)$. The emergent intensities corresponding to the first two were found in Paper I; those corresponding to the last two are found in the next section.

3. *The solution of* (2.16) *when* $B_\nu(t)=E_n(t_1-t)$.—In this section I shall revert to the notation of Paper I in order to be able to quote formulae from that paper without change of notation. These will be quoted in the form I(1.1) etc.

We have to solve the integral equation

$$\mathfrak{J}^n(\tau)=\varpi\bar{\Lambda}_\tau\{\mathfrak{J}^n(t)\}+E_n(\tau_1-\tau) \qquad (0<\varpi<1) \tag{3.1}$$

for $n=2,3,\ldots,\mathfrak{J}^n(\tau)$ being the unknown function. We shall solve for the functions $\mathfrak{j}_0{}^n(\mu^{-1})$ and $\mathfrak{j}_1{}^n(\mu^{-1})$, where

$$\mathfrak{j}_0{}^n(s)=s\int_0^{\tau_1}\mathfrak{J}^n(t)e^{-st}\,dt, \tag{3.2}$$

$$\mathfrak{j}_1{}^n(s)=s\int_0^{\tau_1}\mathfrak{J}^n(\tau_1-t)e^{-st}\,dt. \tag{3.3}$$

As in I(2.17), we have the relation

$$\mathfrak{j}_1{}^n(\mu^{-1})=-e^{-\tau_1/\mu}\mathfrak{j}_0{}^n(-\mu^{-1}). \tag{3.4}$$

Since also, by I(4.26),

$$Y(\mu)=e^{-\tau_1/\mu}X(-\mu), \tag{3.5}$$

the value of $\mathfrak{j}_1{}^n(\mu^{-1})$ can be written down from that of $\mathfrak{j}_0{}^n(\mu^{-1})$ if this is known in terms of X- and Y-functions.

When $n=2$, the solution of (3.1) can be found from Section 9 of Paper I in which the equation

$$\Phi^2(\tau)=\varpi\bar{\Lambda}_\tau\{\Phi^2(t)\}+\tfrac{1}{2}\varpi E_2(\tau) \qquad (0<\varpi<1) \tag{3.6}$$

was solved. In (3.1) the surfaces $\tau=0$ and $\tau=\tau_1$ are interchanged. Hence

$$\mathfrak{j}_0{}^2(\mu^{-1})=2\varpi^{-1}\phi_1{}^2(\mu^{-1}), \qquad \mathfrak{j}_1{}^2(\mu^{-1})=2\varpi^{-1}\phi_0{}^2(\mu^{-1}), \tag{3.7}$$

and therefore, by I(9.15) and I(9.16),*

$$\mathfrak{j}_0{}^2(\mu^{-1})=2\varpi^{-1}\{y_0X(\mu)+(1-x_0)Y(\mu)-e^{-\tau_1/\mu}\}, \tag{3.8}$$

$$\mathfrak{j}_1{}^2(\mu^{-1})=2\varpi^{-1}\{1-(1-x_0)X(\mu)-y_0Y(\mu)\}. \tag{3.9}$$

Now let $n>2$. Then on using the differentiation formula I(3.3) and the relation

$$\frac{d}{d\tau}E_n(\tau)=-E_{n-1}(\tau). \tag{3.10}$$

We obtain from (3.1)

$$\frac{d}{d\tau}\mathfrak{J}^n(\tau)=\varpi\bar{\Lambda}_\tau\left\{\frac{d}{dt}\mathfrak{J}^n(t)\right\}+\tfrac{1}{2}\varpi\mathfrak{J}^n(0)E_1(\tau)$$
$$-\tfrac{1}{2}\varpi\mathfrak{J}^n(\tau_1)E_1(\tau_1-\tau)+E_{n-1}(\tau_1-\tau),$$

and hence

$$\frac{d}{d\tau}\mathfrak{J}^n(\tau)-\mathfrak{J}^{n-1}(\tau)=\varpi\bar{\Lambda}_\tau\left\{\frac{d}{dt}\mathfrak{J}^n(t)-\mathfrak{J}^{n-1}(t)\right\}$$
$$+\tfrac{1}{2}\varpi\mathfrak{J}^n(0)E_1(\tau_1)-\tfrac{1}{2}\varpi\mathfrak{J}^n(\tau_1)E_1(\tau_1-\tau). \tag{3.11}$$

* $x_r=\frac{1}{2}\varpi\int_0^1\mu^rX(\mu)\,d\mu$, $y_r=\frac{1}{2}\varpi\int_0^1\mu^rY(\mu)\,d\mu$, where $r=0,1,2,\ldots$.

On subtracting from (3.11) $\frac{1}{2}\varpi\mathfrak{B}^n(0)$ times I(4.3) and adding $\frac{1}{2}\varpi\mathfrak{B}^n(\tau_1)$ times I(4.4), we get the homogeneous Milne equation

$$\frac{d}{d\tau}\mathfrak{B}^n(\tau)-\mathfrak{B}^{n-1}(\tau)-\tfrac{1}{2}\varpi\mathfrak{B}^n(0)\int_1^\infty J(\tau,x)\frac{dx}{x}+\tfrac{1}{2}\varpi\mathfrak{B}^n(\tau_1)\int_1^\infty J(\tau_1-\tau,x)\frac{dx}{x}$$
$$=\varpi\bar{\Lambda}_\tau\left\{\frac{d}{dt}\mathfrak{B}^n(t)-\mathfrak{B}^{n-1}(t)-\tfrac{1}{2}\varpi\mathfrak{B}^n(0)\int_1^\infty J(t,x)\frac{dx}{x}+\tfrac{1}{2}\varpi\mathfrak{B}^n(\tau_1)\int_1^\infty J(\tau_1-t,x)\frac{dx}{x}\right\}$$

and, ignoring solutions which increase at exponential rate, the solution of this is

$$\frac{d}{d\tau}\mathfrak{B}^n(\tau)-\mathfrak{B}^{n-1}(\tau)-\tfrac{1}{2}\varpi\mathfrak{B}^n(0)\int_1^\infty J(\tau,x)\frac{dx}{x}+\tfrac{1}{2}\varpi\mathfrak{B}^n(\tau_1)\int_1^\infty J(\tau_1-\tau,x)\frac{dx}{x}=0.\quad(3.12).$$

Multiply (3.12) by $e^{-s\tau}$ and integrate with respect to τ over $(0,\tau_1)$ integrating the first term by parts. Then, by (3.2) and by I(4.7) and I(4.10), we have

$$e^{-s\tau_1}\mathfrak{B}^n(\tau_1)-\mathfrak{B}^n(0)+\mathfrak{j}_0{}^n(s)-s^{-1}\mathfrak{j}_0{}^{n-1}(s)$$
$$=\tfrac{1}{2}\varpi\mathfrak{B}^n(0)\int_1^\infty R(s,x)\frac{dx}{x}-\tfrac{1}{2}\varpi\mathfrak{B}^n(\tau_1)e^{-s\tau_1}\int_1^\infty R(-s,x)\frac{dx}{x}.$$

By I(4.12) and I(4.13), this becomes

$$\mathfrak{j}_0{}^n(s)-s^{-1}\mathfrak{j}_0{}^{n-1}(s)=\mathfrak{B}^n(0)J(0,s)-\mathfrak{B}^n(\tau_1)J(\tau_1,s).\quad(3.13)$$

Finally, on putting $s=\mu^{-1}$ and using I(4.21), we have

$$\mathfrak{j}_0{}^n(\mu^{-1})-\mu\mathfrak{j}_0{}^{n-1}(\mu^{-1})=\mathfrak{B}^n(0)X(\mu)-\mathfrak{B}^n(\tau_1)Y(\mu).\quad(3.14)$$

This holds for $n=3,4,\ldots$.

The solution of (3.14) in terms of $\mathfrak{j}_0{}^2(\mu^{-1})$ is

$$\mathfrak{j}_0{}^n(\mu^{-1})=X(\mu)\{\mathfrak{B}^n(0)+\mu\mathfrak{B}^{n-1}(0)+\ldots+\mu^{n-3}\mathfrak{B}^3(0)\}+\mu^{n-2}\mathfrak{j}_0{}^2(\mu^{-1})$$
$$-Y(\mu)\{\mathfrak{B}^n(\tau_1)+\mu\mathfrak{B}^{n-1}(\tau_1)+,..+\mu^{n-3}\mathfrak{B}^3(\tau_1)\},\quad(3.15)$$

and, by (3.4) and (3.5),

$$\mathfrak{j}_1{}^n(\mu^{-1})=X(\mu)\{\mathfrak{B}^n(\tau_1)-\mu\mathfrak{B}^{n-1}(\tau_1)+\ldots+(-\mu)^{n-3}\mathfrak{B}^3(\tau_1)\}+(-\mu)^{n-2}\mathfrak{j}_1{}^2(\mu^{-1})$$
$$-Y(\mu)\{\mathfrak{B}^n(0)-\mu\mathfrak{B}^{n-1}(0)+\ldots+(-\mu)^{n-3}\mathfrak{B}^3(0)\}.\quad(3.16)$$

The functions $\mathfrak{j}_0{}^2(\mu^{-1})$ and $\mathfrak{j}_1{}^2(\mu^{-1})$ are given by (3.8) and (3.9).

We now have to determine the $(2n-4)$ constants $\mathfrak{B}^r(0)$, $\mathfrak{B}^r(\tau_1)$ $(r=3,4,\ldots,n)$. On putting $\tau=0$ and $\tau=\tau_1$ in (3.1) and proceeding as in I(7.12) and I(7.13), we get

$$\mathfrak{B}^n(0)=\tfrac{1}{2}\varpi\int_0^1\mathfrak{j}_0{}^n(\mu^{-1})\,d\mu+E_n(\tau_1),\quad(3.17)$$

$$\mathfrak{B}^n(\tau_1)=\tfrac{1}{2}\varpi\int_0^1\mathfrak{j}_1{}^n(\mu^{-1})\,d\mu+\frac{1}{n-1}.\quad(3.18)$$

When the values of $\mathfrak{j}_0{}^n(\mu^{-1})$ and $\mathfrak{j}_1{}^n(\mu^{-1})$ given by (3.15) and (3.16) are substituted into these equations we get the following equations for the constants:

$$\mathfrak{B}^n(0)(1-x_0)-\mathfrak{B}^{n-1}(0)x_1-\ldots-\mathfrak{B}^3(0)x_{n-3}+\mathfrak{B}^n(\tau_1)y_0+\mathfrak{B}^{n-1}(\tau_1)y_1+\ldots$$
$$+\mathfrak{B}^3(\tau_1)y_{n-3}=\tfrac{1}{2}\varpi\int_0^1\mu^{n-2}\mathfrak{j}_0{}^2(\mu^{-1})\,d\mu+E_n(\tau_1),\quad(3.19)$$

$$\mathfrak{B}^n(\tau_1)(1-x_0)+\mathfrak{B}^{n-1}(\tau_1)x_1-\ldots+(-1)^{n-2}\mathfrak{B}^3(\tau_1)x_{n-3}+\mathfrak{B}^n(0)y_0-\mathfrak{B}^{n-1}(0)y_1+\ldots$$
$$+(-1)^{n-3}\mathfrak{B}^3(0)y_{n-3}=(-1)^{n-2}\tfrac{1}{2}\varpi\int_0^1\mu^{n-2}\mathfrak{j}_1{}^2(\mu^{-1})\,d\mu+\frac{1}{n-1}.\quad(3.20)$$

From (3.8) and (3.9),

$$\tfrac{1}{2}\varpi\int_0^1 \mu^{n-2}\mathfrak{i}_0^2(\mu^{-1})\,d\mu = 2\varpi^{-1}\{y_0x_{n-2}+(1-x_0)y_{n-2}\}-E_n(\tau_1), \tag{3.21}$$

$$\tfrac{1}{2}\varpi\int_0^1 \mu^{n-2}\mathfrak{i}_1^2(\mu^{-1})\,d\mu = \frac{1}{n-1}-2\varpi^{-1}\{(1-x_0)x_{n-2}+y_0y_{n-2}\}. \tag{3.22}$$

The equations (3.19)–(3.22) enable us to determine successively the coefficients $\mathfrak{I}^r(0)$, $\mathfrak{I}^r(\tau_1)$ with $r=3,4,\ldots$.

When $n=3$, (3.19) and (3.21) give

$$\mathfrak{I}^3(0)(1-x_0)+\mathfrak{I}^3(\tau_1)y_0 = 2\varpi^{-1}\{y_0x_1+(1-x_0)y_1\}. \tag{3.23}$$

Also (3.20) and (3.22) give

$$\mathfrak{I}^3(0)y_0+\mathfrak{I}^3(\tau_1)(1-x_0) = 2\varpi^{-1}\{(1-x_0)x_1+y_0y_1\}, \tag{3.24}$$

and hence we have

$$\mathfrak{I}^3(0)=2\varpi^{-1}y_1, \qquad \mathfrak{I}^3(\tau_1)=2\varpi^{-1}x_1. \tag{3.25}$$

On substituting these values into (3.15) and (3.16) (with $n=3$) and using (3.8) and (3.9), we obtain

$$\mathfrak{i}_0^3(\mu^{-1}) = 2\varpi^{-1}\{[y_1+y_0\mu]X(\mu)-[x_1-(1-x_0)\mu]Y(\mu)-\mu e^{-\tau_1/\mu}\}, \tag{3.26}$$

$$\mathfrak{i}_1^3(\mu^{-1}) = 2\varpi^{-1}\{[x_1+(1-x_0)\mu]X(\mu)-[y_1-y_0\mu]Y(\mu)-\mu\}. \tag{3.27}$$

Equations (3.26) and (3.8) are the ones needed to complete the solution of the problem in Section 2.

4. *The emergent intensity.*—We now return to the notation of Section 2. By I(2.5), the emergent intensity in the problem given by (2.13) and (2.14) is

$$I_\nu(0,+\mu) = (b_0+b_1n_\nu t_1+b_1\mu)e^{-\tau_1/\mu}+\mathfrak{i}_0(\mu^{-1}), \tag{4.1}$$

where

$$\mathfrak{i}_0(\mu^{-1}) = \int_0^{t_1}\mathfrak{I}_\nu(t)e^{-t/\mu}\frac{dt}{\mu}. \tag{4.2}$$

This is the sum of I(7.21) (with $a_1=\lambda_\nu b_0$, $a_0=\lambda_\nu b_1n_\nu$), (3.8) multiplied by $\frac{1}{2}(1-\lambda_\nu)(b_0+b_1n_\nu t_1)$ and (3.26) multiplied by $\frac{1}{2}(1-\lambda_\nu)b_1$. In each case τ_1 is replaced by t_1. Since $\varpi=1-\lambda_\nu$, we obtain the following expression for the emergent intensity:

$$\begin{aligned} I_\nu(0,+\mu) = {} & X(\mu)\{b_0(1-x_0)+b_1[n_\nu x_1+(1-n_\nu)y_1]+b_1\mu[n_\nu(1-x_0)+(1-n_\nu)y_0]\} \\ & +Y(\mu)\{b_0y_0-b_1[(1-n_\nu)x_1+n_\nu y_1]+b_1\mu[(1-n_\nu)(1-x_0)+n_\nu y_0]\}. \end{aligned} \tag{4.3}$$

In (5), Chandrasekhar and Elbert have given the moments α_r, β_r ($r=0,1$), where

$$\alpha_r=\int_0^1 X(\mu)\mu^r\,d\mu, \qquad \beta_r=\int_0^1 Y(\mu)\mu^r\,d\mu, \tag{4.4}$$

so that, in our case,

$$x_r=\tfrac{1}{2}(1-\lambda_\nu)\alpha_r, \qquad y_r=\tfrac{1}{2}(1-\lambda_\nu)\beta_r. \tag{4.5}$$

Hence for calculations (4.3) must be written in the form

$$I_\nu(0, +\mu) = \tfrac{1}{2}(1-\lambda_\nu)X(\mu)\{b_0[2(1-\lambda_\nu)^{-1}-\alpha_0] + b_1[n_\nu\alpha_1 + (1-n_\nu)\beta_1] + b_1\mu[n_\nu(2[1-\lambda_\nu]^{-1}-\alpha_0) + (1-n_\nu)\beta_0]\} + \tfrac{1}{2}(1-\lambda_\nu)Y(\mu) \times \{b_0\beta_0 - b_1[(1-n_\nu)\alpha_1 + n_\nu\beta_1] + b_1\mu[(1-n_\nu)(2[1-\lambda_\nu]^{-1}-\alpha_0) + n_\nu\beta_0]\}. \quad (4.6)$$

As a check on this formula we can let $t_1 \to \infty$. Then $X(\mu) \to H(\mu)$ and $Y(\mu) \to 0$, and we have

$$I_\nu(0, +\mu) = \tfrac{1}{2}(1-\lambda_\nu)H(\mu)\{b_0[2(1-\lambda_\nu)^{-1}-\alpha_0] + b_1 n_\nu\alpha_1 + b_1\mu n_\nu[2(1-\lambda_\nu)^{-1}-\alpha_0]\}, \quad (4.7)$$

where

$$\alpha_r = \int_0^1 H(\mu)\mu^r\, d\mu. \quad (4.8)$$

By (**3**), Chap. V, Theorem 1, α_0 satisfies the equation

$$\tfrac{1}{2}(1-\lambda_\nu)\alpha_0 = 1 - \lambda_\nu^{1/2}.$$

On using this and the values for λ_ν and n_ν given by (2.12), (4.7) reduces to equation (66) of (**3**), Chap. XII.

5. *Numerical results.*—The residual intensity in the line at frequency ν (expressed as a percentage) is

$$r_\nu(\mu) = 100 I_\nu(0, +\mu)/I(0, +\mu), \quad (5.1)$$

where $I_\nu(0, +\mu)$ is given by (4.6) and $I(0, +\mu)$ by (2.8). In the following calculations we have taken $b_1/b_0 = 1{\cdot}5$, $\epsilon = 0$ and (for comparison) $\epsilon = 1$.

If $\epsilon = 0$, then $n_\nu = \lambda_\nu$. On writing $\varpi_\nu = 1 - \lambda_\nu$, we get the following formula for $r_\nu(\mu)$:

$$\frac{r_\nu(\mu)}{100} = \frac{\varpi_\nu X(\mu)}{2+3\mu}\{2\varpi_\nu^{-1} - \alpha_0 + \tfrac{3}{2}(\lambda_\nu\alpha_1 + \varpi_\nu\beta_1) + \tfrac{3}{2}\mu[\lambda_\nu(2\varpi_\nu^{-1}-\alpha_0) + \varpi_\nu\beta_0]\} + \frac{\varpi_\nu Y(\mu)}{2+3\mu}\{\beta_0 - \tfrac{3}{2}(\varpi_\nu\alpha_1 + \lambda_\nu\beta_1) + \tfrac{3}{2}\mu[\varpi_\nu(2\varpi_\nu^{-1}-\alpha_0) + \lambda_\nu\beta_0]\}. \quad (5.2)$$

The X- and Y-functions are tabulated in (**5**) as functions of τ, ϖ and μ, where

$$\left.\begin{aligned} \tau &= 0{\cdot}05,\ 0{\cdot}10,\ 0{\cdot}15,\ 0{\cdot}20,\ 0{\cdot}25,\ 0{\cdot}50,\ 1{\cdot}00, \\ \varpi &= 0{\cdot}50,\ 0{\cdot}80,\ 0{\cdot}90,\ 0{\cdot}95,\ 1{\cdot}00, \end{aligned}\right\} \quad (5.3)$$

and $0 \leqslant \mu \leqslant 1$. In our case,

$$\tau = t_1 = (1+\eta_\nu)\tau_1, \qquad \varpi = \varpi_\nu = \eta_\nu/(1+\eta_\nu). \quad (5.4)$$

Thus we get the following possible values of η_ν:

$$\eta_\nu = 1,\ 4,\ 9,\ 19;$$

and corresponding to these, the largest possible values of τ_1 are

$$\tau_1 = 0{\cdot}5,\ 0{\cdot}2,\ 0{\cdot}1,\ 0{\cdot}05 \quad (5.5)$$

respectively.

The following table gives the values of $r_\nu(1)$ and $r_\nu(0)$ whenever these can be calculated from the tables. The values in italics were estimated graphically. They could, of course, have been obtained by interpolation, but I doubt whether greater accuracy would have been achieved. The last line of the table gives the Milne–Eddington case ($\tau_1 = \infty$).

TABLE I

$r_\nu(1)$ and $r_\nu(0)$ when $\epsilon = 0$

τ_1	μ	$\eta_\nu = 1$	$\eta_\nu = 4$	$\eta_\nu = 9$	$\eta_\nu = 19$
0·05	1	96·98	88·00	77·83	61·93
	0	91·85	80·00	68·25	53·89
0·1	1	94·31	80·35	64·08	..
	0	90·51	74·05	58·44	..
0·2	1	*90·00*	68·24	..	..
	0	*88·50*	66·67	..	..
0·5	1	80·43	..	..	..
	0	85·26	..	..	..
∞	1	67·60	42·81	31·03	22·78
	0	82·03	53·55	37·19	25·57

The value of $r_\nu(0)$ has been given in Table I because it enables us to see at a glance which lines will be strengthened towards the limb for the values of η_ν shown. Moreover, by considering the difference $r_\nu(1) - r_\nu(0)$, it is seen that the change in residual intensity is almost independent of η_ν for a given τ_1. Hence in studying the centre to limb variations of $r_\nu(\mu)$ it is enough to consider the values of η_ν and τ_1 corresponding to the extreme right-hand member in each row. The corresponding values of $r_\nu(\mu)$ for $0{\cdot}2 \leqslant \mu \leqslant 1$ are given in Table II. When $\tau_1 = \infty$, I have taken $\eta_\nu = 1$ because this gives about the same intensity when $\mu = 1$ as in three of the other cases.

TABLE II

Centre to limb variations in $r_\nu(\mu)$ when $\epsilon = 0$

μ	$\tau_1 = 0{\cdot}05$ $\eta_\nu = 19$	$\tau_1 = 0{\cdot}1$ $\eta_\nu = 9$	$\tau_1 = 0{\cdot}2$ $\eta_\nu = 4$	$\tau_1 = 0{\cdot}5$ $\eta_\nu = 1$	$\tau_1 = \infty$ $\eta_\nu = 1$
1·0	61·93	64·08	68·24	80·43	67·60
0·9	60·86	63·09	67·42	80·00	68·56
0·8	59·86	62·17	66·67	79·64	69·63
0·7	58·97	61·38	66·04	79·39	70·82
0·6	58·25	60·77	65·62	79·32	72·16
0·5	57·77	60·42	65·50	79·52	73·67
0·4	57·62	60·43	65·77	80·12	75·36
0·3	57·76	60·79	66·50	81·22	77·26
0·2	57·90	61·30	67·56	82·89	79·39

From Table II the following conclusions can be drawn:

(i) The shallower the atmosphere, the more are lines (for the given values of η_ν) strengthened towards the limb. For $\tau_1 = 0{\cdot}05$, $\eta_\nu = 19$, the greatest strengthening, viz. $\max[r_\nu(1) - r_\nu(\mu)]$, is about 7 per cent of the intensity at the centre. For $\tau_1 = 0{\cdot}5$, $\eta_\nu = 1$, it is only about 1·4 per cent.

(ii) The greatest strengthening occurs at about $\mu = 0{\cdot}4$ for $\tau_1 = 0{\cdot}05$ and the position moves towards the centre with increasing τ_1 until, for sufficiently large τ_1, the line is strongest in the centre.

When $\epsilon = 1$ then [by (2.12)] $\lambda_\nu = 1$ and $\varpi_\nu = 0$. As $\varpi_\nu \to 0$, $X(\mu) \to 1$ and $Y(\mu) \to e^{-t_1/\mu}$.* Hence on letting $\lambda_\nu \to 1$ in (4.6), we have

$$I_\nu(0, +\mu) = b_0 + b_1 n_\nu \mu + b_1(1 - n_\nu)\mu e^{-t_1/\mu}, \tag{5.6}$$

and, with $b_1/b_0 = 3/2$,

$$r_\nu(\mu) = 100\{1 - 3\mu(1 - n_\nu)(1 - e^{-t_1/\mu})/(2 + 3\mu)\}, \tag{5.7}$$

a formula which can be verified independently.

The following table for $\epsilon = 1$ corresponds to Table II.

TABLE III

Centre to limb variations in $r_\nu(\mu)$ when $\epsilon = 1$

μ	$\tau_1 = 0{\cdot}05$ $\eta_\nu = 19$	$\tau_1 = 0{\cdot}1$ $\eta_\nu = 9$	$\tau_1 = 0{\cdot}2$ $\eta_\nu = 4$	$\tau_1 = 0{\cdot}5$ $\eta_\nu = 1$	$\tau_1 = \infty$ $\eta_\nu = 1$
1·0	63·79	65·87	69·66	81·04	70·00
0·9	63·39	65·32	69·17	80·73	71·28
0·8	63·03	64·97	68·87	80·54	72·73
0·7	63·00	64·95	68·84	80·53	74·39
0·6	63·50	65·42	69·26	80·79	76·32
0·5	64·80	66·65	70·36	81·47	78·57
0·4	67·30	69·02	72·46	82·73	81·25
0·3	71·57	73·06	76·06	85·04	84·48
0·2	78·22	79·37	81·66	88·54	88·46

From Table III it is seen that the greatest strengthening is in every case less than 1·6 per cent of the intensity at the centre; the position of greatest strengthening is near the centre ($\mu = 0{\cdot}7$); the lines fade away rapidly towards the limb. (Actually $r_\nu(\mu) \to 100$ as $\mu \to 0$.)

6. *Discussion and conclusions.*—The values of $r_\nu(\mu)$ found above for $\tau_1 \leqslant 0{\cdot}5$ are comparable with the residual intensities in faint lines or in the wings of strong ones. Unfortunately, the results given by Dr Adam in (1) are mainly expressed in terms of equivalent widths and are not comparable with the results found here. It is evident from Tables II and III that the observed strengthening can be accounted for theoretically only by taking $\epsilon = 0$ or, perhaps, small, and the following discussion will therefore be concerned with the results when $\epsilon = 0$ (Tables I and II).

First consider the values of $r_\nu(1)$ in Table I. For a given value of η_ν the difference between the values of $r_\nu(1)$ for two different values of τ_1 gives a measure†

* This follows at once on letting $\varpi \to 0$ in equations (4.22) and (4.23) of Paper I.

† This is not strictly correct because the values are calculated on the assumption that there is no scattering in the layers below them.

of the contribution of the corresponding layer to the total absorption in the Milne–Eddington model. Thus for $\eta_\nu = 4$, the total absorption $1 - r_\nu(1)$ is 57·19 per cent, of which about 12 per cent arises from the layer $0 \leqslant \tau \leqslant 0{\cdot}05$, 8 per cent from the layer $0{\cdot}05 \leqslant \tau \leqslant 0{\cdot}1$, and so on. The larger the value of η_ν, the larger is the contribution from each successive layer, the increase getting bigger as the layer approaches the surface. In particular, when $\eta_\nu = 19$ a contribution of about 38 per cent towards the total absorption of 77·22 per cent comes from the topmost layer. This is what is meant by saying that strong lines are formed high in the atmosphere and weak ones low down.

Nevertheless, it is also true that *the larger the value of* τ_1, *the stronger will be the total absorption over* $(0, \tau_1)$ *for a given* η_ν. Moreover, the same residual intensity can be produced by taking different pairs of values of τ_1 and η_ν. For instance, $r_\nu(1)$ is approximately 66 per cent for $\eta_\nu = 9$, $\tau_1 = 0{\cdot}1$, for $\eta_\nu = 4$, $\tau_1 = 0{\cdot}2$, and for $\eta_\nu = 1$, $\tau_1 = \infty$ (cf. Table II, line 1). Only a more detailed knowledge of the conditions in the atmosphere of the Sun (including the variations of η_ν with depth) than we at present possess would enable us to decide between these pairs of values in the case of a particular line in the solar spectrum.

However, Table II shows that, even though the values of $r_\nu(1)$ may be about the same, the behaviour of $r_\nu(\mu)$ from centre to limb is very different. The smaller the value of τ_1, the more is the line strengthened towards the limb. This suggests that faint lines which are strengthened towards the limb must be formed in layers of optical depth τ_1 less than 0·5 (for which the strengthening is negligible); lines which are not strengthened must be formed in layers of optical depth τ_1 greater than 0·5. Since, as has been emphasised above, the total absorption over $(0, \tau_1)$ for a given η_ν increases with τ_1, the former would probably be weaker lines than the latter.

In order to account physically for the strengthening of any particular faint line according to this theory, one would have to show that, for the line in question, η_ν varied with depth in such a way that it could be well represented by a constant value for (say) $0 \leqslant \tau \leqslant 0{\cdot}2$ and by zero for $\tau > 0{\cdot}2$.

Acknowledgment.—I am indebted to Dr Adam, Dr Stibbs and Professor Plaskett for criticisms from the physical point of view and for some helpful suggestions.

St. Hugh's College,
Oxford:
1955 *December* 7.

References

(1) M. G. Adam, *M.N.*, **98**, 112, 1937; **100**, 595, 1940.
(2) V. A. Ambartsumian, *A.J. (USSR)*, **19**, 30, 1942.
(3) I. W. Busbridge, *M.N.*, **115**, 521, 1955.
(4) S. Chandrasekhar, *Radiative Transfer*, Oxford, 1950.
(5) S. Chandrasekhar, D. Elbert and A. Franklin, *Ap. J.*, **115**, 244 and 269, 1952.
(6) J. Houtgast, *Dissertation*, Utrecht: Schotanus & Jens, 1942.
(7) A. Unsöld, *Ann. der Phys.* (6), **3**, 124, 1948.

SOLAR ATMOSPHERIC HEATING BY HYDROMAGNETIC WAVES

J. H. Piddington

(Received 1956 January 31)

Summary

Previous estimates of solar atmospheric heating by hydromagnetic waves (due to Joule loss and viscosity) showed negligible heating. A new mechanism is described, involving neutral atoms, which leads to absorption (and heating) many orders of magnitude greater than previously believed. If hydromagnetic waves are present they must cause strong heating effects.

The formation of such waves from granules is described, their absorption at low levels, and partial reflection being discussed in some detail. A very rough order-of-magnitude estimate of energy flow is obtained. The region in which heating effects are important is restricted to the transition zone between lightly ionized and fully ionized gas. The energy absorbed in this region is estimated as $\sim 10^5$ erg cm^{-2}. sec^{-1}. Numerous particles with energies $\sim$100 EV are released in this region and these may account for the quiet (non-spot) corona.

The mechanism is likely to be important in connection with sunspot heating and flares and perhaps also interstellar hydromagnetic waves and cosmic ray generation.

---

1. *Introduction.*—Of the many theories advanced to explain the heating of the solar corona and chromosphere the most promising are those depending on energy transfer by wave motion upwards from sub-photospheric sources. The types of wave which have been considered are hydromagnetic (Alfvén (**1, 2**)) and pressure (Biermann (**3**) and others).

Recent observations of solar magnetic fields (**4**) indicate that these are widespread, covering polar and other extensive areas as well as spot regions. Furthermore the greatest heating effects are generally observed in regions permeated by magnetic fields. Hence if waves are effective in transporting energy they travel through ionized gas permeated by a magnetic field. Four and only four types of wave may propagate in such a medium (**5**) and at the frequencies concerned (presumably much below radio-frequencies) one of these, the space-charge or electron pressure wave, is excluded. The remaining three are all hydromagnetic waves although one has pressure (sound) waves as a special limiting case. Thus, in general, any waves which heat the solar atmosphere must be hydromagnetic waves.

It is desirable here to separate hydromagnetic waves into two categories (see, for example, ref. (**6**)). Two of the waves have velocities of order $V = H_0(4\pi\rho)^{-1/2}$ where H_0 is the magnitude of the steady magnetic field and ρ the gas density. These waves are largely transverse, they are called the ordinary (O) and extra-ordinary (E) waves according to their polarizations and have as limiting cases, when heavy ion motion is negligible, the corresponding radio O and E waves of the well-known magneto-ionic theory. The remaining (S) wave has a velocity

of the order of sound and is mainly longitudinal; it may be regarded as a modified sound wave. The present paper is primarily concerned with the O and E waves.

Alfvén's theory concerns the O and E waves; he considered that the associated electric fields and currents might cause Joule loss sufficient to account for the heating. Cowling (**7**) investigated the Joule loss and decided it was much too small to cause significant heating.* A more detailed investigation (**8, 6**) gave an estimated chromospheric heating rate about 10^8 or more times lower than that required to explain the observed effects. The possibility of effective heating by the O and E waves appeared to be remote. Incidentally, similar considerations (and others) dispose of the possibility of effective heating by more or less steady electric currents, a mechanism which has been suggested by a number of authors.

There is no theory of heating by the S wave but such would be a logical development from existing theories invoking sound waves.

It is the object of the present paper to re-discuss the absorption rates of the O and E waves in the solar atmosphere. A new factor, involving neutral atoms, is revealed which may enormously increase absorption; in some regions factors like 10^{10} are involved.

Although most solar atmospheric heating appears to take place near sunspots the new heating mechanism is not discussed here in that connection. The example chosen for more or less detailed analysis concerns O and E waves caused by solar granules in regions of weak but extensive magnetic fields, such as near the poles. This simpler example allows a discussion of the formation and partial reflection of the waves, as well as their absorption. However, the results given and some further calculations indicate that the mechanism may be very important in connection with heating near spots, flare formation and interstellar phenomena.

2. *Heating by hydromagnetic waves.*—The Joule loss of hydromagnetic waves has been found (**6**) from *conductivity* transport equations† and in the solar atmosphere is generally negligible. Another effect which causes absorption and hence heating, is viscosity which has been considered by van de Hulst (**9**). The ratio of viscosity loss to Joule loss is $4\pi\sigma\mu$ where σ is the electrical conductivity and μ the kinematic viscosity (c.g.s. electromagnetic units used throughout). The ratio may be considerably greater than unity in parts of the chromosphere but the heating effect due to viscosity is still negligible. .

When neutral atoms are present in numbers comparable with the heavy ions they have a negligible effect on the electron collision frequency, the reason is their very much smaller collision cross-section. However, for varying electric fields (as in hydromagnetic waves), neutral atoms do change the electrodynamic properties of the gas since the mass of the gas can no longer be considered situated in the ions (as in a binary gas) but to some extent in the neutral atoms. The two gases tend to move independently, thus causing a frictional loss. Consider a rather extreme case when the collision period of a neutral atom is of the same order as the wave period. Since the electromagnetic forces necessary to maintain hydromagnetic oscillations act only on the ions, the ion plasma (electrons and

* Even this reduced estimate of Joule loss appears much too large. The " dimension " of the wave (Cowling's L on p. 581) should be identified with the wavelength in the corona (**6**) and not with the size of the granule. If the steady magnetic field is 100 gauss this results in a further reduction of absorption by a factor of 10^6 or more.

† As opposed to Maxwell's momentum transfer equations which are also transport equations. A combination of the two is found necessary below.

heavy ions) tends to perform oscillations independently of the neutral atom gas while collisions between the gases tend to promote forced oscillations of the latter as discussed previously (ref. (**10**), p. 660). At times there will be considerable relative velocity between the two gases so that a collision between a heavy ion and a neutral atom will cause a substantial dissipation of wave energy, which reappears as thermal, excitation or ionization energy. On the other hand all ions share the common hydromagnetic oscillations so that collisions between them are not significant in this way.

The new dissipative process is not an ordinary Joule loss; nor is it an ordinary viscosity effect since it occurs (for finite wave amplitude) when the gas particles have no thermal motions. It may, if desired, be regarded as Joule loss due to Hall *drift* in the ternary gas. This drift may be large but as the plasma moves nearly as a whole the Hall *current* may be small or zero.

When the atom collision period is much less than the wave period the two gases move nearly in unison. However, the loss may be far greater than the ordinary Joule loss even under these conditions.

3. *Hydromagnetic waves in a partially ionized gas.*—The properties of hydromagnetic waves in a partially ionized gas may be studied in either of two ways. They may be found from a set of field equations already given (ref. (**8**), equations (14), (16) and their companion), combined with a dynamic equation describing the gas velocity in terms of the various forces acting on it. The conductivity components are those of a *partially ionized gas*; they comprise σ_0 parallel to the magnetic field and σ_1 and σ_2 perpendicular to the magnetic field, in and perpendicular to the plane of the electric field respectively. The composite or "effective" conductivity σ_3 is given by $\sigma_3 \equiv \sigma_1 + \sigma_2^2/\sigma_1$ and when small is associated with strong damping of the wave.* The gas velocity is the weighted mean velocity of the ion plasma and neutral atoms.

The alternative approach, permissible under conditions described below, is to regard the ion plasma (heavy ions and electrons only) as an entirely separate gas. The relevant field equation is that for a *fully ionized gas* (ref. (**8**), equation (17)):

$$\nabla^2 \mathbf{H} = 4\pi\sigma_3 \left\{ \frac{\partial \mathbf{H}}{\partial t} - \operatorname{curl}(\mathbf{v} \times \mathbf{H}) \right\} + \frac{\sigma_2}{\sigma_1} \frac{\partial}{\partial z} \operatorname{curl} \mathbf{H}, \qquad (1)$$

where $\mathbf{H}$ is the magnetic field, having a steady component $\mathbf{H}_0$ along Oz. The conductivity components and gas velocity $\mathbf{v}$ now refer to a *fully ionized gas*; this means that σ_2 and σ_3 are large when the collision frequency is low.

The effect of the neutral atoms is introduced through their frictional drag on the ion plasma and its effect on $\mathbf{v}$. Thus, instead of a single gas momentum equation, there are two. For simplicity the terms in gas pressure are omitted from these equations. The relative magnitude of these terms in the region of main interest (mid-chromosphere and above) is small and they may be neglected. At lower levels they are large but it has been shown (**6**) that even under these circumstances the velocity and absorption of the O and E waves in a fully ionized

* The small value of σ_3 in a partially ionized gas when collision frequencies are low has been discussed (**10**) for the case when only collisions with neutral atoms are important. Since the communication of the present paper T.G.Cowling has kindly sent me a copy of his paper *The dissipation of magnetic energy in an ionized gas* (*M.N.*, **116**, 114, 1956) in which he completes the discussion and shows that the effect may lead to unexpectedly rapid decay of magnetic energy in certain cases of astronomical interest.

gas are unaffected because the waves are mainly transverse. It seems safe at this stage to neglect the pressure terms, in which case the momentum equations are

$$\frac{\partial \mathbf{v}}{\partial t} + (\mathbf{v} - \mathbf{v}')\frac{\eta}{\tau_n} + \frac{V^2}{H_0^2}(\mathbf{H}_0 \times \operatorname{curl} \mathbf{H}) = 0, \tag{2}$$

$$\frac{\partial \mathbf{v}'}{\partial t} = (\mathbf{v} - \mathbf{v}')\frac{1}{\tau_n}, \tag{3}$$

where $\mathbf{v}'$ and τ_n are the velocity of the neutral atom gas and the collision period* of an atom and η is the ratio of mass densities of neutral atoms and ions.

Strictly speaking, either method of investigation is applicable only to weak waves (**10**), although the results may be suggestive of the effects of strong waves. No further limitation in this respect is necessitated by the use of separate gas velocities since $(\mathbf{v} - \mathbf{v}')$ and also its effect on collision periods must both be small. The second method of investigation imposes a further restriction: the collision rate of electrons with heavy ions must be substantially greater than with neutral atoms; this is assumed in calculating σ_1 and σ_2. Because of the larger collision cross-section of heavy ions the requirement is satisfied even though neutral atoms are about 1000 times more plentiful.

An advantage of the second method is that it discloses more about the relative velocity of the two gases; this is particularly important when the wave period is comparable with the neutral atom collision period. The second method may also reveal more about the underlying physical processes in the wave and is adopted here.

Plane wave solutions of equations (1)–(3) are sought of the form $\exp i(\omega t - k\xi)$ in a right-handed system x, y, z where $O\xi$ lies in the xz plane at an angle ψ to Oz, the direction of the steady magnetic field. Now let H_x, H_y, H_z be the maximum values of the components of the perturbation field $(\mathbf{H} - \mathbf{H}_0)$ and v_x, v_y, v_z those of the plasma velocity $\mathbf{v}$. In all cases the perturbation field lies in the phase planes so that $H_z = -\tan\psi H_x$. Substitute in the component equations:

$$\frac{\partial}{\partial t} = i\omega, \qquad \frac{\partial}{\partial x} = -ik\sin\psi,$$

$$\frac{\partial}{\partial y} = 0, \qquad \frac{\partial}{\partial z} = -ik\cos\psi,$$

$$\epsilon = \frac{4\pi\sigma_3}{\omega}, \qquad Q = \{1 + \eta(1 + i\omega\tau_n)^{-1}\}^{-1},$$

and

$$V = H_0(4\pi\rho)^{-1/2},$$

ρ being the mass density of the ion plasma alone. We find

$$(k^2 + i\epsilon\omega^2)H_x + i\epsilon H_0 \cos\psi k\omega v_x + \frac{\sigma_2}{\sigma_1}\cos^2\psi k^2 H_y = 0, \tag{4}$$

$$(k^2 + i\epsilon\omega^2)H_y + i\epsilon H_0 \cos\psi k\omega v_y - \frac{\sigma_2}{\sigma_1}k^2 H_x = 0, \tag{5}$$

* The mean period which elapses before atoms loose their ordered motion *relative to the ion plasma*. In equations of this nature, the mean velocity of the whole gas mixture is usually introduced and the collision period defined as the mean period which elapses before the atoms loose their ordered motion relative to the gas mixture (that is their peculiar velocity). The simplification results in a different value of collision period, the factor involved being small enough to neglect under the conditions assumed here.

$$H_0 \cos\psi Q^{-1}\omega v_x + V^2 k H_x = 0, \tag{6}$$

$$H_0 Q^{-1}\omega v_y + V^2 \cos\psi h H_y = 0, \tag{7}$$

which are identical with those of a binary gas (**6**) except for the term Q.

4. *Solution of the equations.*—The equations are solved as before (**6**); for convenience terms $(\epsilon\sigma_1 V^2)/\sigma_2$ are replaced by Ω/ω where Ω is the heavy-ion gyromagnetic frequency.* The polarization of the waves $(R=(H_y\cos\psi)/H_x)$ is found to be:

$$R = \frac{i}{2}\left\{\frac{Q\Omega}{\omega}\frac{\sin^2\psi}{\cos\psi} \pm \left(\frac{Q^2\Omega^2}{\omega^2}\frac{\sin^4\psi}{\cos^2\psi} + 4\right)^{1/2}\right\}. \tag{8}$$

Since Q is a complex quantity, R has both real and imaginary parts; the waves are partly plane, partly elliptically polarized. In the absence of neutral atoms they are elliptically polarized.

The dispersion equation is found to be:

$$\omega^2/k^2 = QV^2S^2 + \frac{i}{\epsilon}, \tag{9}$$

where

$$S = \left\{1 + \frac{\sin^2\psi}{2} \mp \left(\frac{\sin^4\psi}{4} + \frac{\omega^2\cos^2\psi}{\Omega^2 Q^2}\right)^{1/2}\right\}. \tag{10}$$

In a magnetic field of only one gauss $\Omega \sim 10^4$ rad sec^{-1} and as we are dealing with much lower wave frequencies the last term of equation (10) may be neglected so that $S=\cos\psi$ for the O wave; $S=1$ for the E wave, just as for waves in the absence of neutral atoms. The corresponding wave velocities are $Q^{1/2}V\cos\psi$ and $Q^{1/2}V$. The quantity Q has real and imaginary parts, the latter being caused by the presence of neutral atoms. When $\eta \to 0$, $Q \to 1$ in agreement with the results for a binary gas (**6**). When $\omega\tau_n \gg 1$ and $\omega\tau_n \gg \eta$ so that the two gases move independently we again have $Q \to 1$ as would be anticipated. In this case, although the wave velocity is not appreciably affected by the neutral atoms, there may still be considerable absorption. When $\omega\tau_n \ll 1$ so that the two gases are effectively bound together, $Q \sim (1+\eta)^{-1}$ and the velocities are $V'\cos\psi$ and $V' = V(1+\eta)^{-1/2}$, being smaller† than V because of the additional gas density. Finally when $\omega\tau_n \sim 1$ and η is not small a type of forced oscillation occurs associated with a considerable change in wave velocity and a high degree of absorption.

The wave absorption coefficient κ is equal in magnitude and opposite in sign to the imaginary part of k. When no neutral atoms are present ($Q=1$) this absorption is due to collisions between electrons and heavy ions and is given by the last term in equation (9). This contribution has been shown negligible (**8**) and will be neglected for the time being. Thus we have:

$$\kappa = -\left(\frac{\omega}{Q^{1/2}SV}\right)_{\text{imag.}}$$

* This is seen by substituting for ϵ and V, which were defined in the previous section, and also for σ_1, σ_2 and σ_3 whose values for a binary gas have been given (see, for example ref. (10), p. 658, noting that there the term ω represents the electron gyro-frequency $H_0 e/m$, where m is the electron mass). The ion gyro-frequency is $\Omega = H_0 e/M$ where M is the ion mass.

† V' and not V was the velocity previously found (**6**); the apparent discrepancy occurs because in the present paper the density determining V is that of the ion plasma alone. The real hydromagnetic velocity, provided the gases move together, is V' and this value is used below.

When $\omega\tau_n \ll 1$ (wave frequency is much less than the relevant collision frequency) this reduces to:

$$\kappa \simeq \frac{\omega^2\tau_n\eta}{2VS(1+\eta)^{1/2}} = \frac{\omega^2\tau_n\eta}{2V'S(1+\eta)}. \qquad (11)$$

This absorption coefficient, due to friction between the two interpenetrating gases, may be compared with that due to Joule losses (ref. (**6**), equation (20)). At the chromospheric level where the hydrogen is half ionized ($\eta = 1$) the electron density is about $3 \times 10^9\,\mathrm{cm}^{-3}$, the conductivity σ_0 about 2×10^{-8} e.m.u. and $\tau_n \sim 1$ (see Appendix 1). In a steady magnetic field of 100 gauss the absorption given by equation (11) is about 10^{10} times greater than that due to Joule heating (and 10^9 times greater than that due to normal viscous effects). In the corona the ratio is lower but heating by either mechanism at these levels is unimportant.

5. *Hydromagnetic waves from granules.*—Granules are convective cells moving upwards with velocities of about 1 km sec^{-1} and having lifetimes of a few minutes. The gas density in the granule is about $10^{-7}\,\mathrm{g\,cm}^{-3}$ so that the upward flow of kinetic energy is about $5 \times 10^7\,\mathrm{erg\,cm}^{-2}\,\mathrm{sec}^{-1}$, perhaps a thousand times or more that needed to maintain the corona in non-spot regions. Alfvén (**2**) has suggested that some of this energy is transferred upwards by hydromagnetic waves.

The actual processes involved in the upward transfer of this energy are largely speculative. However, there are sufficient data available to allow a semi-quantitative discussion which may be of some value.

Upward transfer of energy by mass motion may be ruled out. Even if the granules were moving into a vacuum above the photosphere, its total energy (thermal motion of its particles plus mass motion) would only raise it one or two hundred kilometres. If it were being thrust up from below by a large pressure gradient then the whole granule would be seen to emerge into the chromosphere.* The transfer must be by wave motion and in a weak magnetic field of say 5 gauss the only effective wave is the S wave (see Section 1). This has a velocity of about 10 km sec^{-1} compared with about 0·2 km sec^{-1} for the O and E waves, which gives a measure of the relative effectiveness of energy transfer.

As the waves travel upwards the density decreases while the magnetic field strength remains nearly unchanged. The elastic forces in the medium become increasingly electromagnetic in character and there is a tendency for the O and E waves to grow at the expense of the S wave. This process is no doubt helped by collision between waves from different granules and collision of the waves with irregularities in the gas distribution.

A critical level is reached at about 1500 km above the photosphere where (when $H_0 = 5$ gauss) the gas pressure† and the magnetic pressure $H_0^2/8\pi$ attain equality. Above this level the O and E waves outstrip the S wave attaining velocities of ~ 130 km sec^{-1} at 6000 km where the gas density has a value $\sim 2 \times 10^{-14}\,\mathrm{g\,cm}^{-1}$. It is likely that a significant proportion of the energy of the original granules is contained in these waves.

* Additional energy in the form of higher gas temperature or mass velocity, as suggested by Thomas (**11**), also seems to be contrary to observational evidence.

† For this and other such data a model of the lower chromosphere given by van de Hulst (ref. (**12**), p. 238) is used.

The "period" of the granules is a few (say 3) minutes (**12**), corresponding to an angular frequency $\omega \sim 0{\cdot}03\ \mathrm{sec}^{-1}$. The O and E waves will contain harmonics of this frequency, the proportion of which will be increased by collisions with irregularities and with other waves. An application of the absorption formula indicates that waves with angular frequency $\geqslant 0{\cdot}3\ \mathrm{sec}^{-1}$ are absorbed too strongly to be effective at the upper levels. We will assume that ten per cent of the original energy (that is $5 \times 10^6\ \mathrm{erg\,cm^{-2}\,sec^{-1}}$) is retained in the form of O and E waves of frequency $0{\cdot}1 < \omega < 0{\cdot}3$ and determine the likely effect of these waves.

The fate of the S waves is not clear. When propagated along or in the absence of a magnetic field they are sound waves and the evidence suggests that they would be dissipated around the 1500 km level (**12**). However, when propagated obliquely to a magnetic field, they should have greater coherence and may reach higher levels and possibly play a part in heating the corona and perhaps in the formation of spicules.

6. *Absorption and reflection.*—Up to the critical level near 1500 km the wave motions are controlled mainly by hydrodynamic forces. Hence the absorption discussed above, due to electromagnetic forces, is not appreciable. At a level of 2000 km the gas density $\sim 5 \times 10^{-13}\ \mathrm{g\,cm^{-3}}$ and if $H_0 = 5$ gauss, $V' \sim 20\ \mathrm{km\,sec^{-1}}$. The value of τ_n will be about one-tenth that at 6000 km (given in Appendix 1), that is $\tau_n \sim 0{\cdot}1$ sec. Equation (11) then gives $\kappa \sim 10^{-9}$ so that the wave decays by a factor e in a distance 10^4 km. As far as absorption is concerned most of the wave energy should reach a level of 6000 km.

Reflection of plane hydromagnetic waves in a horizontal, stratified atmosphere with wave normal and H_0 both vertical has been discussed by Ferraro (**13**). The gas density varies as $\rho = \rho_0 e^{-z/z_0}$ where z_0 is the scale-height of the atmosphere; the corresponding variation in the perturbation magnetic field is found to be

$$e^{i\omega t} \cdot e^{-z/2z_0} \cdot J_1\left(\frac{2\omega z_0}{V_0'} e^{-z/2z_0}\right)$$

where J_1 is Bessel's function of order unity and V_0' the wave velocity at the base of the atmosphere. Since $e^{-z/2z_0} = (\rho/\rho_0)^{1/2} = V_0'/V'$ the Bessel function may be written $J_1[(4\pi z_0)/\lambda]$ where λ is the wave-length at level z. When $(2\pi z_0)/\lambda \gg 1$ the perturbation magnetic field is found to vary as $\rho^{1/4}$. But this is just the variation necessary to maintain a constant Poynting flux in the variable-density medium so that no reflection occurs but merely an increase in wave-length. When the latter increases to equality with the scale height, reflection occurs, the last maximum of the standing wave pattern occurring when $(2\pi z_0)/\lambda \simeq 0{\cdot}9$. Above that level the field decays by a factor of 10 in about three scale-heights.

Ferraro's discussion concerned a medium with z_0 constant. However, it seems safe to assume the same general result if z_0 varies (as in the chromosphere): that is, no reflection until $(2\pi z_0)/\lambda \simeq 1$. The results may be further extended to the case of oblique propagation provided we consider only the O wave whose perturbation magnetic field remains perpendicular to the steady magnetic field (**6**). The equations remain unchanged except that z_0 is replaced by $z_0 \sec\psi$, where ψ is the angle of inclination of the wave normal to the vertical. It is seen that the waves penetrate not only to greater distances but to greater heights.

In the middle chromosphere $z_0 \simeq 1200$ km or more so that reflection commences above a level where $\lambda \simeq 7500$ km. If $\omega = 0{\cdot}2\ \mathrm{rad\,sec^{-1}}$, then

$V' \simeq 240\,\mathrm{km\,sec^{-1}}$, corresponding to a density of about $3{\cdot}5 \times 10^{-15}\,\mathrm{g\,cm^{-3}}$ and a level of about 10 000 km. As we are interested in absorption at lower levels reflection is not important at the frequency concerned. However, waves of much lower frequencies will be reflected before reaching levels where their heating effect is important.

7. *Heating at higher levels.*—The above discussion suggests that above solar granules there may be an upward flow of electromagnetic energy of perhaps $5 \times 10^{6}\,\mathrm{erg\,cm^{-2}\,sec^{-1}}$. Averaged over the solar surface there may be a flow of $5 \times 10^{5}\,\mathrm{erg\,cm^{-2}\,sec^{-1}}$ which penetrates to levels of 10^{4} km or more. The region where heating is most important is the transition zone from mainly neutral to mainly ionized hydrogen centred at a level between 6000 km and 7000 km.

In the H I → H II zone we have $\tau_n \simeq 1$ sec (see Appendix 1) and the proton and neutral atom densities are about $3 \times 10^{9}\,\mathrm{cm^{-3}}$ so that $\eta \simeq 1$ and $V' \simeq 1{\cdot}4 \times 10^{7}\,\mathrm{cm\,sec^{-1}}$. The absorption coefficient (equation (11)) is about $10^{-9}\,\mathrm{cm^{-1}}$ for waves of frequency $0{\cdot}2\,\mathrm{rad\,sec^{-1}}$. At levels where the hydrogen and helium are mainly ionized the absorption is negligible owing to the small value of η. At levels where the gas is mainly unionized the absorption is much the same as in the H I → H II zone but the heating effect is negligible because of the high gas density. The total thickness of the heated layer, allowing for some oblique propagation, is likely to be a few thousand km and the total energy absorbed about $10^{5}\,\mathrm{erg\,cm^{-2}\,sec^{-1}}$. This is comparable with the estimate of energy needed to replenish the quiet or spot-free solar atmosphere, in which only a small proportion of the *average* coronal energy is released (**14**).

The peak gas velocity due to a passing hydromagnetic wave is $V'H_p/H_0$ where H_p is the maximum of the perturbation magnetic field. In the upper part of the transition zone V' may exceed $2 \times 10^{7}\,\mathrm{cm\,sec^{-1}}$ and occasionally H_p may equal H_0 in magnitude. The corresponding kinetic energy of a proton is $3{\cdot}4 \times 10^{-10}$ ergs or ~200 eV. If the proton collides with a neutral atom which does not share the plasma velocity then each particle receives energy of order 100 eV, resulting in ionization and thermal motion corresponding to a temperature of order 10^{6} deg. K. Since the wave quarter-period ($\omega = 0{\cdot}2\,\mathrm{rad\,sec^{-1}}$) is ~8 sec and the collision period $\tau_n > 1$ sec such collisions will be reasonably frequent. The process might be likened to the boiling away of a liquid (the dense unionized gas) to form an overlaying vapour.

8. *Discussion.*—The new mechanism of absorption of hydromagnetic waves disposes of the main objection to the theory of solar heating by these waves. It seems likely that waves due to granules cause enough heating in the H I → H II zone (and the corresponding He zone) to account for the quiet corona.

Corresponding effects on a much larger scale are likely to occur in the neighbourhood of sunspots where violent hydromagnetic disturbances are often observed. In extreme cases the heating mechanism may cause flares.

A prediction of the theory is that most of the significant heating should occur in the surface layer of lightly ionized gas, that is near the surface of the visible chromosphere or of prominence material. In this region there should be a very marked departure from conditions of local thermodynamic equilibrium.

The theory of energy transfer by hydromagnetic waves seems to have advantages over corresponding theories involving purely hydrodynamic effects.

A discussion of these theories of solar atmospheric heating, due to Biermann, Schwarzschild and others is given by van de Hulst (**12**). The main difficulty seems to be that energy is dissipated at too low a level in the chromosphere. The most recent suggestion, made by Schwarzschild, is that the pressure waves concerned might have initial material velocities of only 10^{-2} or 10^{-3} that of the granulation. The energy of these waves would tend to be dissipated in the upper chromosphere and corona. The obvious objections to this suggestion, which involves throwing away all but a tiny fraction of the initially available energy, are avoided when the extra-elastic forces introduced by a magnetic field are taken into account.

APPENDIX

The collision period of neutral atoms.—A plasma of density N (N electrons and N protons or other heavy ions) drifting with velocity v_r through an atomic gas of density N_a ($=\eta N$) will experience a force $\mathbf{F}\,\mathrm{cm}^{-3}$ retarding its motion. To a reasonable approximation we may write

$$\mathbf{F} = N\mathbf{v}_r\left(\frac{m}{\tau_e} + \frac{M}{\tau_i}\right) \qquad (12)$$

where m and M are the electron and heavy ion masses and τ_i and τ_i their respective collision periods *with neutral atoms*.

For weak hydromagnetic waves the values of τ_i and τ_e are found from the collision cross-sections at gas kinetic energies. The cross-section of helium atoms for slow protons is about 2·6 in units of πa_0^2 (Mott and Massey (**15**), p. 289). The relative mobilities of various heavy ions in He and H_2 gases (**16**) are in the ratio about 2 : 1. Allowing for the decrease in mobility because the hydrogen was in the molecular form the collision cross-section of H atoms (for protons) is about $2{\cdot}3 \times 10^{-16}\,\mathrm{cm}^2$. The corresponding cross-section for electrons (ref. (**15**), Fig. 21) is about $3{\cdot}6 \times 10^{-16}\,\mathrm{cm}^2$. The collision period of electrons is less than that of heavy ions because of the greater collision cross-section and the greater velocity. However, these effects are more than offset by the much smaller electron mass so that the term m/τ_e may be neglected in a reasonable approximation.

From equations (2) and (12) we now have (remembering that $\mathbf{v}_r = (\mathbf{v} - \mathbf{v}')$ and $NM = \rho$)

$$\tau_n = \eta\tau_i$$

as would be expected when electron collisions are neglected.

At the chromospheric transition level H I → H II reasonable values of proton density and temperature are about $3 \times 10^9\,\mathrm{cm}^{-3}$ and 10^4 deg. K. The corresponding value of τ_n is 0·9 sec.

Division of Radiophysics, C.S.I.R.O.,
University Grounds,
Sydney, Australia:
1956 *January.*

References

(1) H. Alfvén, *M.N.*, **107,** 211, 1947.
(2) H. Alfvén, *Cosmical Electrodynamics*, Oxford, Clarendon Press, 1950.
(3) L. Biermann, *Zeit. f. Astrophys.*, **25,** 161, 1948.
(4) H. W. Babcock and H. D. Babcock, *Ap. J.*, **121,** 349, 1955.
(5) J. H. Piddington, *Phil. Mag.*, **46,** 1037, 1955.
(6) J. H. Piddington, *M.N.*, **115,** 671, 1955.
(7) T. G. Cowling, *The Solar System:* vol. 1 *The Sun*, ed. by G. P. Kuiper, Chicago University Press 1953, Chap. 8.
(8) J. H. Piddington, *M.N.*, **114,** 638, 1954.
(9) H. C. van de Hulst, *Problems of Cosmical Aerodynamics*, I.U.T.A.M. and I.A.U. Symposium, Paris 1949, (Dayton, Ohio), Chap. VI.
(10) J. H. Piddington, *M.N.*, **114,** 651, 1954.
(11) R. N. Thomas, *Ap. J.*, **108,** 130, 1948.
(12) H. C. van de Hulst, *The Solar System:* vol. 1 *The Sun*, ed. by G. P. Kuiper, Chicago University Press 1953, Chap. 5.
(13) V. C. A. Ferraro, *Ap. J.*, **119,** 393, 1954.
(14) J. H. Piddington and R. D. Davies, *M.N.*, **113,** 582, 1953.
(15) N. F. Mott, and H. S. W. Massey, *The Theory of Atomic Collisions*, Oxford 1949.
(16) A. M. Tyndall, *Mobility of Positive Ions in Gases*, Cambridge, p. 92, 1939.

ON THE EQUILIBRIUM OF MAGNETIC STARS

L. Mestel

(Received 1956 April 14)*

The effect of a magnetic field on the equilibrium of a gaseous star is studied by a perturbation method. It is shown that the pressure-temperature field reacts on the meridional magnetic field not through the condition of hydrostatic support, as in a liquid or barytropic star, but through the energy equation. This reaction is in general very small, so that the imposed field may be considered as arbitrary, in contrast to Ferraro's result for a liquid star (**1**). The electron-pressure and magnetic force terms in the equation of conduction lead on the average to a slight modification of the law of isorotation.

---

1. *Introduction.*—In a recent paper, Ferraro (**1**) has considered the mechanical equilibrium of an incompressible, uniformly rotating magnetic star; he shows that the equation of hydrostatic support implies that the magnetic field (assumed symmetric about the axis of rotation) must satisfy a certain non-linear condition. He derives the explicit solution for a dipole-type field, finding the dependence on radial distance to differ considerably from Cowling's decaying field (**2**). He therefore concludes that Cowling's field will not satisfy the conditions of equilibrium, and so must set up mass motions.

Ferraro's result can be generalized to state that if the density of the stellar material is strictly a function of pressure alone, then the star can remain in equilibrium only if the non-spherical perturbing fields (centrifugal and magnetic) satisfy jointly a certain complicated condition. The physical reason is that polytropic equilibrium is neutral for purely internal displacements, so that the star lacks the extra degree of freedom necessary for it to withstand an arbitrary perturbing force; if one component is given, the pressure field adjusts itself in a way that severely limits the other component.

However, it can be seen that this conclusion does not hold if the equation of state is that of a perfect gas, as in real stars; for then an arbitrary perturbing field can be balanced by non-spherical variations in temperature as well as in pressure. In a convectively stable region, the pressure field reacts on the meridional magnetic field not through the equation of support, but through the thermal equation. Through the bulk of the star, this reaction is small as long as the magnetic force is small compared with gravity, and so the imposed magnetic field may be considered as essentially arbitrary.

An important point of method is involved here. Normally in applied mathematics if a problem is difficult, the model is simplified and the results treated as a first approximation to the truth. Such a procedure is justified only if we know on general grounds that the results obtained are qualitatively correct, although quantitatively approximate. For this reason, the assumption in the present problem of incompressibility or barytropy is misleading.

* Received in original form 1955 January 21.

The discussion is limited to fields symmetric about the axis of rotation. In Section 2 the equation of support is discussed for incompressible, barytropic and perfect gas stars respectively. In Sections 3–8 the mutual interaction of the magnetic, thermal and rotation fields is studied by a method of successive approximation.

2. *The condition of mechanical equilibrium.*—Consider a fluid mass of density ρ (not necessarily uniform), in equilibrium under a magnetic field $\mathbf{H}$ maintained by currents $\mathbf{j}$, and with an arbitrary rotation field $\boldsymbol{\Omega}$. The equation of hydrostatic support is

$$\left(\frac{\mathbf{j}\wedge\mathbf{H}}{c}\right)_m - \rho\boldsymbol{\Omega}\wedge(\boldsymbol{\Omega}\wedge\mathbf{r}) + \rho\nabla\phi - \nabla p = 0, \tag{1}$$

where ϕ is the gravitational potential, p the gas pressure, $\mathbf{r}$ the position vector from the centre, and c the velocity of light (Gaussian units being used). The suffix m selects the meridional component.

On taking the curl of (1), we have

$$\nabla\rho\wedge\nabla\phi + \nabla\wedge\left(\left(\frac{\mathbf{j}\wedge\mathbf{H}}{c}\right)_m - \rho\boldsymbol{\Omega}\wedge(\boldsymbol{\Omega}\wedge\mathbf{r})\right) = 0. \tag{2}$$

If ρ is constant, (2) reduces to

$$\nabla\wedge\left\{\left(\frac{\mathbf{j}\times\mathbf{H}}{\rho c}\right)_m - \boldsymbol{\Omega}\wedge(\boldsymbol{\Omega}\wedge\mathbf{r})\right\} = 0; \tag{3}$$

or in cylindrical polar coordinates (ϖ,θ,z) referred to the centre and the rotation axis

$$\frac{1}{c}\left\{\frac{\partial}{\partial z}(j_\theta H_z) + \frac{\partial}{\partial\varpi}(j_\theta H_\varpi)\right\} - \frac{1}{4\pi\varpi}\frac{\partial}{\partial z}(H_\theta)^2 + \rho\varpi\frac{\partial}{\partial z}|\boldsymbol{\Omega}|^2 = 0, \tag{4}$$

where use has been made of the equation $\nabla\wedge\mathbf{H} = 4\pi\mathbf{j}/c$. If the magnetic field is zero, (4) implies that in equilibrium $|\boldsymbol{\Omega}|$ must be a function only of ϖ, the distance from the rotation axis. In a magnetic star with such a rotation law, condition (4) restricts the form of the magnetic field: Ferraro's result

$$\frac{\partial}{\partial z}(j_\theta H_z) + \frac{\partial}{\partial\varpi}(j_\theta H_\varpi) = 0 \tag{5}$$

follows if the field is assumed purely meridional.

If ρ is not a constant, but is strictly a function of *pressure* only, then the same result (3) holds, as is seen by subtracting from (2) the vector product of (1) with $\nabla\rho/\rho$; but now ρ is determined by the equation of support (1) and Poisson's equation $\nabla^2\phi = -4\pi G\rho$. In a non-magnetic star, the same condition $\partial|\boldsymbol{\Omega}|/\partial z = 0$ restricts the rotation field: if $\mathbf{H}$ does not vanish, however, the constraint exerted on the rotation and magnetic fields is in general more complicated than (4), because of the dependence of ρ on the non-spherical perturbing forces.

Thus in both the incompressible and barytropic cases, the condition of mechanical equilibrium exerts a constraint on the magnetic and rotation fields; if they do not in fact satisfy this condition (3), rapid mass motions are set up. As in a highly conducting fluid the field is dragged by the matter, while each element of fluid tends to conserve its angular momentum, both the rotation and magnetic fields are distorted until they jointly satisfy (3).

By contrast, consider a gaseous star with $p \propto \rho T$, T being the absolute temperature. Equations (1) and (2) can now be satisfied, for arbitrary perturbing

forces, by allowing non-spherical variations in T as well as in ρ and p. In a convectively stable region, mechanical equilibrium is maintained at the expense of radiative, leading to slow material currents in meridional planes, which maintain thermal balance through the energy they transport (**3**). The electromagnetic effects of flow across the field can then be determined in a higher approximation. In a convectively unstable region, strong interaction between the perturbation and the convection currents is likely. Turbulent viscosity will tend to reduce non-uniformities of rotation; a weak magnetic field will be tangled up by the convection, while a stronger field will inhibit flow across the lines of force. But whatever modifications the perturbing fields undergo, mechanical equilibrium will be preserved by temperature variations, to which the convection currents adjust themselves. In the rest of the paper, only stable regions will be treated.

However, in considering the interaction between a spherical gaseous star and a perturbing rotation or magnetic field, a distinction must be drawn between fields that are imposed "rapidly" or "gradually". If changes in the fields take place in a time comparable with or longer than the Kelvin–Helmholtz time-scale, then the temperature field has the time to adjust itself to the slowly changing density and pressure fields so as to preserve mechanical equilibrium. This is the case, for example, if the star's magnetic field is a distorted part of the local galactic field dragged in with the condensing proto-star; or if the field has been built up against self-induction in a time of the order of Cowling's decay-time (**2**). Displacements of the elements of the star by the perturbing forces will react back on the rotation and magnetic fields, but provided the forces are small compared with gravity the distortion of the imposed fields will be small.

On the other hand, suppose the rotation and magnetic fields are changing in a time short compared with the Kelvin–Helmholtz time-scale. The resulting variations in the density of an element of matter are accompanied by *adiabatic* variations in pressure, as there is no time for the temperature field to adjust itself so as to preserve mechanical equilibrium. Mass motions, with distortion of the rotation and magnetic fields must take place, but it is difficult to draw any general conclusions about any quasi-equilibrium state that may be reached. In particular, it is not obvious that the distorted magnetic field should differ only slightly from the imposed field, even if the magnetic pressure is small compared with the thermal pressure. However, except briefly in Section 8, we shall deal only with slowly varying fields.

It should be emphasized that Ferraro's result (5) and its generalization (3) do depend on the pressure being strictly independent of temperature. In a real liquid or degenerate body there will always be a small thermal contribution to pressure, and again it is possible to satisfy the condition of equilibrium (1) by allowing non-spherical temperature variations, whatever the shape of the perturbing fields. In fact, equation (3) is just the condition that the perturbations to the temperature be of the same order as those in the pressure and density; if (3) does not hold, larger temperature variations are required, with correspondingly larger thermal currents. Thus even for liquid bodies or white dwarfs, it is doubtful whether (3) represents a real limitation.

3. *Gaseous magnetic stars.*—We now assume that the star is in mechanical equilibrium under a meridional magnetic field $\mathbf{H}_1$, maintained by azimuthal currents $\mathbf{j}_1$. For the moment rotation is ignored. That perturbations to the field $\mathbf{H}_1$ must arise can be seen from the equation that replaces Ohm's law in a

highly ionized gas (**4**)

$$\mathbf{j}=\sigma\left(\mathbf{E}+\frac{\mathbf{v}\wedge\mathbf{H}}{c}+\frac{\nabla p_e}{n_e e}-\frac{1}{n_e e}\frac{\mathbf{j}\wedge\mathbf{H}}{c}\right), \tag{6}$$

where σ is the unreduced conductivity, $\mathbf{E}$ the electric field, p_e, n_e the electron pressure and density, and $-e$ the electron charge. The non-spherical pressure–density field yields an effective e.m.f. in meridional planes, while thermally-driven material currents induce electric currents by flow across the field. The following scheme of successive approximation therefore suggests itself:

In the absence of a magnetic field $\mathbf{H}_1$, the electron pressure term $\nabla p_e/n_e e$ is given by

$$\frac{A}{(Z+1)}\frac{m_{\mathrm{H}}}{e}\frac{\nabla p_0}{\rho_0}=\frac{Am_{\mathrm{H}}}{(Z+1)e}\nabla\phi_0, \tag{7}$$

where again the suffix zero refers to the unperturbed spherical star, and A and Z are the mean atomic weight and number respectively. This force on each electron is just cancelled out by an electrostatic force

$$\mathbf{E}_0=-\frac{Am_{\mathrm{H}}}{(Z+1)e}\nabla\phi_0. \tag{8}$$

This is the Pannekoek–Rosseland field, with a corresponding charge density $\nabla.\mathbf{E}_0/4\pi$ e.s.u. The field is built up in the very short time $1/\sigma$, the same as the decay-time of charge density within a conductor without any non-electric force acting on the electrons.

The currents $\mathbf{j}_1$ maintaining the field $\mathbf{H}_1$ are driven by an electric field $\mathbf{E}_1$, so that

$$\begin{aligned}\nabla\wedge\mathbf{H}_1&=\frac{4\pi}{c}\mathbf{j}_1=\frac{4\pi}{c}\sigma_0\mathbf{E}_1,\\ \nabla\wedge\mathbf{E}_1&=-\frac{1}{c}\frac{\partial\mathbf{H}_1}{\partial t},\\ \nabla.\mathbf{H}_1&=0.\end{aligned} \tag{9}$$

As usual in conductors, the displacement current is negligible.

The magnetic force $\mathbf{j}_1\wedge\mathbf{H}_1/c$ in the equation of support involves H_1^2 and so the perturbed quantities ϕ, ρ, p, T are written

$$\begin{aligned}\phi&=\phi_0+\phi_2+\ldots & \rho&=\rho_0+\rho_2+\ldots\\ p&=p_0+p_2+\ldots & T&=T_0+T_2+\ldots.\end{aligned} \tag{10}$$

The perturbations satisfy

$$\nabla^2\phi_2=-4\pi G\rho_2 \tag{11}$$

from Poisson's equation;

$$p_2=\frac{\mathfrak{R}}{\mu}(\rho_0T_2+\rho_2T_0) \tag{12}$$

from the equation of state; and the perturbed equation of support

$$\left(\frac{\mathbf{j}_1\wedge\mathbf{H}_1}{c}\right)+\rho_0\nabla\phi_2+\rho_2\nabla\phi_0-\nabla p_2=0. \tag{13}$$

The electron pressure term in (6) now yields, besides (7),

$$\frac{Am_{\mathrm{H}}}{(Z+1)e}\left\{\frac{\nabla p_2}{\rho_0}-\rho_2\frac{\nabla p_0}{\rho_0^2}\right\}=\frac{Am_{\mathrm{H}}}{(Z+1)e}\left\{\nabla\phi_2+\frac{\mathbf{j}_1\wedge\mathbf{H}_1}{c\rho_0}\right\}. \tag{14}$$

Thus the last two terms in (6) give electromagnetic effects of order H_1^2; we therefore write

$$\begin{aligned}\mathbf{j}_2&=\sigma_0\left(\mathbf{E}_2+\frac{Am_{\mathrm{H}}}{(Z+1)e}\left(\nabla\phi_2+\frac{\mathbf{j}_1\wedge\mathbf{H}_1}{c\rho_0}\right)-\frac{Am_{\mathrm{H}}}{Ze}\left(\frac{\mathbf{j}_1\wedge\mathbf{H}_1}{c\rho_0}\right)\right)\\&=\sigma_0\left(\mathbf{E}_2+\frac{Am_{\mathrm{H}}}{(Z+1)e}\nabla\phi_2-\frac{Am_{\mathrm{H}}}{(Z+1)Ze}\left(\frac{\mathbf{j}_1\wedge\mathbf{H}_1}{c\rho_0}\right)\right).\end{aligned} \tag{15}$$

and also

$$\begin{aligned}\nabla\wedge\mathbf{H}_2&=\frac{4\pi}{c}\mathbf{j}_2,\\\nabla\wedge\mathbf{E}_2&=-\frac{1}{c}\frac{\partial\mathbf{H}_2}{\partial t},\\\nabla.\mathbf{H}_2&=0.\end{aligned} \tag{16}$$

The term in $\nabla\phi_2$ and the irrotational part of the term in $\mathbf{j}_1\wedge\mathbf{H}_1/c$ merely change slightly the electrostatic field and the charge density, but in general the last term leads to non-vanishing electric currents in meridional planes, maintaining an azimuthal field. The interaction of these currents with the meridional field $\mathbf{H}_1$ and the rotation of the star (neglected so far) will be considered in Section 6.

The velocity $\mathbf{v}$ of matter flow in meridional planes is given by the energy equation

$$\begin{aligned}\frac{\mathfrak{R}}{\mu}\left(\frac{1}{(\gamma-1)}\frac{\partial T}{\partial t}-\frac{T}{\rho}\frac{\partial\rho}{\partial t}\right)+\frac{\mathfrak{R}T}{\mu}\mathbf{v}.\nabla\left(\ln\frac{T^{1/(\gamma-1)}}{\rho}\right)\\=\epsilon-\frac{\nabla.\mathbf{F}}{\rho}+\frac{\mathbf{j}_1^2}{\rho\sigma},\end{aligned} \tag{17}$$

where $\mathbf{F}$ is the energy flux, ϵ the energy liberation per gram, and γ the ratio of the two principal specific heats. In the absence of a magnetic field, the Joule heating term $j_1^2/\rho\sigma$ vanishes; all the quantities are spherically symmetric, and the energy equation determines the approach of the star to strict thermal equilibrium, for which $\epsilon-\nabla.\mathbf{F}/\rho=0$, in a time of order of the Kelvin–Helmholtz time-scale. With a perturbing magnetic field present, the radial velocity will vary over a sphere: the spherically symmetric part of the perturbation will expand or contract the sphere as a whole, again in a time of Kelvin–Helmholtz order, while the rest drives the meridional circulation, as in the rotational case (3). The two components of circulation are of order H_1^2, and are related by the equation of continuity

$$\nabla.(\rho\mathbf{v})+\frac{\partial\rho}{\partial t}=0. \tag{18}$$

The terms of order H_1^3 in (6) yield, besides an extra meridional electric current, the azimuthal current

$$\mathbf{j}_3=\sigma_0\left(\mathbf{E}_3+\frac{\mathbf{v}_2\wedge\mathbf{H}_1}{c}-\frac{Am_{\mathrm{H}}}{Zec}\left(\frac{\mathbf{j}_2\wedge\mathbf{H}_1}{\rho_0}\right)+\frac{3}{2}\frac{T_2}{T_0}\mathbf{E}_1\right), \tag{19}$$

the last term arising from the perturbation in the conductivity ($\sigma\propto T^{3/2}$). Again $\mathbf{E}_3$, $\mathbf{j}_3$ and $\mathbf{H}_3$ are related by Maxwell's equations (16) with suffix 3 replacing 2.

If terms of order 4 or higher in H_1 are required in (6), perturbations of the equation of support of second order in magnetic force must be computed.

4. *The field* $\mathbf{H}_1$.—From (9) it follows that $\mathbf{E}_1$ satisfies Cowling's equation of decay (**2**)

$$\nabla \wedge (\nabla \wedge \mathbf{E}_1) = -\frac{4\pi\sigma_0}{c^2}\frac{\partial \mathbf{E}_1}{\partial t}. \tag{20}$$

With $\mathbf{H}_1$ assumed purely meridional, in spherical polar coordinates (r, θ, ϕ) the eigen-solutions of (20) are azimuthal vectors of magnitude

$$r f_{nk}(r)\frac{\partial P_n}{\partial \theta} e^{-t/\tau_{nk}}, \tag{21}$$

where f_{nk} satisfies a second order linear equation. The series of eigenvalues τ_{nk} are found from the conditions of finiteness at the origin and continuity at the stellar surface; however, the order of the decay-time of a field of scale l is seen from (20) to be $\sim 4\pi\sigma_0 l^2/c^2$. For a dipole-type field, the slowest decaying component has a time-constant of about 10^{10} years (**2**). At time $t=0$ an arbitrary magnetic field can be expanded in terms of these eigen-solutions, thus fixing the field $\mathbf{H}_1$ at all later times. The higher order effects may then be considered term by term.

5. *The azimuthal field and the stellar rotation.*—From (15) and (16), the vector potential $\mathbf{A}_2$ of the field $\mathbf{H}_2$ satisfies the supplementary relation

$$\nabla \cdot \mathbf{A}_2 = 0$$

and

$$-\nabla \wedge (\nabla \wedge \mathbf{A}_2) = \frac{4\pi\sigma_0}{c^2}\left(\frac{\partial \mathbf{A}_2}{\partial t} + \frac{Am_{\mathrm{H}}}{Z(Z+1)e}\left(\overline{\frac{\mathbf{j}_1 \wedge \mathbf{H}_1}{\rho_0}}\right)\right). \tag{22}$$

The bar over the last term indicates that the irrotational part has been subtracted. We ignore for the moment the decay of the term in H_1; then, as shown by Cowling (**4**), equation (22) implies that a field is slowly built up against self-induction through the action of the impressed e.m.f. $\{Am_{\mathrm{H}}/Z(Z+1)ec\}(\overline{\mathbf{j}_1 \wedge \mathbf{H}_1/\rho_0})$. The asymptotic azimuthal field $\mathbf{H}_2$ satisfies

$$\nabla \wedge \mathbf{H}_2 = -\frac{4\pi\sigma_0}{c^2}\left(\frac{Am_{\mathrm{H}}}{Z(Z+1)e}\right)\left(\overline{\frac{\mathbf{j}_1 \wedge \mathbf{H}_1}{\rho_0}}\right). \tag{23}$$

This field $\mathbf{H}_2$ can be expanded in terms of the azimuthal eigen-solutions of the decay equation

$$-\nabla \wedge (\nabla \wedge \mathbf{A}_2) = \frac{4\pi\sigma_0}{c^2}\frac{\partial \mathbf{A}_2}{\partial t}; \tag{24}$$

the time of build-up of each eigen-solution is the same as its time of decay, if it were imposed on the star with no quasi-electric forces to drive the maintaining currents. As in fact the driving term in $(\overline{\mathbf{j}_1 \wedge \mathbf{H}_1})$ is itself slowly decaying, it is clear that the field $\mathbf{H}_2$ would grow to a maximum, and then decay along with the field $\mathbf{H}_1$.

However, in fact the star does not allow this azimuthal field $\mathbf{H}_2$ to be built up. So far we have neglected the effect of rotation on the equation of conduction (6). If $\mathbf{k}$ is the unit vector in the positive azimuthal direction, then a rotation field Ω leads to an induced meridional e.m.f.

$$\frac{\Omega r \sin\theta}{c}(\mathbf{k} \wedge \mathbf{H}_1). \tag{25}$$

Let us ignore for the moment the terms in ∇p_e and $\mathbf{j}_1 \wedge \mathbf{H}_1/c$ in equation (6). Then the assumption that $\mathbf{H}_1$ be purely meridional implies that the meridional electric field should be electrostatic, so that no currents flow, maintaining an azimuthal field. The condition for this is

$$\nabla \wedge \left(\frac{\Omega r \sin\theta}{c} (\mathbf{k} \wedge \mathbf{H}_1) \right) = 0, \tag{26}$$

which at once yields Ferraro's well-known law of isorotation, restricting the angular velocity to be uniform along a line of force.

Now reintroduce the last two terms in (6), which we have seen tend to build up slowly a meridional current field. In the presence of the meridional field $\mathbf{H}_1$, the magnetic force has in general a non-vanishing component $\mathbf{j}_2 \wedge \mathbf{H}_1/c$ in the azimuthal direction; as there are opposing it only the very small Coriolis and viscous forces, this force must affect the rotation field, and so also will modify $\mathbf{j}_2$ through the motional induction term $\Omega r \sin\theta \mathbf{k} \wedge \mathbf{H}_1/c$. The change in the rotation law will cease only when $\mathbf{j}_2 \wedge \mathbf{H}_1 = 0$; in general this implies $\mathbf{j}_2 = 0$. The time-scale of adjustment is comparable with the period of a hydromagnetic wave, which for any sizeable magnetic field is much shorter than the characteristic time of growth or decay of the field. We may therefore expect the rotation field to suffer a gentle progressive modification with time; as the impressed meridional e.m.f. slowly overcomes self-induction and tries to build up a current field, the rotation field is immediately altered so as to cancel out the currents. The maximum deviation from isorotation occurs after the time in which the field $\mathbf{H}_2$ would have been built up, if the effect of rotation on (6) could have been ignored; after this time, the impressed e.m.f. will have overcome self-induction, and the rotation field will satisfy

$$\nabla \wedge \left\{ \left(\Omega - \frac{Am_{\mathrm{H}}}{Z(Z+1)e} \frac{|\mathbf{j}_1|}{\rho_0 r \sin\theta} \right) \left(r \sin\theta \, \mathbf{k} \wedge \mathbf{H}_1 \right) \right\} = 0 \tag{27}$$

in place of (26), leading to

$$\Omega - \frac{Am_{\mathrm{H}}}{Z(Z+1)e} \frac{|\mathbf{j}_1|}{\rho_0 r \sin\theta} = \text{constant along a line of force.} \tag{28}$$

However, over the bulk of the star this correction to Ferraro's law is small; e.g. if $\mathbf{H}_1$ is Cowling's dipole-type decaying field, (28) reduces to the constancy of $(\Omega - 10^{-25} H/\rho_0)$ along a line of force. As even a slowly rotating star like the sun has $\Omega \sim 3 \times 10^{-6}$ at the surface, it follows that the departure from isorotation is negligible in all cases of interest.

6. *The perturbation to the meridional field.*—In computing the current $\mathbf{j}_3$ from (19), we may ignore the term in $\mathbf{j}_2 \wedge \mathbf{H}_1/c$, for we have seen that this azimuthal force merely serves so to modify the rotation field as to cancel itself out. The vector potential of $\mathbf{H}_3$ is then an azimuthal vector satisfying

$$-\nabla \wedge (\nabla \wedge \mathbf{A}_3) = \frac{4\pi\sigma_0}{c^2} \left(\frac{\partial \mathbf{A}_3}{\partial t} - \left(\overline{\mathbf{v}_2 \wedge \mathbf{H}_1} + \frac{3}{2} \overline{\frac{cT_2}{T_0} \mathbf{E}_1} \right) \right), \tag{29}$$

again implying a slow build up of $\mathbf{H}_3$ against self-induction to a maximum

$$\nabla \wedge \mathbf{H}_3 = \frac{4\pi\sigma_0}{c^2} \left(\overline{\mathbf{v}_2 \wedge \mathbf{H}_1} + \frac{3}{2} \overline{\frac{cT_2}{T_0} \mathbf{E}_1} \right), \tag{30}$$

and then a slow decay as the primary field $\mathbf{H}_1$ decays.

The velocity $\mathbf{v}_2$ is calculated as in the rotational case (**3**). From (11) and (13) we have an equation for $\partial\phi_2/\partial\theta$; $\partial\rho_2/\partial\theta$, $\partial p_2/\partial\theta$, $\partial T_2/\partial\theta$, and finally $\partial(v_2)_r/\partial\theta$ are then found from (11), (13), (12) and (17). The condition of zero outflow from a sphere of given mass determines $(v_2)_r$ uniquely, and $(v_2)_\theta$ is found from the equation of continuity (18).

The orders of magnitude of the different terms in (17) are as follows

$$\left(\epsilon - \frac{\nabla.\mathbf{F}}{\rho}\right) \sim \frac{L}{M}\left|\frac{\mathbf{j}_1 \wedge \mathbf{H}_1}{c}\right| \Big/ \rho_0(-\phi_0'),$$

$$\frac{\mathfrak{R}}{\mu}\frac{\partial T_2}{\partial t} \sim \frac{\mathfrak{R}}{\mu}\frac{T_0}{\rho_0}\frac{\partial \rho_2}{\partial t} \sim \frac{\mathfrak{R}}{\mu}\frac{T_0}{\tau}\left|\frac{\mathbf{j}_1 \wedge \mathbf{H}_1}{c}\right| \Big/ \rho_0(-\phi_0') \sim \frac{R}{\rho_0 \tau}\left|\frac{\mathbf{j}_1 \wedge \mathbf{H}_1}{c}\right|, \tag{31}$$

$$\frac{\mathbf{j}_1^2}{\rho_0 \sigma_0} \sim \frac{c j_1 H_1}{4\pi l \rho_0 \sigma_0} \sim \left|\frac{\mathbf{j}_1 \wedge \mathbf{H}_1}{c}\right| l/\rho_0 \tau,$$

where L, M, and R are stellar luminosity, mass and radius, τ is the time of magnetic decay, and l again the scale of the field. (If $\mathbf{H}_1$ is a superposition of fields of widely varying dimensions, then we select the largest term).

Consider first a large-scale field, with $l \simeq R$. Then inspection of (31) shows that the last two terms are comparable in magnitude, while the first is larger than the other two by a factor of about 200. Hence from (17) the velocities through the bulk of the star are of the order

$$\frac{L}{M}\frac{H_1^2}{4\pi R} \Big/ \rho_0(-\phi_0')^2 \tag{32}$$

The term $(\frac{3}{2}cT_2/T_0)\,|\,\mathbf{E}_1\,|$ in (19) is small compared with $|\,\mathbf{v}_2 \wedge \mathbf{H}_1\,|$, and so the asymptotic value of $|\,\nabla \wedge \mathbf{H}_3\,|$ is of order $(4\pi\sigma_0/c^2)\,|\,\mathbf{v}_2 \wedge \mathbf{H}_1\,|$, giving

$$\frac{H_3}{H_1} \simeq 10^{-14}\frac{(T/T_c)^{3/2}}{(\rho/\rho_c)} H_1^2\left(\frac{\bar{R}^3}{\bar{M}}\right). \tag{33}$$

(Barred quantities are expressed in solar units, and the suffix c refers to central values. T_c is taken as 2×10^7 deg. K, and ρ_c from Miss Gardiner's integration of a Cowling Model star (**5**)). Thus through the bulk of the star only an enormous field $\mathbf{H}_1$ can give rise to velocities large enough to modify seriously the meridional field.

If $l < R$ then H_3/H_1 is greater than (33) by a factor (R/l); with $l < R/200$ the last two terms in (31) become dominant and give an even larger perturbation. However, the decay-time of such a small-scale field is much shorter than the stellar lifetime, and unless there is operative some process that continually crinkles the large-scale field we may ignore it.

The perturbation technique of this paper may break down near the edge of the star, as $|\,\mathbf{j}_1 \wedge \mathbf{H}_1\,| = \sigma_0\,|\,\mathbf{E}_1 \wedge \mathbf{H}_1/c\,|$ drops to zero less rapidly than $\rho_0(-\phi_0')$. This leads to a large v_r, while the equation of continuity (18) gives v_θ even larger, by a factor $r\rho_0'/\rho_0$. Thus near the surface, with $l \sim R$,

$$\frac{H_3}{H_1} \sim 10^{-14}\left|\frac{r\dfrac{d}{dr}\left(\dfrac{\rho}{\rho_c}\right)\left(\dfrac{T}{T_c}\right)^{3/2}}{\left(\dfrac{\rho}{\rho_c}\right)^2}\right| H_1^3\left(\frac{\bar{R}^3}{\bar{M}}\right). \tag{34}$$

Putting in photospheric values for ρ and T, we have

$$\frac{\left|\dfrac{\mathbf{j}_1 \wedge \mathbf{H}_1}{c}\right|}{\rho_0(-\phi_0')} \sim 3 \times 10^{-11}\frac{H_1^2 \bar{R}^4}{\bar{M}^2} \qquad \frac{H_3}{H_1} \sim 6 \times 10^{-6} H_1^2\left(\frac{\bar{R}^3}{\bar{M}}\right) \tag{35}$$

At the base of the Unsöld convection zone the numerical factors will be much smaller. Thus the perturbation technique seems adequate for main-sequence stars with large-scale magnetic fields unless the fields are of the intensities found by Babcock (**6**). On the other hand, a locally concentrated strong magnetic field, of the sort that may give rise to sunspots cannot be treated as a perturbation, and an entirely new approach is necessary.

If the field $\mathbf{H}_1$ should be such that $H_3/H_1 \simeq 1$, then in fact the thermally driven matter currents would distort the lines of force so that they follow closely the flow; near the surface the field would become more or less horizontal, because of the large horizontal component of flow. Perturbation technique could then be applied to this distorted field unless the magnetic force becomes comparable with the gravitational force. Further discussion of this case is beyond the scope of this paper.

We may conclude, then, that the meridional magnetic field imposed on a star may be considered as essentially arbitrary, provided it is not too strong nor changes too rapidly in space. The contrast with the situation in a liquid or barytropic star has already been pointed out. The results are intuitively satisfactory: as long as the magnetic forces are small compared with gravity we expect them to have small consequences except when they cannot be balanced by small perturbations in gravity and gas pressure, as with azimuthal forces, or with general meridional forces in a barytropic star.

7. *Rotation.*—The effect of rotation on the equation of conduction (6) has been dealt with in Section 5. As long as we are considering only first order perturbations in the equation of support (1), then the distortions of the pressure-density field due to magnetic and centrifugal forces may be computed separately and superposed. Again, the rotational distortion of the star will react back on the imposed fields, but as long as the ratio of centrifugal to gravitational force is small this perturbation will be small; in any case, the field $\mathbf{H}_1$ introduced in Section 3 will be the field present in the magnetically and rotationally distorted star, apart from the perturbations $\mathbf{H}_3$ etc.

We have assumed so far that the field $\mathbf{H}_1$ is purely meridional and have seen that this implies that the angular velocity is initially constant along a line of force, but suffers very slight progressively increasing non-uniformities. However, a rotation field conforming to this law will still in general yield a centrifugal field not derivable from a potential; as first pointed out by Biermann (**7**), such a centrifugal field drives meridional electric currents $\mathbf{j}_m$ that build up an azimuthal field $\mathbf{H}_a$, analogous to the $\mathbf{j}_2$ and $\mathbf{H}_2$ of Section 5. The asymptotic field will be

$$\nabla \wedge \mathbf{H}_a = \frac{4\pi\sigma_0}{c}\left(\frac{Am_{\mathrm{H}}}{(Z+1)e}\right)\overline{(\boldsymbol{\Omega} \wedge (\boldsymbol{\Omega} \wedge \mathbf{r}))}, \tag{36}$$

where again a bar denotes that the potential part has been subtracted out. However, in the presence of the meridional field $\mathbf{H}_1$, as soon as currents $\mathbf{j}_m$ begin to flow, the azimuthal force $\mathbf{j}_m \wedge \mathbf{H}_1/c$ reacts on the rotation field; as in the case discussed in Section 5, we may expect a gentle progressive modification of the rotation field sufficient to keep the magnetic field meridional. The equation analogous to (27) reduces to

$$\frac{\partial\Omega}{\partial\theta}\left[\frac{2Am_{\mathrm{H}}c}{(Z+1)e}(\Omega\sin\theta) - H_\theta\right] = r\frac{\partial\Omega}{\partial r}\left[\frac{2Am_{\mathrm{H}}c}{(Z+1)e}(\Omega\cos\theta) + H_r\right]. \tag{37}$$

Neglect of the first term in each bracket gives Ferraro's law. The deviation from isorotation is of the order of the ratio

$$\frac{2Am_{\mathrm{H}}c}{(Z+1)e}\left(\frac{\Omega}{\bar{H}}\right)\sim 3\times 10^{-4}\left(\frac{\Omega}{\bar{H}}\right). \tag{38}$$

In order that centrifugal force should not be too great compared with gravity, Ω must not much exceed 10^{-4} radians/sec. anywhere within the star; thus only with fields as small as 10^{-7} gauss does (38) approach unity. With such small fields the coupling between the rotation and magnetic fields is in any case negligible, as the period of a hydromagnetic wave along the lines of force is longer than the galactic age.

Thus we see that in the presence of a sizeable meridional field, the electron pressure and magnetic force terms in (6) do not build a large azimuthal magnetic field, but simply lead to a slight non-uniformity of drift across the lines of force. This is a particular case of a result due to Sweet (**8**).

Should the initial rotation field be non-isorotational, then the hydromagnetic interaction between the rotation and meridional magnetic fields will cause an oscillation about the mean state in which the field is meridional. The period of the oscillation is that of a hydromagnetic wave, which for any sizeable field is much shorter than both the time of magnetic growth and decay and the Kelvin–Helmholtz time-scale. The comparatively rapid changes in the centrifugal force and in the meridional magnetic force will therefore lead to adiabatic changes in the density and temperature of each element of matter. As pointed out in Section 2, this perturbed density-temperature field will not in general satisfy the equation of support, and so further mass motion must occur, with rapid distortion of the centrifugal and magnetic fields and adiabatic temperature–density variations, until a state of equilibrium is reached.

The rotational thermal currents $\mathbf{v}_\Omega$ discussed by Sweet (**3**) will also react on $\mathbf{H}_1$ through the induction term $\mathbf{v}_\Omega\wedge\mathbf{H}_1/c$ in (6). This perturbation becomes comparable with $\mathbf{H}_1$ if

$$\left|\frac{\mathbf{v}_\Omega\wedge\mathbf{H}_1}{c}\right|\simeq E_1\simeq\frac{lH_1}{c\tau}\simeq\frac{H_1}{\frac{4\pi\sigma l}{c}}, \tag{39}$$

i.e.

$$\frac{4\pi\sigma l v_\Omega}{c^2}\simeq 1,$$

l being the scale of the field. This condition asserts that the time of flow across a distance of order l should be comparable with the decay time of the field. From Sweet's results with $\sigma\sim 10^{-17}$ e.s.u.

$$v_\Omega\simeq 10^{-10}(\bar{L}\bar{R}^5/\bar{M}^3)\bar{\Omega}^2,$$

and

$$\frac{4\pi\sigma l v_\Omega}{c^2}\simeq 10^{-2}\left(\frac{l}{\bar{R}}\right)\left(\frac{\bar{L}\bar{R}^6}{\bar{M}^3}\bar{\Omega}^2\right). \tag{40}$$

Thus quite moderate angular velocities will drive rotational currents strong enough to distort the field $\mathbf{H}_1$, whereas we saw in Section 6 that the magnetically driven thermal currents have quite negligible effects unless $\mathbf{H}_1$ is enormous.

Either the lines of force will be made to follow the streamlines of the rotational currents, so that $\mathbf{v}_\Omega \wedge \mathbf{H}_1 = 0$, or possibly the field $\mathbf{H}_1$ may be so twisted as to exert much stronger mechanical forces, so that the effect of rotation on the thermal equation is cancelled out. This result is relevant to the oblique rotator theory of magnetic variables, in that only slowly rotating stars will preserve an initial obliquity of the magnetic and rotation axes.

8. *The imposed field non-meridional.*—So far we have assumed $\mathbf{H}_1$ to have only meridional components. If now $\mathbf{H}_1$ is taken as purely azimuthal, then examination of the equations of Section 3 shows that all the perturbing terms $\mathbf{H}_2, \mathbf{H}_3 \ldots$ are also azimuthal. As the rotation velocities are parallel to the field, there is no interaction with the rotation field. The asymptotic value of the ratio j_2/j_1 is of order $\sigma_0 H_1 m_H/\rho_0 ec$, which is comparable with unity in a stellar envelope for quite moderate fields $\mathbf{H}_1$.

However, it is unlikely that the field $\mathbf{H}_i$ will have no meridional component, and so we can again expect interaction with the rotation field through the azimuthal component of magnetic force. In general, the field at each point will possess an azimuthal component which changes sign periodically as the local rotation field fluctuates. Again, the period of hydromagnetic waves along the lines of force will be much shorter, for any sizeable field, than the time of build-up of the fields $\mathbf{H}_2, \mathbf{H}_3 \ldots$, and so only the meridional field exerts a magnetic force having a permanent effect on the electromagnetic equation. A star with an initial purely meridional field and a rotation field not satisfying the modified isorotation law is a special case, in that the magnetic field fluctuates about a state in which it is simultaneously meridional at every point of the star.

Acknowledgments.—This work was done at the University of Leeds while the writer was holding an I.C.I. Research Fellowship. He is indebted to Professor T. G. Cowling for introducing him to the study of hydromagnetics, and for helpful criticisms of the manuscript.

Faculty of Mathematics,
The Arts School,
Bene't St.,
Cambridge :
1956 *April* 13.

References

(1) V. C. A. Ferraro, *Ap. J.*, **119,** 407, 1954.
(2) T. G. Cowling, *M.N.*, **105,** 166, 1945.
(3) P. A. Sweet, *M.N.*, **110,** 548, 1950.
(4) T. G. Cowling, *Solar Electrodynamics* in G. P. Kuiper (Ed.), *The Sun,* Chicago, 1953.
(5) J. G. Gardiner, *M.N.*, **111,** 94, 1951.
(6) H. Babcock, *Pub. A.S. Pac.*, **59,** 112, 1947.
(7) L. Biermann, *Z. f. Naturforsch.*, **5a,** 65, 1950.
(8) P. A. Sweet, *M.N.*, **110,** 69, 1950.

ON THE COORDINATION OF THE RIEMANNIAN AND KINEMATIC TECHNIQUES IN THEORETICAL COSMOLOGY, WITH PARTICULAR REFERENCE TO THE SHIFT-DISTANCE LAW

W. Rindler

(Communicated by G. J. Whitrow)

(Received 1956 June 25)*

Summary

This paper is concerned with homogeneous and isotropic model-universes. The two main alternative descriptions of such universes, (i) by means of a Riemannian space-time map characterised by the Robertson–Walker metric and (ii) as a kinematic equivalence, are compared. The generating function $\psi(t)$ and signal-parameter α of the equivalence are related to the scale-function $R(t)$ and radial coordinate r of the corresponding metric. Milne's distance is related to the other distances commonly used in cosmology, for which expansions in terms of proper distance are given. The empirical determination from nebular red-shift data of the functions $R(t)$ and $\psi(t)$ appropriate to the observable universe is discussed with reference to Whitrow's second-order shift-distance criterion and in the light of recently published observations. Also, new general shift-ratio formulae for kinematic equivalences are derived.

---

1. ***Introduction.***—There are two main techniques for the discussion of cosmological problems including the construction of model-universes. One, which I shall call ***the Riemannian technique***, originated in Minkowski's analysis of Einstein's "Special Theory of Relativity" and depends on the use of a Riemannian space-time map. This became the basic technique of Einstein's "General Relativity". The other is the technique first developed by Milne and Whitrow for "Kinematic Relativity", which I shall therefore call ***the kinematic technique***. Neither of these techniques, however, is restricted to the particular physical theory to which it was first applied, a fact well illustrated by the Riemannian treatment of "Kinematic Relativity" by A. G. Walker and others. The present paper will stress the fact (implicit in the work of Robertson, Walker, Heckmann and others, but still, perhaps, not generally appreciated) that *both* techniques are indeed only techniques and not theories. As such, they can be adapted to the same cosmological hypotheses, and then when applied to a given problem they should furnish equivalent results.

Both techniques have been developed for the investigation of ***homogeneous and isotropic*** model-universes, although the Riemannian technique is certainly capable of incorporating basic hypotheses other than homogeneity and isotropy; the same would appear to be true of the kinematic technique, but this does not seem to have been investigated. The present discussion will be restricted to model-universes of the former type.

Thus, on the one hand, it has been shown by H. P. Robertson (**1**) and, independently, by A. G. Walker (**2**) that any cosmological model which satisfies

* Received in original form 1955 July 5.

the hypotheses of homogeneity and isotropy admits *ipso facto* an invariant quadratic form, now generally known as the Robertson–Walker metric,

$$ds^2 = c^2\,dt^2 - R^2(t)\,\frac{dr^2 + r^2(d\theta^2 + \sin^2\theta\,d\phi^2)}{(1 + kr^2/4)^2}, \qquad (1)$$

which characterizes the model as set out in Section 2 below. Here we need only note that $R(t)$ is an arbitrary function of t, and k is either -1, 0, or 1. The Riemannian 4-space of which (1) is the metric is called the Riemannian map of the model and furnishes a kinematic background against which its properties can be discussed. Additional hypotheses are, however, needed before a particular model can be isolated, that is, before we can assign a particular functional form to $R(t)$ and a particular value to k. It is at this stage only that the various cosmological theories postulating homogeneity and isotropy diverge. For example: (i) if the field equations of "General Relativity" and certain other reasonable assumptions are imposed, some fifteen different models are isolated (**3**); (ii) if Milne's dimensional hypothesis is imposed, a single form of $R(t)$ is isolated (**2**); (iii) the hypotheses of the steady-state theory of Bondi and Gold give rise to a unique model (**4**); (iv) so does the cosmological theory of Dirac (**5**).

On the other hand, it has been shown by Milne and Whitrow (**6**) that the assumptions of homogeneity and isotropy imply certain well-defined relations between the operationally defined coordinates of the fundamental particles of the model. It will be sufficient to recall at this stage that these relations are characterized by an arbitrary generating function $\psi(t)$. Once a particular form of ψ is specified, the kinematic properties of the model are uniquely determined, except for the type of geometry appropriate to it: hyperbolic, spherical or Euclidean. (This property, which in the Riemannian map is governed by the value of k, does not seem to have been adequately discussed by the exponents of the operational technique. It is of importance even in spatially one-dimensional problems like that of the shift-distance law when comparison is made between theory and observation, but its effect does not appear until terms of the third order are considered.) Thus, in this technique also, when applied to homogeneous and isotropic models, the kinematic background is largely characterized by a single unspecified function, $\psi(t)$, which can only be determined by additional hypotheses, such as, for example, Milne's dimensional hypothesis, the "perfect cosmological principle" of the steady-state theory, etc.

It would appear, therefore, that any homogeneous and isotropic model with given kinematic properties should possess a description in terms of either technique and that there should exist a relation between the functions $R(t)$ and $\psi(t)$ appropriate to it. In general, formulae appertaining to the one technique should be translatable into formulae appertaining to the other and results obtained by the two techniques should be comparable. One would not expect to find a complete parallelism, for evidently the kinematic technique is of narrower scope, if only because in it there are difficulties in ascribing *operational* coordinates to particles beyond a possible "horizon of vision" and also because in three dimensions the method still lacks complete development. But within the narrower field of the kinematic technique it is evidently desirable to establish Riemannian equivalents. Undoubtedly, the most important step towards correlating the two techniques has been Robertson's and Walker's

derivations of the metric from the hypotheses of homogeneity and isotropy. This showed that these hypotheses lead either to the metric (1) or to the concept of the kinematic equivalence, depending solely on which technique is used. Walker also showed (**7**) how, by a suitable clock-regraduation, the model characterized by the metric (1) can be made formally identical with the Milne–Whitrow "uniform motion" equivalence. Walker's further investigations, however, were concerned with the Riemannian equivalents of Milne's "Kinematic Relativity" *theory* (free paths, etc.) as distinct from the kinematic *technique*.

In Milne's later work, and in Walker's, only two particular equivalences are considered—the "uniform motion" equivalence and the "stationary" equivalence. These are regarded as alternative descriptions, in terms of two different time-scales, of the unique physical model isolated by the dimensional hypothesis. Yet the kinematic technique can be applied to cosmological problems in its own right, apart from the dimensional hypothesis, just as the Riemannian technique can be applied without the restriction of Einstein's field equations. For a recent example we may point to a paper by Whitrow and Randall (**8**) in which more general equivalences are examined. In connection with such investigations the following hitherto apparently neglected questions are of interest, and it is the primary object of the present paper to attempt to answer them:—

(i) How can one obtain the scale-function $R(t)$ corresponding to an arbitrary generating function $\psi(t)$?

(ii) What is the relation of the coordinate r in the metric (1), specifying a particle on a given line through the origin, and the signal-parameter α which enters into the well-known Milne–Whitrow signal-function $\theta(t)=\psi\alpha\psi^{-1}(t)$ (**9**) and equally specifies a particle on a given line?

(iii) What is the relation of Milne's distance ("radar"-distance) to the distances commonly used in the Riemannian technique?

(iv) Once a relation between $R(t)$ and $\psi(t)$ is established and $\psi(t)$ is found empirically by way of $R(t)$, to what clock-graduation of the universe does $\psi(t)$ correspond?

The last is a question of physics, whereas the others are purely mathematical. Question (iii) is dealt with in Section 2, the remainder in Section 3, which may be read independently of Section 2.

A further object of the present paper is an examination of kinematic equivalences and Riemannian models (which can now be undertaken concurrently) in the light of the shift-distance law with particular reference to a recent paper by G. J. Whitrow (**10**).

All expanding models are characterized by a Doppler red-shift which, to a first approximation, is proportional to distance. The factor of proportionality can usually be made to agree with observation by adjusting a parameter. For many well-known models, however, the second-order term in the expansion of the shift-ratio in the form

$$\frac{\delta\lambda}{\lambda}=ax+bx^2+\ldots,$$

where x denotes distance,* cannot be brought into line with observation by the

* It is a matter of choice which of the several possible cosmological "distances" is to be used in this expansion. The values of the coefficients (with the exception of the first) will, in general, depend on this choice.

mere adjustment of a parameter. The second-order term could thus be used to eliminate such a model. The accurate empirical determination of the shift-distance law is, therefore, of great importance in this connection. The only results available until very recently were those obtained by Hubble before 1937. In view of their unavoidable uncertainties no very definite conclusions could be drawn from the second-order term. Nevertheless, cautious use has been made of that term by Heckmann (**11**) *in conjunction with data obtained from nebular counts*, to determine some of the parameters of "General Relativity" models. A similar procedure seems to have been adopted by most other writers on the subject.

Recently, however, in the above-mentioned paper, G. J. Whitrow re-examined the *direct* use of the second-order term, which is of particular interest now that far more accurate observational results are at our disposal (**12**). He considers not the absolute values of the coefficients but the ratio b/a^2, which we shall denote by η, of the second-order term to the square of the first-order term in the expansion of $\delta\lambda/\lambda$. Whitrow shows, for example, that $\eta = \frac{1}{2}$ for *any* non-recessional theory of the red-shift, provided that the correlation between shift and distance is independent of time and provided also that the expansion of $\delta\lambda/\lambda$ is made in powers of an *additive* distance. Thus the second-order term could be used to eliminate this whole class of models. Another advantage of using η, which has not been stressed, is its independence of any *scale* error made in the distance measurements. This is of particular interest in view of the recent drastic revision of the cosmological distance-scale, by a factor* of about 2 or 3. Several questions concerning η are discussed in Whitrow's paper, but four, in particular, are left open and these will be considered in the present paper:—

(v) Which of the distances commonly used in cosmology are additive in a static model?

(vi) In the general case, how does the particular definition of distance used affect the value of η?

(vii) What is the value of η for the most general kinematic equivalence and Riemannian model?

(viii) What conclusions can be drawn from a comparison of the theoretical values of η with empirical evidence?

The answers to questions (v) and (vi) are contained in Section 2, where expansions of the shift-ratio and auxiliary distances are derived in terms of proper distance, the latter being additive in static models. Various expansions relating shift-ratio, luminosity distance, distance from apparent size and the coordinate r in (1) are well known (**13**), but expansions in terms of proper distance do not seem to be available. The incorporation of Milne's distance into these relations also seems to be new. Regarding question (vi) we may say that the first coefficient in the expansion of $\delta\lambda/\lambda$, usually called Hubble's constant after multiplication by the speed of light, is independent of the particular definition of distance used, since all current cosmological "distances" are equal to a first approximation. But η is more sensitive to the exact definition of distance than was made evident in Whitrow's paper. For example, it will be seen below (Section 4) that the value of η can be changed by as much as 2 when proper

* It is not unlikely, however, that the correction for the more distant nebulae will prove to be more complicated than a mere scale adjustment.

distance (implicit in Whitrow's paper) is replaced by luminosity distance in the expansion.

Question (vii) can be readily answered for the Riemannian models (see Section 2), as general shift-distance formulae are available in this technique. By the correlation of techniques the Riemannian shift-distance formulae can then at once be made applicable also to kinematic equivalences. For the latter no such general formulae have previously been given. In the Appendix it is shown how these shift-distance formulae can be obtained, alternatively, by purely kinematic methods. This serves as a useful illustration of the parallelism between the two techniques.

It was question (viii) that, in fact, first suggested the correlation of the two techniques. For neither of the two main links between theory and observation —the relations between luminosity and red-shift and between luminosity and nebular density—can be satisfactorily treated by the kinematic technique in the absence of a geometrical method. Now, by the correlation effected below, all the relevant formulae of the Riemannian technique can be made available to the models of the kinematic technique also. Section 4 deals with the general problem of comparing theory with observation, as far as the relation between luminosity and red-shift is concerned.

2. *Distance relations.*—In the present section I obtain expansions in terms of proper distance of the shift-ratio, luminosity distance, distance from apparent size and Milne's "radar"- distance. Proper distance, l, as defined below, is the only objective or *cosmic* definition of distance and is therefore suitable as the fundamental variable in a theoretical discussion such as this.

We must now make use of the Robertson–Walker metric (1) which, as already mentioned in Section 1, has been shown to be applicable to *all* theories based on a homogeneous and isotropic substratum. It has the following significance: (i) t is a cosmic time-coordinate; (ii) θ, ϕ are the usual angular measurements made at the spatial origin $r=0$ (which can be identified with *any* fundamental particle); (iii) the world-lines of the fundamental particles are the geodesics r, θ, $\phi=$constant, whence r is a "co-moving" radial coordinate; (iv) light-tracks correspond to the null-geodesics of the metric, and, in particular, light-tracks through the spatial origin have the equations θ, $\phi=$constant and

$$\frac{dt}{R(t)} = \pm \frac{dr}{c(1+kr^2/4)}. \tag{2}$$

It should be noted that at this stage the constant c occurring in (1) need not be identified with the velocity of light. Moreover, in deriving (1) no assumption need be made about the invariance of this velocity nor about the measurement of length (see ref. (**1**), p. 298). In any theory, however, which adopts the convention of the constancy of the local speed of light (and which consequently has related time- and distance-scales) that velocity can be, and usually is, identified with the constant c in (1).

The proper distance, l, between the origin and a fundamental particle with coordinate r_1, at time t_1, is defined (**14**) by the formula

$$l = R(t_1)\int_0^{r_1} \frac{dr}{1+kr^2/4}. \tag{3}$$

In theories of the type just mentioned this distance can be interpreted as the sum of the infinitesimal distance measurements made at the world-moment t_1

by a chain of fundamental observers situated along the space-geodesic joining the particle to the observer. In other theories l must be regarded as conventional.

As a preliminary to obtaining the expansions of the auxiliary distances, as well as for the later discussion of the coefficient η, we derive an expansion of the shift-ratio of the light received at the origin from a fundamental particle. Assuming for the moment that this is a pure Doppler-shift, one easily obtains from (2) the familiar formula (**15**)

$$D=\frac{\lambda+\delta\lambda}{\lambda}=\frac{R(t_0)}{R(t_1)}, \tag{4}$$

where λ and $\lambda+\delta\lambda$ are the emitted and observed wave-lengths and t_1 and t_0 are the times of emission and reception, respectively, of the light-signal in question. Writing $t_1=t_0-\tau$ and expanding, we obtain for $z=D-1$ the series

$$z=\frac{\delta\lambda}{\lambda}=\tau\frac{R'}{R}+\tau^2\left(\frac{R'^2}{R^2}-\frac{1}{2}\frac{R''}{R}\right)+\tau^3\left(\frac{R'^3}{R^3}-\frac{R''R'}{R^2}+\frac{1}{6}\frac{R'''}{R}\right)+\ldots, \tag{5}$$

where we have written R, R', etc., for $R(t_0)$, $R'(t_0)$, etc. To this notation we shall adhere throughout this paper. Integration of (2) along the track of the signal and reference to (3) now gives

$$\int_{t_0-\tau}^{t_0}\frac{dt}{R(t)}=\frac{1}{c}\int_0^{r_1}\frac{dr}{1+kr^2/4}=\frac{l}{cR(t_0-\tau)}. \tag{6}$$

On introducing a new function $s(t)$, defined by the equation $s'(t)=1/R(t)$, the integral on the left becomes $s(t_0)-s(t_0-\tau)$, which can at once be expanded in powers of τ, and the same is true of the denominator on the right. In this way we obtain the series

$$\frac{l}{c}=\tau-\frac{\tau^2}{2}\frac{R'}{R}+\frac{\tau^3}{3}\left(\frac{R''}{R}-\frac{1}{2}\frac{R'^2}{R^2}\right)+\ldots. \tag{7}$$

Inverting, we get

$$\tau=\frac{l}{c}+\frac{1}{2}\frac{l^2}{c^2}\frac{R'}{R}+\frac{1}{3}\frac{l^3}{c^3}\left(2\frac{R'^2}{R^2}-\frac{R''}{R}\right)+\ldots, \tag{8}$$

which, when substituted in (5), gives the required formula

$$z=\frac{l}{c}\frac{R'}{R}+\frac{1}{2}\frac{l^2}{c^2}\left(3\frac{R'^2}{R^2}-\frac{R''}{R}\right)+\frac{1}{6}\frac{l^3}{c^3}\left(16\frac{R'^3}{R^3}-11\frac{R''R'}{R^2}+\frac{R'''}{R}\right)+\ldots. \tag{9}$$

We now turn to the auxiliary distances. The *distance from apparent size*, S, of a given nebula, is defined by the equation

$$\omega=\frac{\Delta}{S^2},$$

where Δ is the supposedly known cross-sectional area of the nebula in question and ω is the solid angle subtended by it at the observer. Taking the observer to be at $r=0$ and the nebula at $r=r_1$, at $t=t_1$, it has been shown (**16**) that

$$S=\frac{R(t_1)r_1}{1+kr_1^2/4}. \tag{10}$$

The *distance from apparent brightness*, or luminosity distance, L, is defined by the equation

$$b=\frac{B}{L^2},$$

where B is the supposedly known absolute brightness of the nebula and b its observed brightness. Again, it has been shown (**17**) that, if t_1 and t_0 are the

times of emission and reception of the light by means of which the nebula at $r=r_1$ is observed, then

$$L=\frac{R^2(t_0)}{R(t_1)}\frac{r_1}{1+kr_1^2/4}. \tag{11}$$

Comparison of (10) and (11) gives, by reference to (4), the well-known relation

$$L=D^2S. \tag{12}$$

On the other hand, comparison of (10) and (3) gives

$$S=R(t_1)\sin\frac{l}{R(t_1)},\ l,\ R(t_1)\sinh\frac{l}{R(t_1)} \tag{13}$$

(according as $k=1$, 0, or -1) and consequently

$$S=l-\frac{kl^3}{6R^2(t_1)}+\ldots.$$

This can be written as

$$S=l-\frac{kl^3}{6R^2}+\ldots, \tag{14}$$

since $R=R(t_0)=R(t_1)+O(l)$. Substituting (14) and (9) in (12), we also obtain the following series expansion for L:

$$L=l+l^2\frac{2R'}{cR}+l^3\left(\frac{4R'^2}{c^2R^2}-\frac{R''}{c^2R}-\frac{k}{6R^2}\right)+\ldots. \tag{15}$$

Finally, ***Milne's distance***, which is the fundamental distance in "Kinematic Relativity" and which will here be denoted by M, is defined by the equation

$$M=\tfrac{1}{2}c(t_0-t_2),$$

where t_2 and t_0 are the instants of emission and reception (after reflection) respectively of a light-signal emitted by the observer and reflected (at time t_1, say) at the particle whose distance is required. Writing $t_1=t_0-\tau$, $t_2=t_0-\sigma$, and integrating (2) once more along the track of the signals, we see that

$$\int_{t_0-\sigma}^{t_0-\tau}\frac{dt}{R(t)}=\int_{t_0-\tau}^{t_0}\frac{dt}{R(t)},$$

whence

$$\int_{t_0-\sigma}^{t_0}\frac{dt}{R(t)}=2\int_{t_0-\tau}^{t_0}\frac{dt}{R(t)}.$$

Expanding both integrals by the method already employed in the derivation of (7), we obtain

$$\frac{\sigma}{R}+\frac{\sigma^2}{2}\frac{R'}{R^2}+\frac{\sigma^3}{6}\frac{2R'^2-RR''}{R^3}+\ldots=2\left(\frac{\tau}{R}+\frac{\tau^2}{2}\frac{R'}{R^2}+\frac{\tau^3}{6}\frac{2R'^2-RR''}{R^3}+\ldots\right),$$

which, when solved for σ, gives

$$\frac{\sigma}{2}=\frac{M}{c}=\tau-\frac{\tau^2}{2}\frac{R'}{R}+\frac{\tau^3}{2}\frac{R''}{R}+\ldots.$$

Substituting for τ from (8) we get the following series expansion for M

$$M=l+\frac{l^3}{6c^2}\left(\frac{R'^2}{R^2}+\frac{R''}{R}\right)+\ldots. \tag{16}$$

This shows that as far as terms of the first and second order are concerned, M and l are interchangeable, which is of particular practical interest in connection with formula (15). (Compare also formulae (9) and (37).)

With reference to the recent paper by Whitrow (**10**) mentioned in the Introduction, we note that $c\tau$ is clearly a *linearly additive* "distance" in the sense employed by Whitrow (i.e. such that, if A, B, C are events along a light-track and in that order, then distance AC = distance AB + distance BC). It follows that the other distances, l, S, L, M, being non-linear functions of $c\tau$ (see (7), (14), (15) and (16)), cannot, in general, be linearly additive in this sense. Only when the model is static, so that $R(t)$ = constant, do we have $c\tau = l = M$. Even in a static model, the distances L and S are not necessarily additive. Only when the model, in addition, is spatially flat ($k = 0$) do we have $c\tau = l = M = S$.

3. *The metric of the ψ-equivalence.*—It has been shown by A. G. Walker (**7**) that, whatever be the form of the function $R(t)$ in the metric (1), it is always possible to find a regraduation from the universal time t to another universal time t' relative to which the model characterized by (1) is equivalent to the "uniform motion" equivalence of "Kinematic Relativity". The required regraduation is given by

$$t' = \exp \int \frac{c\,dt}{R(t)}, \tag{17}$$

and it can easily be verified that this leads to the linear distance–epoch relation $M/T = c \tanh \sigma(r_1)$ for a fundamental particle at $r = r_1$ relative to the origin $r = 0$, where M and T are Milne's conventional distance- and epoch-coordinates assigned in the usual way to the particle in question by means of light-signals and using t'-time, and where

$$\sigma(r_1) = \int_0^{r_1} \frac{dr}{1 + kr^2/4}.$$

Since the origin can be chosen so as to coincide with any fundamental particle, it follows that we have here exactly the situation of the "uniform motion" equivalence.

On the other hand, a well-known formula of "Kinematic Relativity" (**18**), sometimes referred to as expressing the "main theorem on equivalences", gives the regraduation necessary to convert the equivalence generated by the function ϕ into that generated by any other function ψ. If t' is the time of the ϕ-equivalence, then t'', the time of the ψ-equivalence, is given by

$$t'' = \psi(p(\phi^{-1}(t'))^s),$$

where p and s are arbitrary constants which, for our purposes, may be taken as unity. The uniform motion equivalence is generated by the function $\phi(t) = t$ (**19**). Thus a transformation from uniform motion time t' to the time t'' of the ψ-equivalence is given by

$$t'' = \psi(t').$$

The last formula in conjunction with (17) shows that the regraduation

$$t'' = \psi\left\{\exp \int \frac{c\,dt}{R(t)}\right\}$$

will convert the model characterized by the metric (1) into the ψ-equivalence. If (1) is itself the metric of the ψ-equivalence, we must have $t = t''$ and therefore

$$\frac{1}{R(t)} = \frac{1}{c}\frac{d}{dt}\log \psi^{-1}(t). \tag{18}$$

This formula gives the scale function $R(t)$ corresponding to the generating function $\psi(t)$, and vice versa.

An important function in the kinematic technique is the function $\omega(t)$ given by the infinitesimal member of the signal function group, $t+\epsilon\omega(t)$. This function is related to the generating function $\psi(t)$ by the equation $\int(1/\omega(t))\,dt=\log\psi^{-1}(t)$ (**20**). In terms of this function relation (18) takes the very simple form*

$$R(t)=c\omega(t). \tag{19}$$

A further point of interest is the relation between the "co-moving" coordinate r in (1), which permanently appertains to a given fundamental particle, and the signal-parameter α occurring in the Milne–Whitrow signal function (**9**) $\theta(t)=\psi\alpha\psi^{-1}(t)$, which also permanently appertains to a given fundamental particle. From standard formulae of "Kinematic Relativity" (**20**) we obtain the relation

$$\int_{t_1}^{t_0}\frac{dt}{\omega(t)}=\log\alpha_1,$$

t_1 and t_0 being, as before, the times of emission and reception of a light-signal from a particle characterized by the parameter α_1 to the observer. On the other hand, using (19) and (2), we obtain

$$\int_{t_1}^{t_0}\frac{dt}{\omega(t)}=\int_{t_1}^{t_0}\frac{c\,dt}{R(t)}=\int_{0}^{r_1}\frac{dr}{1+kr^2/4}=\sigma(r_1),$$

whence we get the required relation,

$$\alpha=\exp\sigma(r),$$

having discarded the particularizing suffix 1.

The most important application of the correlation here established is to enable us to associate with kinematic equivalences a method for studying questions involving space-geometry. It appears that only with the help of the corresponding metric can such topics as, for example, luminosity distance, distance from apparent size and nebular counts be satisfactorily discussed for a given equivalence.

Conversely, the correlation throws certain light on the Riemannian technique. Milne's concept of clock-equivalence, his recognition of alternative time-scales and of the connection between time-scales and distance-scales (depending on a conventional speed of light) are relevant to all cosmology. The fact that an empirical determination of $R(t)$ automatically determines $\psi(t)$, and our knowledge that $\psi(t)$ depends on the clocks that define t, force us to examine more closely the time-scale implicit in our observational work. This is somewhat hidden, since in practice none of the most significant measurements are actually made with clocks, but rather with photographic plates, spectroscopes, etc. The time-scale enters only when these primary measurements are translated into theoretical terms, usually on the assumption that the observed nebular red-shift is a pure Doppler effect.

If we assume that the red-shift can be regarded as a pure Doppler effect, then when we so regard it we are automatically committed to the uniform time of "atomic vibrators", which I shall call t-time (not to be confused with Milne's dual use of this symbol to signify also the time of the uniform motion equivalence). For in any other time-scale, in which the frequency of atomic vibrators changes secularly, this change constitutes a non-recessional effect contributing to the spectral shift. Thus it appears that t-time is generally implicit in our work

* I owe this observation to Dr G. J. Whitrow.

and the generating function $\psi(t)$ found empirically by way of $R(t)$ will therefore refer to t-time.

The generating function appropriate to the observable universe and a given physical time-scale is, therefore, seen to be amenable to observational determination or, at least, verification. Milne's identification of t-time with the time of the uniformly expanding equivalence, generated by $\psi(t)=t$, can thus be put to the test. Since this identification depended on arguments essentially based on the dimensional hypothesis, we see that the justification of this hypothesis, which is perhaps the cornerstone of Milne's theory, largely depends on the empirical confirmation, subject to the assumptions of "Kinematic Relativity", of this particular form of ψ.

We conclude this section with a table showing the scale-functions $R(t)$ appropriate to some of the more familiar forms of kinematic equivalences. We find that several of these correspond to well-known Riemannian models, provided the curvature index k is suitably chosen. The last column of entries shows the value of Whitrow's coefficient $\eta=3/2-R''R/2R'^2$. This will be of significance in the following section.

TABLE I

$\psi(t)$	Kinematic equivalence	$R(t)$	Riemannian model	η
$a\log(t/b)$	stationary equivalence	ac	Einstein's static model	$(\frac{1}{2})$(**10**)
t	uniform motion equivalence	ct	(*a*) one of the 'empty' models of General Relativity. (*b*) Milne's 'hydrodynamical' model.	$\frac{3}{2}$
$[a\log(b/t)]^{-1}$	Page's uniformly accelerated equivalence (**22**)	act^2		$\frac{5}{4}$
$[a\log(b/t)]^{1/1-n}$	Whitrow and Randall's equivalence (**8**)	$\dfrac{act^n}{n-1}$	for $n=\frac{2}{3}$: Einstein–de Sitter model. for $n=\frac{1}{3}$: Dirac's model (**5**).	$1+\dfrac{1}{2n}$
$-a\log(-1/a\log t)$	Whitrow's equivalence (**23**)	$c\exp\dfrac{t}{a}$	(*a*) de Sitter's model. (*b*) steady state model (**4**).	1

4. *The second-order term in the expansion of the shift-ratio, and its comparison with the empirical data.*—Formula (9), for the shift-ratio interpreted as a pure Doppler effect, may be re-written in the form

$$z=\frac{l}{l_0}+\eta\left(\frac{l}{l_0}\right)^2+\ldots, \tag{20}$$

where, provided $R'\neq 0$, $l_0=cR/R'$ and

$$\eta=\frac{3}{2}-\frac{R''R}{2R'^2}. \tag{21}$$

The coefficient η in the expansion (20) is, in some sense, characteristic of the various cosmological models. In Table I of the preceding section the last

column gives this coefficient for some of the better known kinematic equivalences and Riemannian models evaluated according to (21) except for the first entry.

If, on the other hand, we consider a static model and a red-shift consequently due to some non-Doppler phenomenon, we shall still have a relation of the form (20), although η will not now be given by (21). However, each theory postulated for the explanation of the observed red-shift must predict its own value for η. Whitrow (**10**) has proved the general result that if such a theory gives a *time-independent* shift-ratio then $\eta = \frac{1}{2}$.*

We cannot, of course, rule out the possibility that *both* the expansion of the universe *and* some other phenomenon contribute to the red-shift, but we shall ignore it here.

We now turn to the observational data concerning the shift-ratio. This ratio, z, is correlated by observers with the photographic magnitude of the nebulae, and from these we can calculate the corresponding luminosity distances L. If we assume that

$$z = \alpha L + \beta L^2 + \ldots, \tag{22}$$

we can attempt to find the coefficients α and β by "fitting the best quadratic curve" to the data. Implicit in this procedure is the assumption that the infinite series is fairly represented by its first two terms, at least for the distances so far surveyed. We can obtain some estimate of the validity of this assumption by examining one or two theoretical models. From calculations depending on formula (6) we can find the theoretical value of l/l_0 corresponding to a given shift-ratio z in a given model, which may then be substituted in (20) to exhibit the pattern of the series. To take two widely different cases, consider the models characterized by (*a*) $R(t) = e^{t/T}$, $k = 0$ (e.g. the steady-state model) and (*b*) $R(t) = t$, $k = 0$ (a "uniformly expanding" model). For (*a*) we find $l/l_0 = z/(1+z)$ and for (*b*) $l/l_0 = \ln(1+z)/(1+z)$. Taking $z = 0{\cdot}25$ we find that the series (20) takes the following forms in these cases:

(*a*) $0{\cdot}25 = 0{\cdot}200 + 0{\cdot}040 + 0{\cdot}008 + \ldots,$
(*b*) $0{\cdot}25 = 0{\cdot}178 + 0{\cdot}048 + 0{\cdot}016 + \ldots.$

From (12) and (13) we have that $L = (1+z)^2 l$ in our cases ($k = 0$), whence we find that the series (22) takes the following forms:

(*a*) $0{\cdot}25 = 0{\cdot}312 - 0{\cdot}097 + 0{\cdot}061 + \ldots,$
(*b*) $0{\cdot}25 = 0{\cdot}278 - 0{\cdot}039 + 0{\cdot}014 + \ldots.$

We therefore see that for these models and a shift-ratio of $0{\cdot}25$ the second-order term in (22) is about two or three times as large as all the remaining terms put together. For smaller shift-ratios the convergence of course improves, and the value $z = 0{\cdot}25$ may be regarded as about the frontier of present observations. The maximum error in the empirical value of β in (22), obtained by "fitting the best quadratic" to the data, may, therefore, be of the order of 50 per cent so that we can have some confidence in at least the sign of β so obtained, provided that additional sources of error are not excessive.

Let us now rewrite (22) in the form

$$z = \frac{L}{L_0} + \eta' \left(\frac{L}{L_0}\right)^2 + \ldots \tag{23}$$

where $L_0 = 1/\alpha$ and $\eta' = \beta/\alpha^2$. Then if we know α and β we can calculate η'.

* Whitrow's result here applies, since it refers to the expansion of z in powers of an "additive" distance, which l is in the case of a static model. See the remark at the end of Section 2.

In order to relate η' to the coefficient η of (20) and (21) let us set

$$L = D^p S. \tag{24}$$

It was seen in Section 2 that $p = 2$ on a purely Doppler interpretation of the red-shift and on the assumption of constant nebular brightness. However, in a static model in which some non-Doppler agency causes the red-shift, the absence of the so-called number effect (or recession effect) in the calculations for L can be shown to lead to the value $p = \frac{1}{2}$ (**24**). In "Kinematic Relativity", on the other hand, the variation of the absolute brightness of nebulae ($B\alpha t^{-1}$) implied by the dimensional hypothesis (**21**) leads to $p = \frac{3}{2}$, as can easily be verified. Only if we allow for the possibility, mentioned earlier, of a red-shift caused by more than one agency, would the relation between L and S be of an altogether more complicated type than (24).

Referring to (14) we can rewrite (24) as

$$L = D^p l + O(l^3),$$

whence, using (20),

$$L = l + p\frac{l^2}{l_0} + O(l^3),$$

which is a general relation analogous to (15). When this is substituted in (23) we obtain an expression which must be identical with (20). Comparing coefficients we then obtain $l_0 = L_0$ and

$$\eta = \eta' + p. \tag{25}$$

This relation allows us to compare our theoretical results with observation.

There are two published sets of figures available for analysis. The first set was obtained by Hubble before 1937 and analysed by Heckmann (**25**). It comprised data concerning ten nebulae with shift-ratios ranging from 0·0041 to 0·1403. With due stress on the uncertainties both of the data and of the series expansion method as such, Heckmann gave the following values for the coefficients in (22) (the unit of distance being 10^8 parsec):

$$\left.\begin{aligned} &\text{(i)}\ \alpha = 0{\cdot}1789 \pm 0{\cdot}0160, \quad \beta = -0{\cdot}0071 \pm 0{\cdot}0160 \\ &\text{(ii)}\ \alpha = 0{\cdot}1782 \pm 0{\cdot}0035, \quad \beta = -0{\cdot}0150 \pm 0{\cdot}0035 \end{aligned}\right\}, \tag{26}$$

the second set being obtained by omitting from the analysis the three most doubtful nebulae. The following are the corresponding values of η' in (23):

$$\text{(i)}\ \eta' = -0{\cdot}22 \pm 0{\cdot}50, \quad \text{(ii)}\ \eta' = -0{\cdot}47 \pm 0{\cdot}11. \tag{27}$$

Although the distance scale has been drastically revised since these results were published, that portion of the correction which is merely multiplicative will affect only the values of α and β but not of η'. I have, therefore, included the above figures for purposes of comparison with the new ones.

Hubble's data are now superseded by the publication, by Humason, Mayall and Sandage (**12**), of new data obtained with the most modern apparatus and corrected in accordance with the most refined theoretical techniques. These authors, moreover, carefully analysed their data—amongst other things—for much the same purpose as ours, namely to determine second-order terms. The publication of the present alternative analysis would, perhaps, be unjustified if its results completely agreed with those of Humason, Mayall and Sandage. The fact, however, that there is a difference (significant, though not large enough to affect the main conclusion) seems to indicate some uncertainty in both results.

The discrepancy can be traced to the use of different variables in the fitting of theoretical curves to the empirical data, and the sensitivity of the "least squares" method to such differences. Whereas these authors seek to determine the coefficients in the relation $m = 5 \log cz + Bz + D$, I seek α and β in the relation $z = \alpha L + \beta L^2$. I shall comment on our differences below.

The relevant data are contained in Table XIII of the above-mentioned paper (**12**). We begin by converting the (corrected) photographic magnitudes, P_c, into luminosity distances, L, by the usual formula $\log L = 0{\cdot}2(P_c - M_0) + 1$, where for the absolute magnitude M_0 we take the authors' value of $-19{\cdot}78$. This leads to the following correlation between the shift-ratio, z, and L (in 10^8 parsec).

TABLE II

z	L	z	L	z	L
0·004	0·061	0·052	1·253	0·131	2·618
0·018	0·287	0·053	0·995	0·134	2·618
0·022	0·334	0·065	1·355	0·159	2·716
0·035	0·603	0·072	1·000	0·173	2·443
0·043	0·817	0·072	1·387	0·192	2·911
0·044	0·920	0·078	1·614	0·202	3·342

Then, fitting the best quadratic curve to these data by the method of least squares, I find that

$$z = 0{\cdot}0472 L + 0{\cdot}0042 L^2. \tag{28}$$

The first term in this quadratic would imply a Hubble coefficient of 142 km/sec per megaparsec.

Although we have here neglected the tricky question of the magnitude of the possible errors involved, the convex trend of the z–L graph and therefore the positive sign of the quadratic term in (28) seem beyond doubt. From (28) and (23), we obtain, in fact,

$$\eta' = 1{\cdot}9. \tag{29}$$

Some months ago Professor G. C. McVittie kindly informed me that he had computed the values of R'/R and R''/R from data on red-shifts available in 1954 July and that these implied a value of η' lying between 1 and 3, which is compatible with (29).

The values (27) of η' which result from Heckmann's analysis of Hubble's data would present fewer theoretical difficulties than the new value (29). By (25) the former permit the ranges

$$\text{(i)}\ -0{\cdot}22 \leqslant \eta \leqslant 0{\cdot}78, \quad \text{(ii)}\ -0{\cdot}08 \leqslant \eta \leqslant 0{\cdot}14$$

for static models with time-independent red-shift ($p = \frac{1}{2}$);

$$\text{(i)}\ 0{\cdot}78 \leqslant \eta \leqslant 1{\cdot}78, \quad \text{(ii)}\ 0{\cdot}92 \leqslant \eta \leqslant 1{\cdot}14$$

for the model of "Kinematic Relativity" ($p = \frac{3}{2}$); and

$$\text{(i)}\ 1{\cdot}28 \leqslant \eta \leqslant 2{\cdot}28, \quad \text{(ii)}\ 1{\cdot}42 \leqslant \eta \leqslant 1{\cdot}64$$

for other expanding models ($p = 2$).

Thus the stricter sets of figures (ii) would rule out static models with time-independent red-shift ($\eta = \frac{1}{2}$) and the model of "Kinematic Relativity" ($\eta = \frac{3}{2}$).

Both (i) and (ii) would rule out, amongst others, the model of the steady-state theory ($\eta = 1$). A uniformly expanding model ($R = t$, $\eta = \frac{3}{2}$) without the particular assumptions of "Kinematic Relativity" regarding intrinsic brightness would appear to be well favoured by Heckmann's figures.

The new data indicate that the value of η' implicit in Hubble's data was too low. The former lead to a convex z–L graph (viewed from the axis of L), whereas Hubble's data led to a slightly concave graph. If, for the moment, we accept no other consequence of the new data than this, i.e. that $\eta' > 0$, we find from (25) that $\eta > 2$ for the ordinary expanding model ($p = 2$). Reference to (21) shows that this implies $R'' < 0$, and so we are led to a class of models which, until recently, were rejected because of the well-known time-scale difficulty inherent in them (**26**). (Owing to a more rapid expansion in the past they are of even more recent origin than models with uniform expansion at the present rate, and the latter led to a low age of the universe not consistent with geological and other data.) The newly revised scale resolves this difficulty to some extent. However, before we discard, on the basis of criterion (29), practically all the models that have been put forward in the last two decades* we must carefully consider the following possibilities: (i) the shift-ratios of the absorption-line spectra of the most distant nebulae may have been systematically increased by some non-Doppler agency; (ii) the distances of the remote nebulae may be systematically underestimated, owing perhaps to (iii) the possible non-constancy of absolute nebular brightness in t-time. Two further possible sources of systematic distance errors are (iv) the Stebbins Whitford effect and (v) internebular absorption. Both these, however, make for overestimates rather than underestimates of distance.

Humason, Mayall and Sandage find that the coefficient B in their relation $m = 5 \log cz + Bz + D$ is $-1{\cdot}180 \pm 0{\cdot}875$. From the theoretical expression

$$B = 1{\cdot}086\left(1 + \frac{RR''}{R'^2} - 2\mu\right),$$

where μ is a correction term depending on the factors (iii), (iv) and (v) above and which we shall neglect for the moment, this is found to imply

$$\frac{RR''}{R'^2} = -2{\cdot}0 \pm 0{\cdot}8$$

whence $\eta' = 0{\cdot}5 \pm 0{\cdot}4$ for an ordinary expanding model. When an "aperture correction" is applied, these authors find

$$\frac{RR''}{R'^2} = -3{\cdot}0 \pm 0{\cdot}8$$

whence $\eta' = 1{\cdot}0 \pm 0{\cdot}4$. This is considerably lower than our value of 1·9. Even so, the authors consider that on present theories of nebular evolution and with the present data concerning the Stebbins Whitford effect, the term μ cannot be made sufficiently large for the tentative conclusion $R'' < 0$ to be avoided.

5. *Acknowledgments.*—I wish to express my sincere thanks to Dr G. J. Whitrow, who suggested the present investigations to me, for his many constructive criticisms and help in clarifying portions of the exposition. I also wish to thank Professor G. C. McVittie for the interest which he has shown in this work and for his valuable criticisms of a first draft of it; and Dr M. L. Humason and

* Dirac's model (**5**) formed an exception, having $R'' < 0$, but for it, too, the new value of η' is too high.

Dr A. R. Sandage for kindly making available to me observational material prior to publication, and for answering in detail my queries.

Mathematics Department,
Imperial College of Science and Technology,
London, S.W.7:
1956 *June* 25.

APPENDIX

Shift-distance formulae obtained by the kinematic technique

The two results of this Appendix, viz. formulae (33) and (37), could be written down at once by translating the Riemannian formulae (4) and (9) into their kinematic equivalents according to Sections 2 and 3. I here obtain these formulae by purely kinematic methods as an example of the parallelism between the two techniques. Such general formulae for the shift-distance relation in the kinematic technique do not appear to have been obtained previously.

Consider two fundamental particles, A and B, belonging to a kinematic equivalence and let $\theta(t)$ be the signal function appertaining to these two particles. Let an observer attached to A emit a light-signal at time t_2, which is received at B at time t_1, whereupon the observer attached to B instantly emits a signal which arrives at A at time t_0, all times being measured by the local clock, so that

$$t_1=\theta(t_2), \qquad t_0=\theta(t_1). \tag{30}$$

A second signal is then emitted at B at time t_1+dt_1 and received at A at time t_0+dt_0. If dt_1 is the duration at B of a single pulse of the emitted light, then the Doppler-shift in this light when received at A is given by

$$D=\frac{\lambda+\delta\lambda}{\lambda}=\frac{dt_0}{dt_1}=\theta'(t_1), \tag{31}$$

where λ and $\lambda+\delta\lambda$ are the wave-lengths as measured at B and A respectively, the last equation resulting from differentiation of the second member of (30).

If $\omega(t)$ is the function occurring in formula (19) we have the relation (**20**)

$$\theta'(t)=\frac{\omega(\theta(t))}{\omega(t)}. \tag{32}$$

On substituting this in (31) and using (30), we obtain

$$D=\frac{\omega(t_0)}{\omega(t_1)}. \tag{33}$$

If we write $t_1=t_0-\tau$, we can expand the right-hand side of this equation in powers of τ, thus:

$$D=1+\tau\frac{\omega'}{\omega}+\tau^2\left(\frac{\omega'^2}{\omega^2}-\frac{1}{2}\frac{\omega''}{\omega}\right)+\tau^3\left(\frac{\omega'^3}{\omega^3}-\frac{\omega''\omega'}{\omega^2}+\frac{1}{6}\frac{\omega'''}{\omega}\right)+\ldots, \tag{34}$$

where we have written ω, ω', etc., for $\omega(t_0)$, $\omega'(t_0)$, etc. It now remains to relate τ to the distance AB.

From equation (32) we obtain

$$\int_{t_2}^{t_1}\frac{dt}{\omega(t)}=\int_{t_2}^{t_1}\frac{\theta'(t)\,dt}{\omega(\theta(t))}=\int_{\theta(t_2)}^{\theta(t_1)}\frac{dt}{\omega(t)}=\int_{t_1}^{t_0}\frac{dt}{\omega(t)}$$

and therefore

$$\int_{t_2}^{t_0}\frac{dt}{\omega(t)}=2\int_{t_1}^{t_0}\frac{dt}{\omega(t)}. \tag{35}$$

If we introduce a new function $s(t)$, defined by the equation $s'(t) = 1/\omega(t)$, and write $t_2 = t_0 - \sigma$, then equation (35) reduces to

$$s(t_0) - s(t_0 - \sigma) = 2[s(t_0) - s(t_0 - \tau)],$$

both sides of which can now be expanded, thus

$$\frac{\sigma}{\omega} + \frac{\sigma^2}{2}\frac{\omega'}{\omega^2} + \frac{\sigma^3}{6}\frac{2\omega'^2 - \omega''\omega}{\omega^3} + \ldots = 2\left[\frac{\tau}{\omega} + \frac{\tau^2}{2}\frac{\omega'}{\omega^2} + \frac{\tau^3}{6}\frac{2\omega'^2 - \omega''\omega}{\omega^3} + \ldots\right]. \quad (36)$$

Now, by the usual definition (in "Kinematic Relativity") of the distance M between A and B, we have $\sigma = 2M/c$, so that equation (36) can be solved for τ in terms of M, giving

$$\tau = \frac{M}{c} + \frac{1}{2}\frac{M^2}{c^2}\frac{\omega'}{\omega} + \frac{1}{2}\frac{M^3}{c^3}\left(\frac{\omega''}{\omega} - \frac{\omega'^2}{\omega^2}\right) + \ldots,$$

which, when substituted in equation (34), leads to the following shift-distance relation:

$$z = D - 1 = \frac{M}{c}\frac{\omega'}{\omega} + \frac{1}{2}\frac{M^2}{c^2}\left(3\frac{\omega'^2}{\omega^2} - \frac{\omega''}{\omega}\right) + \frac{1}{6}\frac{M^3}{c^3}\left(9\frac{\omega'^3}{\omega^3} - 6\frac{\omega''\omega'}{\omega^2} + \frac{\omega'''}{\omega}\right) + \ldots. \quad (37)$$

References

(1) H. P. Robertson, *Astrophys. J.*, **82,** 284, 1935.
(2) A. G. Walker, *Proc. London. Math. Soc.* (2), **42,** 90, 1937.
(3) H. Bondi, *Cosmology*, Cambridge, p. 105, 1952.
(4) H. Bondi, *loc. cit.*, p. 146.
(5) P. A. M. Dirac, *Proc. Roy. Soc.* A, **165,** 199, 1938. See also H. Bondi, *loc. cit.*, p. 162.
(6) E. A. Milne and G. J. Whitrow, *Z. Astrophys.* **15,** 263, 1938.
(7) A. G. Walker, *M.N.*, **95,** 263, 1935.
(8) G. J. Whitrow and D. G. Randall, *M.N.*, **111,** 455, 1951.
(9) E. A. Milne, *Kinematic Relativity*, Oxford, p. 22, 1948.
(10) G. J. Whitrow, *M.N.*, **114,** 180, 1954.
(11) O. Heckmann, *Theorien der Kosmologie*, Berlin, p. 65 *et seq.*, 1942.
(12) M. L. Humason, N. U. Mayall, and A. R. Sandage, *Astr. J.* **61,** 97, 1956.
(13) See, for example, W. H. McCrea, *Z. Astrophys*, **9,** 290, 1935; G. C. McVittie, *Proc. Phys. Soc.* Lond, **51,** 529, 1939; O. Heckmann, *loc. cit.* p. 62 *et seq.*
(14) R. C. Tolman, *Relativity, Thermodynamics and Cosmology*, Oxford, formula (155.11), 1934; or G. C. McVittie, *Cosmological Theory*, London, formula (4.20), 1937.
(15) H. Bondi, *loc. cit.*, formula (10.18).
(16) W. H. McCrea, *loc. cit.*, formula (5).
(17) W. H. McCrea, *loc. cit.*, formula (15).
(18) E. A. Milne, *loc. cit.*, section (16).
(19) E. A. Milne, *loc. cit.*, section (24).
(20) E. A. Milne, *loc. cit.*, section (12).
(21) A. G. Walker, *Proc. Roy. Soc. Edin.* (Sect. A), **62,** 221, 1946.
(22) E. A. Milne, and G. J. Whitrow, *Z. Astrophys.*, **15,** 342, 1938.
(23) G. J. Whitrow, unpublished work.
(24) W. H. McCrea, *loc. cit.*, p. 300.
(25) O. Heckmann, *loc. cit.*, pp. 66, 67.
(26) H. Bondi, *loc. cit.*, p.116.

BOYLE'S LAW AND GRAVITATIONAL INSTABILITY

W. B. Bonnor

(Communicated by H. Bondi)

(Received 1956 February 2)

Summary

A modified form of Boyle's Law is derived for a spherical mass of gas at uniform temperature in equilibrium under its own gravitation and an external pressure, and a typical p–V curve is shown. Any such mass of gas is gravitationally unstable if sufficiently compressed. It is shown also that a sufficiently large isothermal gas sphere is unstable, and the condition for this is compared with Jeans' formula for gravitational instability.

The relevance of the phenomenon to the formation of the nebulae is briefly considered.

---

1. *Introduction.*—It has recently been suggested by Terletsky (**7**) that for a large mass M of gas, of volume V and temperature T, containing N molecules under boundary pressure p, the equation of state should be not

$$pV = NkT \tag{1.1}$$

but

$$pV = NkT - \alpha GM^2V^{-1/3}, \tag{1.2}$$

where k is Boltzmann's constant, G is Newton's constant of gravitation, and α is a constant depending on the shape of the mass. The proposed correction of Boyle's Law arises because, for a large mass, one has to take account of the gravitational interactions between the molecules.

Terletsky is interested in the statistical fluctuations in density of the gas, and he uses the ordinary formula for the volume fluctuation

$$\frac{\overline{(V-\bar{V})^2}}{\bar{V}^2} = -\frac{kT}{V^2(\partial p/\partial V)_T}, \tag{1.3}$$

where $\bar{V}$ is the mean volume. If this is applied to (1.1) the right-hand side becomes $1/N$ and the volume (or density) fluctuation diminishes as the mass increases; if, however, it is applied to (1.2), one finds

$$\frac{\overline{(V-\bar{V})^2}}{\bar{V}^2} = \frac{1}{N}\left[1 - \frac{4}{3}\frac{\alpha Gm^2N}{kTV^{1/3}}\right]^{-1}, \tag{1.4}$$

where $m = M/N$. From (1.4) it follows that the fluctuation can become large for large masses as well as for small ones. For example, supposing that the gas is hydrogen at 10^5 deg. K, and is a uniform sphere (in which case $\alpha = \frac{1}{5}(\frac{4}{3}\pi)^{1/3}$, as will be shown later), one finds that the right-hand side of (1.4) becomes large when the ratio mass/radius is about 2×10^{20}.

This result is especially interesting because of the present situation in cosmology. One of the difficulties of the point-source cosmological models of general relativity concerns the formation of the nebulae. If one supposes that the

primordial matter was uniformly distributed but subject to ordinary fluctuations, it seems from the work of Lifshitz (**6**) that the time of 4×10^9 years which has elapsed since the start of the universal expansion is not long enough to allow the development of the present degree of heterogeneity. Some mechanism which allows large fluctuations in the cosmic medium might help to explain the formation of the nebulae.

In discussing formula (1.2) Terletsky seems to have in mind a static mass of gas of uniform density. This is unsatisfactory because if the mass is finite the equation of hydrostatic equilibrium is not satisfied, and if it is infinite the gravitational field strength at a point is not properly defined and the use of Newtonian gravitation theory is questionable. There is also the objection that in a proper treatment of fluctuations one should consider, as $(\partial p/\partial V)_T$ tends to zero, the higher derivatives such as $(\partial^2 p/\partial V^2)_T$, as is done in the theory of gases near the critical point. Further, if for a certain value of the ratio mass/radius $(\partial p/\partial V)_T$ changes sign (as it does for (1.2)) this suggests that such a mass of gas would be unstable, and not that it would be in a critical state as Terletsky proposes.

In this paper I obtain the equation of state for a large gas sphere of constant mass and temperature, but non-uniform density, and I construct its p–V curve. This amounts to an investigation of the equilibrium under its own gravitation and an applied external pressure of an isothermal gas sphere containing a fixed mass. Boyle's Law (1.1) is obeyed only as $V \to \infty$. If the mass/radius ratio is large enough the sphere is unstable and the gas tends to collapse towards the centre; there is, however, no evidence that gravitation, though responsible for the instability, could confer on the gas the properties of a critical state.

The p–V curve is obtained in Section 2, and this is followed in Section 3 by a discussion of the stability and a comparison of the results with those of Jeans on gravitational stability. The paper ends with Section 4, in which the main conclusions are briefly summarized.

2. *The p–V curve.*—Consider a spherical mass of perfect gas (of uniform chemical composition) in isothermal equilibrium under its own gravitation, and let O be the centre. At every point P the gas obeys the local equation of state

$$p = k\rho T/m, \tag{2.1}$$

where p, ρ and T are the pressure, density and temperature at P, and m is the mass of a molecule. The gas satisfies also the equation of hydrostatic equilibrium:

$$-\frac{dp}{dr} = \frac{4\pi G\rho}{r^2}\int_0^r \rho y^2 dy,$$

or

$$\frac{1}{r^2}\frac{d}{dr}\left(\frac{r^2}{\rho}\frac{dp}{dr}\right) = -4\pi G\rho\,. \tag{2.2}$$

Eqns. (2.1) and (2.2) together give the equation for the density distribution of an isothermal gas sphere:

$$\frac{1}{r^2}\frac{d}{dr}\left(\frac{r^2}{\rho}\frac{d\rho}{dr}\right) = -\frac{4\pi Gm\rho}{kT}. \tag{2.3}$$

This equation was studied in detail by Emden (**2**), and is discussed in standard textbooks. (See, for example, Chandrasekhar (**1**).)

Eqn. (2.3) may be put into a form analogous with Terletsky's equation (1.2) in the following way. Consider a spherical volume V, with centre O and radius

r, containing N molecules and under pressure p at the boundary. We have

$$N = \frac{4\pi}{m}\int_0^r \rho y^2 dy, \tag{2.4}$$

and we may write

$$pV - NkT = \frac{4\pi}{3} r^3 p - \frac{4\pi kT}{m}\int_0^r \rho y^2 dy$$

$$= \frac{4\pi}{3}\int_0^r y^3 \frac{dp}{dy} dy,$$

using (2.1). Using (2.2) we now find

$$pV = NkT - \frac{16}{3}\pi^2 G \int_0^r \rho y dy \int_0^y \rho x^2 dx. \tag{2.5}$$

This is the corrected form of (1.1) when gravitation is taken into account, ρ being given by (2.3).

Although we have obtained it for an isothermal gas sphere by using the local equation of state (2.1) and the equation of hydrostatic equilibrium (2.2), equation (2.5) may be derived without assuming either (2.1) or (2.2). If one uses the virial of Clausius, (2.5) follows on the assumptions, first, that the spherical mass of gas is in a steady state, secondly, that its mean kinetic energy is equal to $(3/2)\,NkT$, and thirdly that one may in computing the virial use ordinary Newtonian gravitation theory. Included in the last assumption is that the gravitational force at a point distant r from the centre arises only from matter within radius r. Strictly, therefore, ρ does not need to satisfy (2.3) for (2.5) to be true, and Terletsky's expression (1.2) (with $\alpha = 1/5(4\pi/3)^{1/3}$) follows from (2.5) by taking $\rho = \text{const.}$ The objection to this, as already stated, is that if the sphere is finite, $\rho = \text{const.}$ does not satisfy the equation of equilibrium, and if it is infinite the gravitational force is not defined, and the third assumption above is not justified.

Let us now transform (2.3) by making the following substitutions:

$$\rho = \lambda e^{-\psi}, \quad r = \beta^{1/2}\lambda^{-1/2}\xi, \tag{2.6}$$

where λ is an arbitrary constant, and

$$\beta = kT/4\pi Gm. \tag{2.7}$$

Then (2.3) becomes

$$\xi^{-2}\frac{d}{d\xi}\left(\xi^2 \frac{d\psi}{d\xi}\right) = e^{-\psi}. \tag{2.8}$$

The boundary conditions to be satisfied at the centre $r = 0$ are

$$\rho = \rho_c, \quad \frac{d\rho}{dr} = 0,$$

where ρ_c is the central density, supposed given. If we choose $\lambda = \rho_c$ these conditions become, in the new variables

$$\psi = 0, \qquad \frac{d\psi}{d\xi} = 0 \text{ at } \xi = 0,$$

which completely determine the solution of (2.8). The solution, so determined, may be applied to gas spheres of different central densities by choosing different values of λ. Thus we may regard λ as the parameter of the family of isothermal gas spheres. Any complete isothermal gas sphere extends to infinity: this means that in (2.8) $e^{-\psi}$ (and therefore p and ρ) has no zero for finite positive values of ξ.

To construct the p–V curve, let us imagine a Boyle's Law experiment conducted in a spherical container of variable radius which contains a fixed number N_0 of molecules of gas, and which is kept at constant temperature T. If the pressure p_0 on the outside is successively varied, and after each variation the gas is allowed to come to equilibrium, it will assume the configurations of the central cores of a series of isothermal gas spheres. To each point (p_0, V_0) (V_0 being the volume of the container) of the Boyle's Law curve will correspond a different value of λ.

Although it does not seem possible to find a closed formula for p_0 in terms of V_0 at constant N_0 and T, we can find the derivative $(\partial p_0/\partial V_0)_{N_0, T}$ in the following way. From (2.2), (2.4), (2.6) and (2.7), we have

$$N = \frac{4\pi}{m}\beta^{3/2}\lambda^{-1/2}\xi^2\frac{d\psi}{d\xi}. \tag{2.9}$$

We are interested in variations of p_0 and V_0 at constant N_0, so we take

$$\delta N_0 = \frac{4\pi}{m}\beta^{3/2}\delta\left\{\lambda^{-1/2}\xi_0^{\,2}\left(\frac{d\psi}{d\xi}\right)_0\right\} = 0, \tag{2.10}$$

where the suffix 0 means that the value of a quantity on the boundary is to be taken. Equation (2.10) gives

$$-\tfrac{1}{2}\lambda^{-3/2}\xi_0^{\,2}\left(\frac{d\psi}{d\xi}\right)_0\delta\lambda + \lambda^{-1/2}\left\{\frac{d}{d\xi}\left[\xi^2\frac{d\psi}{d\xi}\right]\right\}_0\delta\xi_0 = 0; \tag{2.11}$$

and from (2.8)

$$\left\{\frac{d}{d\xi}\left[\xi^2\frac{d\psi}{d\xi}\right]\right\}_0 = \xi_0^{\,2}e^{-\psi_0}. \tag{2.12}$$

Now
$$\delta\xi_0 = \left(\frac{\partial\xi_0}{\partial r_0}\right)_\lambda \delta r_0 + \left(\frac{\partial\xi_0}{\partial\lambda}\right)_{r_0}\delta\lambda;$$

substituting this and (2.12) into (2.11), and using (2.6), we find

$$0 = \delta\lambda\left[-\tfrac{1}{2}\lambda^{-3/2}\xi_0^{\,2}\left(\frac{d\psi}{d\xi}\right)_0 + \tfrac{1}{2}\lambda^{-3/2}\xi_0^{\,3}e^{-\psi_0}\right] + \beta^{-1/2}\xi_0^{\,2}e^{-\psi_0}\delta r_0$$

which gives, on using (2.6) and (2.9)

$$\delta\lambda = \frac{2\lambda\rho_0\delta r_0}{mN_0/4\pi r_0^{\,2} - r_0\rho_0}. \tag{2.13}$$

From (2.1), we have

$$\left(\frac{\partial p_0}{\partial V_0}\right)_{N_0, T} = \frac{kT}{m}\left(\frac{\partial\rho_0}{\partial V_0}\right)_{N_0, T} = \frac{kT}{4\pi m r_0^{\,2}}\left(\frac{\partial\rho_0}{\partial r_0}\right)_{N_0, T}, \tag{2.14}$$

and
$$\begin{aligned}\delta\rho_0 = \delta(\lambda e^{-\psi_0}) &= e^{-\psi_0}\delta\lambda - \lambda e^{-\psi_0}\left(\frac{d\psi}{d\xi}\right)_0\delta\xi_0\\ &= e^{-\psi_0}\left\{\delta\lambda\left[1 - \lambda\left(\frac{d\psi}{d\xi}\right)_0\frac{\partial\xi_0}{\partial\lambda}\right] - \lambda\left(\frac{d\psi}{d\xi}\right)_0\frac{\partial\xi_0}{\partial r_0}\delta r_0\right\}\\ &= e^{-\psi_0}\left\{\delta\lambda\left(1 - \frac{mN_0}{8\pi\beta r_0}\right) - \frac{mN_0\lambda}{4\pi r_0^{\,2}\beta}\delta r_0\right\},\end{aligned} \tag{2.15}$$

where (2.6) and (2.9) have been used. Reintroducing ρ from (2.6) into (2.15) and using (2.13), we find that (2.14) gives after simplification

$$\left(\frac{\partial p_0}{\partial V_0}\right)_{N_0, T} = -\frac{2p_0}{3V_0}\cdot\frac{1 - \left(\frac{4\pi}{3}\right)^{1/3}\frac{Gm^2N_0^{\,2}}{6p_0V_0^{4/3}}}{1 - \frac{N_0kT}{3p_0V_0}}. \tag{2.16}$$

If in (2.16) one puts $G=0$ and supposes that the density is uniform one finds the usual expression for $\partial p/\partial V$ for an ideal gas.

Although I have not been able to integrate (2.16) in finite form, it is not difficult to sketch the solution curves. It is rather easier, however, to obtain the solution of physical interest from Emden's data (2) in the following way. This procedure amounts to choosing that integral of (2.16) in which p_0 is of order V_0^{-1} for large V_0.

Emden gave the solutions of (2.8) in the form of a table of values of ψ and $d\psi/d\xi$ corresponding to certain values of the independent variable ξ. If one assumes a definite constant value of λ one can find from the table the density distribution for an isothermal gas sphere of given central density λ by using (2.6). Instead of doing this, let us allow λ to vary whilst keeping N (number of molecules inside radius r) constant; in this case we have from (2.9)

$$\lambda^{1/2}=\frac{4\pi}{mN}\beta^{3/2}\xi^2\frac{d\psi}{d\xi}. \tag{2.17}$$

Then points on the p–V curve are obtained by expressing $p(=kT\rho/m)$ and $V(=\frac{4}{3}\pi r^3)$ in terms of ψ and $d\psi/d\xi$, and using Emden's data to calculate them. From (2.6), (2.7) and (2.17) we find

$$p=\frac{k^4T^4}{4\pi G^3m^6N^2}\xi^4\left(\frac{d\psi}{d\xi}\right)^2 e^{-\psi},$$

$$V=\frac{4\pi}{3}\left[\frac{Gm^2N}{kT\xi d\psi/d\xi}\right]^3.$$

Using this method we find p–V curves such as that shown in Fig. 1. which refers to a mass of 10^{30} gm. of hydrogen at 0°C. For large volumes the curve approaches the ordinary curve $p=NkT/V$, but for larger values of p it spirals round the singular point

$$p=\frac{2}{\pi}\frac{k^4T^4}{G^3m^6N^2}, \qquad V=\frac{\pi}{6}\left[\frac{Gm^2N}{kT}\right]^3,$$

of the differential equation (2.16).

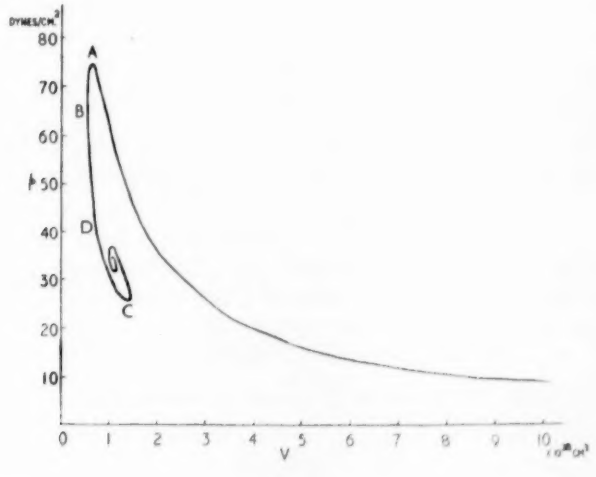

FIG. 1.

3. *Stability.*—For points on the curve between $V=\infty$ and A, the highest maximum of p, $\partial p/\partial V$ is negative and the equilibrium is stable. At A the equilibrium is unstable because a small increase in the external pressure causes a decrease in the volume which results in a reduction of the internal boundary pressure as the state of the gas moves along the part AB of the curve. Thus an isothermal sphere of gas, if sufficiently compressed, is unstable, because a small increase in external pressure will make it collapse.

It follows also that any sufficiently large isothermal gas sphere is unstable. For consider a sphere of radius R in equilibrium under the correct boundary pressure, and with definite central density. Let $p(r)$ be the pressure at radius $r(<R)$ and $V(r)$ and $N(r)$ the volume and number of molecules inside r. Throughout the sphere there will be slight pressure and volume fluctuations, and for spherically symmetric fluctuations $(\partial p/\partial V)_{N,T}$ at radius r is given by (2.16). Now the numerator and denominator of the second fraction on the right-hand side of (2.16) may be written

$$1-\frac{(4\pi/3)^{1/3}Gm^2N^2}{6pV^{4/3}}=1-\tfrac{1}{2}\,e^v\left(\frac{d\psi}{d\xi}\right)^2, \tag{3.1}$$

$$1-\frac{kTN}{3pV}=1-\frac{e^v}{\xi}\frac{d\psi}{d\xi}, \tag{3.2}$$

in which form the two expressions may readily be calculated from Emden's data. For smaller values of ξ (or r) both these functions are positive and $\partial p/\partial V$ is negative as in Boyle's Law. For larger values of r both (3.1) and (3.2) oscillate in sign, (3.1) becoming zero before (3.2). Let $V=v$ be the smallest volume for which (3.1) (and therefore $\partial p/\partial V$) becomes zero; then one easily finds

$$\left(\frac{\partial^2 p}{\partial V^2}\right)_{N,\,T(V=v)}<0.$$

Thus for a small fluctuation dV in the volume of the sphere of mean volume v, we have

$$dp=\left(\frac{\partial^2 p}{\partial V^2}\right)_{V=v}dV^2+O(dV^3)\quad<0.$$

Therefore if a fluctuation occurs which results in a slight decrease in the volume of this sphere, this will produce a decrease in the pressure inside its boundary which will lead to a further reduction in its volume. Thus an isothermal gas sphere of volume greater than v will be unstable because small fluctuations will make the volume v collapse towards the centre.

The lowest value of ξ at which $\partial p/\partial V$ becomes zero is found from (3.1) and Emden's table to be about 6·5. Hence from (2.6) the critical radius is

$$r_c=6{\cdot}5\beta^{1/2}\lambda^{-1/2}=1{\cdot}8\left(\frac{kT}{mG\lambda}\right)^{1/2}, \tag{3.3}$$

where, it will be recalled, λ is the central density. Formula (3.3) may be written in various forms. For example, we find

$$r_c=0{\cdot}76\left(\frac{kT}{mG\bar{\rho}}\right)^{1/2}, \tag{3.4}$$

where $\bar{\rho}$ is the mean density inside the sphere of radius r_c;

or

$$r_c=0{\cdot}49\left(\frac{kT}{mG\rho_c}\right)^{1/2}, \tag{3.5}$$

where ρ_c is the density at the critical radius. Finally the critical ratio of mass/radius is

$$\frac{M(r_c)}{r_c} = 2{\cdot}4\,\frac{kT}{mG}. \tag{3.6}$$

Reverting to the p–V curve for a fixed mass of gas we can now see that any point on the spiral part of the curve below A refers to a state of unstable equilibrium. (It is necessary to point this out because along BC, for example, $\partial p/\partial V$ is positive, so it might seem that this part of the curve refers to stable states.) The point A refers to the critical value of ξ ($\xi_c = 6{\cdot}5$), and on the spiral part below A, for example at D, $\xi > \xi_c$. Thus for an isothermal gas sphere represented by D, there must be some interior value r_c of r at which $\xi = \xi_c$, and the gas inside r_c is unstable to small fluctuations. It therefore follows that the only stable part of the p–V curve is the part from $V = \infty$ to A.

Finally, I shall compare the criterion of gravitational instability derived here with that discovered by Jeans (**4**). Jeans considered a mass of gas, uniform except for small condensations and rarefactions which are supposed to propagate through it as waves of length l. He found that the velocity of propagation was

$$\left[\frac{dp}{d\rho} - \frac{G\rho l^2}{\pi}\right]^{1/2}.$$

This becomes imaginary if

$$l^2 > \frac{\pi}{G\rho}\frac{dp}{d\rho}, \tag{3.7}$$

and Jeans concluded that if the linear dimensions of the mass of gas were greater than $(\pi/G\rho\ dp/d\rho)^{1/2}$ the motion would be unstable and the mass would break up. If one considers a sphere and uses $p = kT\rho/m$, one finds that to the three criteria for instability (3.3), (3.4) and (3.5) there corresponds the single equation

$$r_c = 0{\cdot}89\left(\frac{kT}{mG\rho}\right)^{1/2} \tag{3.8}$$

and to (3.6) corresponds

$$\frac{M(r_c)}{r_c} = 3{\cdot}3\,\frac{kT}{mG}. \tag{3.9}$$

It seems worth while to emphasize that the Jeans' condition for instability of a gaseous mass is (3.7) and not, as some writers seem to think, that the gravitational energy (taken as positive) shall exceed twice the thermal energy. If a gas is under no forces except its own gravitation, then, from the virial theorem, a necessary condition for it to be in a steady state is that the gravitational energy shall be equal to twice the thermal energy. It happens, as Jeans pointed out, that the equilibrium dimensions, as given by the virial theorem, are about the same as the maximum dimensions for a stable mass as given by (3.7). Hence Jeans concluded that an isolated mass in equilibrium would have no tendency to break up. The situation is quite different if the mass under consideration is not isolated: if, for example, it consists of a local concentration in a gaseous medium which exerts a pressure on it. In this case the virial theorem does not apply, but the mass might still be unstable.

From a comparison of formulae (3.3) to (3.6) with (3.8) and (3.9), it seems that the instability investigated in this work occurs in masses with sizes and

densities roughly the same as those predicted by Jeans' formula. However, the question is not so straightforward as it appears, for the following reasons.

In the first place, Jeans' formula is open to the criticism, already mentioned, that one should not assume a constant density for a gravitating mass of gas, whether it is finite or infinite. Secondly, it does not follow that Jeans' method will give similar results when applied to a non-uniform mass: in fact, Jeans (**5**) came to the conclusion that similar perturbations applied to an isothermal gas sphere did not make it unstable. Thirdly, the numerical factors in equations (3.4) and (3.6) are important because, owing to the non-uniform density, $r\bar{\rho}^{1/2}$ and $M(r)/r$ are not monotonically increasing functions of r; they have in fact maxima and minima, and tend to limits as $r \to \infty$, so that they each lie within a certain numerical range. The upper limit of the range is in each case less than the value from (3.8) or (3.9), in the direction of which ρ is assumed to be constant. Thus, for example, the critical ratio $M(r_c)/r_c$ in (3.9) is not achieved for any isothermal gas sphere.

4. *Conclusion.*—From Sections 2 and 3 it appears that, at any rate for an isothermal gas sphere, the corrections to Boyle's Law proposed by Terletsky result in gravitational instability, and not in the gas having the properties of a critical state. Although one condition for a critical state, i.e. $\partial p/\partial V = 0$, is satisfied at an appropriate volume, the second condition, $\partial^2 p/\partial V^2 = 0$, is not, and the fact that the second derivative is non-zero implies instability.

The instability is interesting because the condition for it resembles the well-known Jeans' condition, but it is here obtained without assuming that the gas has a uniform density. The difference between the two conditions suggests that Jeans' formula should be used with caution, and with due regard to the fact that no large cloud of gas actually existing in nature satisfies the conditions assumed in deriving it.

The bearing of this work on cosmology is as follows. According to the point-source models of relativistic cosmology, there was, during the early history of the universe, a finite or infinite expanding mass of gas which at any given time was of uniform density. In order to find out whether such a model can explain the formation of the nebulae two additional theories are required: first, one which gives the probability that density fluctuations of a given magnitude shall occur; and secondly, a theory which describes the motion and growth of such perturbations once they have occurred.

A rigorous formulation of the first theory, which would involve an adaptation of statistical mechanics to general relativity, is not available, and for want of something more appropriate, one naturally falls back on classical statistical mechanics, and obtains the likely fluctuations by the formula (1.3). One then uses these in the second theory, available in the work of Lifshitz, and finds that the probable fluctuations could not have given rise to the nebulae in the time available. This implies that in the point-source models the formation of the nebulae is vastly improbable.

To save the point-source models one might make some special hypothesis about the early history of the universe; for example, that the primordial cosmic medium was turbulent, as has been suggested by Gamow (though it is not in fact clear that primordial turbulence would explain the formation of the nebulae); or one might even suppose that the universe started its expansion complete with inhomogeneities of the required size, at some time slightly later than the singular

state of the point-source models. Alternatively, one may examine more carefully the application to cosmology of classical fluctuation theory.

It was as a contribution to this latter examination that the present work was undertaken. If it had turned out that large density fluctuations could take place without upsetting the stability of a system such as an isothermal gas sphere, this would have been some indication that a rigorous treatment of fluctuations in the expanding universe might yield perturbations of the magnitude required to explain the formation of the nebulae. In fact, however, the investigation lends no support to this idea because it reveals no large fluctuations, but shows that the isothermal gas sphere is unstable.

The instability could be of interest only for the later nebular evolution. An isothermal gas sphere of nebular mass represents a considerable inhomogeneity, and for its formation within the appropriate time a large initial fluctuation in the homogeneous cosmic medium would be required. Thus the instability by itself does not solve the problem because one first needs a mechanism to produce density concentrations corresponding to the isothermal gas spheres.

Granted some mechanism to produce the isothermal gas spheres, the criterion for instability fits quite well the hypothesis that the nebulae were formed from them. For example, if one takes $\bar{\rho} = 10^{-28}$ g/cm^3 one finds that the biggest stable sphere of hydrogen has the mass of a nebula (10^{44} g) if the temperature is about 10^5 deg. K. This agrees well with the temperature of a condensing nebula deduced by Hoyle (3) on other grounds.

The University,
Liverpool:
1956 *February* 2.

References

(1) Chandrasekhar, S., *An Introduction to the Study of Stellar Structure*, Chicago, 1939, Chapter IV.
(2) Emden, R., *Gaskugeln*, Leipzig and Berlin, 1907, Table 14.
(3) Hoyle, F., *Astrophysical Journal*, **118**, 513 (1953).
(4) Jeans, J. H., *Astronomy and Cosmogony*, Cambridge, 1929, page 345.
(5) Jeans, J. H., Philosphical Transactions, Series A, **199**, 1.
(6) Lifshitz, E., Journal of Physics, (U.S.S.R.) X, 116, (1946).
(7) Terletsky, Y. P., Zh. Eksper. Teor. Fiz., **22**, 506 (1952).

CONTENTS

Meeting of 1956 March 9: PAGE

Fellows elected .. 241
Junior members elected .. 241
Presents announced .. 241

Meeting of 1956 April 13:

Fellows elected .. 242
Associates elected .. 242
Presents announced .. 242

W. D. Heintz, Six visual double star orbits .. 243

W. D. Heintz, Micrometer observations of double stars .. 248

F. Schmeidler, Measures of double stars and their systematic errors .. 256

William Buscombe, The orbit of the spectroscopic binary HD 170523 .. 262

University of London Observatory, Stellar parallaxes determined at Mill Hill (Third List) .. 267

W. N. Abbott, Ionized and neutral calcium in the atmospheres of the Cepheids η Aquilae and ζ Geminorum .. 269

Antoinette de Vaucouleurs, Equivalent widths of the *K* line .. 277

F. G. Smith, P. A. O'Brien and J. E. Baldwin, The radio source in the direction of the galactic centre .. 282

R. v. d. R. Woolley and Denise A. Robertson, Studies in the equilibrium of globular clusters (II) .. 288

R. v. d. R. Woolley, On the equilibrium of clusters. III. The Pleiades .. 296

I. W. Busbridge, Finite atmospheres with isotropic scattering. II. Increase of line strength to the limb .. 304

J. H. Piddington, Solar atmospheric heating by hydromagnetic waves .. 314

L. Mestel, On the equilibrium of magnetic stars .. 324

W. Rindler, On the coordination of the Riemannian and kinematic techniques in theoretical cosmology, with particular reference to the shift-distance law .. 335

W. B. Bonnor, Boyle's law and gravitational instability .. 351

Printed in London by Taylor & Francis, Ltd., 1957 January